

# **Study of lower Sampling Intervals on Rainfall Queue Characteristics over Radio Links in South Africa**

By

Godfrey Nkululeko Mazibuko

Dissertation submitted in fulfillment of the requirement for the degree

**MASTER OF SCIENCE IN ENGINEERING:**

**ELECTRONIC ENGINEERING**



**UNIVERSITY OF KWAZULU-NATAL**

November 2017

**Supervisor:**

Prof. Thomas Joachim Odhiambo Afullo

**Co-supervisor:**

Dr. Akintunde Ayodeji Alonge

As the candidate's Supervisors we agree to the submission of this dissertation

Prof. Thomas Joachim Odhiambo Afullo

Signed .....

Date: .....

Dr. Akintunde Ayodeji Alonge

Signed .....

Date: .....

### **Declaration 1 - Plagiarism**

I, **Godfrey Nkululeko Mazibuko**, declare that:

1. The research reported in this thesis, except where otherwise indicated, is my original research.
2. This dissertation has not been submitted for any degree or examination at any other university.
3. This dissertation does not contain other persons' data, pictures, graphs or other information, unless specifically acknowledged as being sourced from other persons.
4. This dissertation does not contain other persons' writing, unless specifically acknowledged as being sourced from other researchers. Where other written sources have been quoted, then:
  - a) Their words have been re-written but the general information attributed to them has been referenced;
  - b) Where their exact words have been used, their writing has been placed inside quotation marks, and referenced.
5. Where I have reproduced a publication of which I am an author, co-author or editor, I have indicated in detail which part of the publication was actually written by myself alone and have fully referenced such publications.
6. This dissertation does not contain text, graphics or tables copied and pasted from the Internet, unless specifically acknowledged, and the source being detailed in the dissertation and in the References sections.

Signed .....  
**Godfrey Nkululeko Mazibuko**

Date: .....

**Declaration 2 – Publication**

**Godfrey N. Mazibuko, Thomas J. Afullo and Akintunde A. Alonge**, “Effects of Lower Sampling Interval on Rainfall Queue Characteristics over Radio Links in South Africa”, presented in the 2017 *IEEE AFRICON Conference*, Cape Town, S.A, September 18-20.

Signed .....  
**Godfrey Nkululeko Mazibuko**

Date: .....

## **Acknowledgements**

Firstly, I would like to give thanks to my GOD who gave me the strength and understanding for the completion of this work in the name of JESUS CHRIST my lord and savior. If it wasn't for the blood of JESUS CHRIST which made me right with GOD, I would have not been at this stage. Hence I boldly say, indeed my GOD bursts through like a raging flood (1 Samuel 5 vs 20).

Secondly, many thanks go to my supervisors, Professor Thomas J. Afullo and Dr. Akintunde A. Alonge for their excellent guidance during the period of this research. They were always available and prepared to help me all times. Working and being around them was one of those experiences that are priceless.

Thirdly, big thanks to my family especially Miss L. N. Ndlovu (my mother), Mr Mndeni Mbhele (my brothe), Mrs Wendy Mbhele (my sister), Sphehile Mbhele (my brother) and Hlanzeka Mbatha (my sister) for their support and encouragement throughout the period of this research.

I would also like to thank Telkom for funding this research; their financial contribution was one of the major influences for the completion of this research.

Again, thanks to all staff members in the School of Electrical, Electronics and Computer Engineering, University of KwaZulu-Natal, South Africa, for their contribution in the success of this research work. A big thank you to Dr. Modisa Mosalaosi for his constructive suggestions, Mr. Khaye Dlamini, the school administrator, for his great assistance.

Lastly, to my postgraduate colleagues, a big thank you – especially Mrs. Mary Ahunah, Mr. Olabamidele Kolawole and Babajide Afolayan.

## Abstract

Rainfall attenuation in tropical and subtropical regions of the world has continued to attract great interest; as there is a urgent emphasis on proper spectrum management and sharing, particularly at microwave and millimeter bands above 10 GHz. To this end, there have been arguments pertaining to the need to improve the ‘sensing’ of rainfall events to enhance the opportunities provided by adaptive rain fade mitigation schemes, while conserving base station power requirements during rainy events. To implement this approach, an extensive understanding of rainfall time series via the available statistical tools is often required to properly harness the characteristics of rainfall behavior. To this end, a study was undertaken to examine the behavior of rainfall and its impact on radio links at 1-minute sampling time by using the Queueing Theory Technique (QTT). Interesting results were obtained in the process of the study, except that the effect of the sampling time on rainfall queues remained unknown. Therefore, this thesis presents the investigation of the sampling time effects on rainfall queues over radio links in Durban, South Africa. Rainfall measurements were collected at 30-second sampling time using the RD-80 Joss–Waldvogel (JW) distrometer in Durban (29°52’S, 30°58’E), the same location where the 1-minute data was previously collected. As before, the rainfall data is classified into four rainfall regimes, namely drizzle, widespread, shower and thunderstorm. The queue parameters required for rainfall traffic analysis such as inter-arrival time and service-time distribution are empirically determined to be Erlang-k distributed, whereas the overlap time is exponentially distributed. It is thus established that the queue discipline for rain spikes over radio waves is a non-Markovian process ( $E_k/E_k/s/\infty/FCFS$ ). Comparison between the 30-second rainfall queues results and previous results of 1-minute sampling time, shows that more rainfall spikes are revealed at 30-second sampling time. Furthermore, it is determined that there is a strong polynomial relationship between the 30-second and 1-minute sampling time data – hence some of the 1-minute data may be converted into 30-second data by using the polynomial function, with the appropriate polynomial coefficients according to rainfall queue parameters in each regime. The converted data is amalgamated with the actual 30-second data for the investigation of the rainfall long-term behavior. It is found that the rainfall long-term behavior resembles the behavior of the short-term data - hence implying that the rainfall process at 30-second sampling time in Durban has the attributes of a self-similar process. From rain attenuation investigation, it is determined that since more rain spikes are evident in the 30-second data, the former has higher rain attenuation exceedance values ( $R_{0.01}$ ) compared to the 1-minute data.

## Table of Content

Title Page.....	i
Declaration 1 - Plagiarism.....	iii
Declaration 2 - Publication .....	iv
Acknowledgements.....	v
Abstract.....	vi
Table of Content.....	vii
List of Figures.....	xi
List of Tables.....	xiv
List of Abbreviations.....	xvi

### CHAPTER ONE

#### Introduction of the Study

1.1 Introduction.....	1
1.2 Problem Statement.....	1
1.3 Objectives.....	2
1.4 Methodological Approach.....	2
1.5 Organization of the Dissertation .....	3
1.6 Publication.....	4

### CHAPTER TWO

#### Literature Review

2.1 Introduction.....	5
2.2 Specific RainAttenuation.....	5
2.3 Rain Attenuation Models.....	7
2.3.1 ITU-R Model.....	7
2.3.2 Moupfouma Model.....	7
2.3.3 Crane’s Global Model.....	8
2.4 Rain Rate Models.....	9
2.4.1 Rice-Holmberg (R-H) Rain Rate.....	9
2.4.2 Crane Rain Rate Model.....	9
2.4.3 The Moupfouma I Model.....	11

2.4.4	The Moupfouma and Martin Model.....	12
2.5	Rain Drop Size Distribution (DSD) Models.....	13
2.5.1	Lognormal Rainfall DSD Model.....	13
2.5.2	Modified Gamma Rainfall DSD Model.....	13
2.6	Markov chain Model on Rainfall Process.....	14
2.7	Rainfall Studies in South Africa.....	14
2.7.1	Rainfall DSD Studies.....	14
2.7.2	Rainfall Queueing Theory.....	15
2.7.2.1	Data Collection.....	16
2.7.2.2	Rainfall Spikes Queue Analysis.....	16
2.8	Chapter Summary.....	19

## **CHAPTER THREE**

### **Impact of the Sampling Time on the Rainfall Queues in Durban**

3.1	Introduction.....	20
3.2	Sampled Rain Spikes.....	21
3.3	Rainfall Queue Parameters Modeling and Results Analysis at 30-second sampling time.....	21
3.3.1	Service Time.....	21
3.3.2	Inter-Arrival Time.....	24
3.3.3	Overlap Time.....	26
3.3.4	Overall Queue Parameters.....	27
3.3.5	Error Analysis of the Suggested Distributions.....	29
3.4	Investigation of the` Number of Servers.....	30
3.5	Investigation of the Relationship between the Overall Number of Spikes and Event Duration...32	
3.6	Comparison of the Rainfall Queue Parameters at 30-second and 1 minute Sampling Time.....34	
3.6.1	Service Times .....	34
3.6.2	Inter-Arrival Times.....	36
3.6.3	Overlap Times .....	37
3.6.4	Overall Queue Parameters.....	39
3.7	Chapter Summary.....	41

## **CHAPTER FOUR**

### **Long Term Modeling of the Rainfall Spikes at 30-second Sampling Time in Durban**

4.1	Introduction .....	42
4.2	Investigation of the Typical Relationship between the 30-second and 1-minute Data.....	42
4.3	Modeling Results of the Converted Queue Parameters.....	49
4.3.1	Service Time.....	50
4.3.2	Inter-Arrival Time.....	51
4.3.3	Overlap Time.....	53
4.3.4	Overall Queue Parameters.....	53
4.4	Error Analysis of the Proposed Distributions.....	56
4.5	Validation of the Conversion Method.....	57
4.5.1	Service Times Comparison .....	59
4.5.2	Inter-Arrival Times Comparison .....	59
4.5.3	Overlap Times Comparison.....	62
4.5.4	Overall Queue Parameters Comparison.....	63
4.6	Long Term Modeling Results Analysis.....	65
4.6.1	Long-Term Service Time.....	66
4.6.2	Long-Term Inter-Arrival Time.....	66
4.6.3	Long-Term Overlap Time.....	67
4.6.4	Long-Term Overall Parameters .....	70
4.6.5	Error Analysis of the Long-Term Proposed Distribution.....	71
4.7	Chapter Summary .....	72

## **CHAPTER FIVE**

### **Effect of the Sampling Time on Rainfall Attenuation along Radio Links**

5.1	Introduction.....	74
5.2	Rain Rate Cumulative Distributions.....	74
5.3	Prediction and Comparison of Specific Attenuation .....	75
5.3.1	Determination of Conversion Factors .....	75
5.3.2	Comparison of the Specific Attenuation at Different Sampling Times.....	76
5.4	Prediction of Path Attenuation Using Existing Models.....	77
5.5	Investigation of Annual Attenuation Exceeded Along the Path Length of 10 km at 10 GHz and 40 GHz.....	79

5.6 Significance of Lower Sampling Time on Rainfall Data.....80  
5.7 Chapter Summary.....81

**CHAPTER SIX**

**Conclusion and Future Work**

6.1 Conclusions.....82  
6.2 Future Work.....84  
**References.....85**  
**Internet References.....91**

**APPENDICES**

Appendix A: Frequency-dependent coefficients for estimation of specific rain attenuation.....92

## List of Figures

<b>Figure 2.1:</b>	The Process of Rainfall Spikes Delivering Rain Droplets over Radio Links.....	16
<b>Figure 2.2:</b>	Rainfall measurement equipment setup (Joss-Waldvogel RD-80 distrometer).....	17
<b>Figure 3.1:</b>	Service Time PDFs of Actual and Simulated Rainfall Data in Durban at 30-second Sampling Time.....	23
<b>Figure 3.2:</b>	Inter-Arrival Time PDFs of Actual and Simulated Rainfall Data in Durban at 30-second Sampling Time.....	25
<b>Figure 3.3:</b>	Overlap Time PDFs of Actual and Simulated Rainfall Data in Durban at 30-second Sampling Time.....	27
<b>Figure 3.4:</b>	Overall Queue Parameter's PDFs of Actual and Simulated Rainfall Data in Durban at 30-second Sampling Time.....	28
<b>Figure 3.5:</b>	Relationship between the Overall Number of Rainfall Spikes and Rainfall Duration.....	33
<b>Figure 3.6:</b>	Plots of the Proposed Queue Models and Actual Data Sets for the Service Time at 30-Second and 1- min Sampling Time According to the Regimes.....	35
<b>Figure 3.7:</b>	Plots of the Proposed Queue Models and Actual Data Sets for the Inter-Arrival Time at 30-Second and 1- min Sampling Time According to the Regimes.....	37
<b>Figure 3.8:</b>	Plots of the Proposed Queue Models and Actual Data Sets for the Overlap Time at 30-Second and 1- min Sampling Time According to the Regimes.....	38
<b>Figure 3.9:</b>	Plots of the Proposed Queue Models and Actual Data Sets for the Overall Queue Parameters at 30-Second and 1- min Sampling Time According to the Regimes.....	39
<b>Figure 4.1:</b>	Comparison Procedure of the 30-second and 1-minute Cumulative Distribution Functions (CDFs).....	43

<b>Figure 4.2:</b>	Relationship between the Regime Service Times of the 1-minute and 30-second Data.....	45
<b>Figure 4.3:</b>	Relationship between the Regime Inter-Arrival Times of the 1-minute and 30-second Data.....	46
<b>Figure 4.4:</b>	Relationship between the Regime Overlap Times of the 1-minute and 30-second Data.....	47
<b>Figure 4.5:</b>	Relationship between the Overall Queue parameters of the 1-minute and 30-second Data.....	48
<b>Figure 4.6:</b>	Converted regime service time PDFs of the actual and simulated data.....	51
<b>Figure 4.7:</b>	Converted regime inter-arrival time PDFs of the actual and simulated data.....	52
<b>Figure 4.8:</b>	Converted regime overlap time PDFs of the actual and simulated data.....	54
<b>Figure 4.9:</b>	Converted Overall Queue Parameters PDFs of Actual and Simulated Data.....	55
<b>Figure 4.10:</b>	Comparison of the Service Times Proposed Models for the 30-second Actual Data and Converted Data.....	60
<b>Figure 4.11:</b>	Comparison of the Inter-Arrival Times Proposed Models for the 30-second Actual Data and Converted Data.....	61
<b>Figure 4.12:</b>	Comparison of the Overlap Times Proposed Models for the 30-second Actual Data and Converted Data.....	62
<b>Figure 4.13:</b>	Comparison of the Overall Queue Parameters Proposed Models for the 30-second Actual Data and Converted Data.....	64
<b>Figure 4.14:</b>	Long-Term Modeling Plots of the Service Time Parameter at 30-second Sampling Time in Durban.....	66
<b>Figure 4.15:</b>	Long-Term Modeling Plots of the Inter-Arrival Time Parameter at 30-second Sampling Time in Durban.....	67
<b>Figure 4.16:</b>	Long-Term Modeling Plots of the Overlap Time Parameter at 30-second Sampling Time in Durban.....	69

<b>Figure 4.17:</b>	Long-Term Modeling Plots of the Overall Parameters at 30-second Sampling Time in Durban.....	70
<b>Figure 5.1:</b>	Rainfall rate cumulative distribution for the 30-second and 1-minute sampling times.....	75
<b>Figure 5.2:</b>	Conversion of the 30-second rain rate into 1-minute rain rate.....	76
<b>Figure 5.3:</b>	Predicted specific attenuation at 30-second and 1-minute sampling on different frequencies for horizontal frequency polarization.....	77
<b>Figure 5.4:</b>	Predicted path attenuation using existing models at 30-second and 1-minute sampling on different path length in Durban.....	78
<b>Figure 5.5:</b>	Rain attenuation cumulative distribution for the 30-second and 1-minute sampling time data.....	79

## List of Table

Table 2.1:	ITU-R parameters for Moupfouma models.....	12
Table 2.2:	Rainfall Queue Parameters Statistical Information at 1-minute Sampling Time in Durban.....	18
Table 3.1:	Number of Sampled Rainfall Spikes According to their Time Bounds and Queue Parameters at 30- second Sampling Time.....	22
Table 3.2:	Rainfall Queue Parameters Modeling Results at 30-second Sampling Time.....	23
Table 3.3:	Overall Queue Parameters at 30-second Sampling Time in Durban.....	27
Table 3.4:	Proposed Queue Parameters Distribution Error Investigation.....	31
Table 3.5:	Proposed Overall Queue Parameters Distribution Error Investigation.....	31
Table 3.6:	The Minimum Number of Servers for the four Rainfall Regimes.....	32
Table 3.7:	Relationship Between the Number of Rainfall Spikes and Rainfall Events Duration.....	33
Table 4.1:	Coefficient of Determination Values ( $R^2$ ) Between the 1-minute and 30-second Rainfall Queue Parameters.....	43
Table 4.2:	Modeling Results of the Converted Rainfall Queue Parameters from 1-minute to 30-second Sampling Time.....	49
Table 4.3:	Modeling Results of the Converted Overall Queue Parameters from 1-minute to 30-second Sampling Time.....	54
Table 4.4:	Error Analysis of the Proposed Distributions for the Converted Queue Parameters.....	56
Table 4.5:	Error Analysis of the Proposed Distributions for the Overall Converted Queue Parameters.....	57
Table 4.6:	Error Analysis between the Queue Parameters Proposed pdfs of the 30-second Actual Data and Converted Data.....	58
Table 4.7:	Error Analysis between the Overall Queue Parameters Proposed pdfs of the 30-second Actual Data and Converted Data.....	62
Table 4.8:	Long-Term Rainfall Queue Parameters Modeling Results at 30-second Sampling Time.....	65
Table 4.9:	Long-Term Rainfall Overall Queue Parameters Modeling Results at 30-second Sampling Time.....	70
Table 4.10:	Error Analysis of the Long-Term Queue Parameters Proposed Distributions.....	72

Table 4.11:	Error Analysis of the Long-Term Overall Queue Parameters Proposed Distributions....	72
Table 5.1:	Rain Attenuation Exceedence at Different Percentage of Time for the 30-second and 1-minute data.....	80

## LIST OF ABBREVIATIONS

BD	Birth-Death
CDF	Cumulative Distribution Function
CV	Coefficient of Variation
DMCP	Discrete Markov Chain Process
DRFM	Dynamic Rain Fade Mitigation
DSD	Drop Size Distribution
DTH	Direct-To-Home
DTMC	Discrete Time Markov Chains
FCFS	First-Come, First-Served
FMT	Fade Mitigation Technique
IEEE	Institution of Electrical and Electronics Engineers
ITU-R	International Telecommunication Union – Radiocommunication Sector
JW	Joss-Waldvogel
MC	Markov Chains
PDF	Probability Density Function
RMSE	Root Mean Square Error
SRFM	Static Rain Fade Mitigation
SST	Synthetic Storm Technique
PCS	Personal Communication System
GPS	Global Positioning Satellite
WLANS	Wireless Local Area Computer Network
DBS	Direct Broadcast Satellite
QTT	Queueing Theory Technique
L-P	Laws and Parsons
M-P	Marshall and Palmer

# CHAPTER ONE

## Introduction of the Study

### 1.1 Introduction

Most of telecommunication services in our days are provided through radio links, which utilize frequencies that range between 3 GHz and 300 GHz. Wireless communications such as personal communication system (PCS), global positioning satellite (GPS) system, wireless local area computer networks (WLANS), direct broadcast satellite (DBS) television and many more are applications of radio services operating in the aforementioned frequency range. Over the years, new ideas have been brought into the field of communication to make the means of communication simpler. Telecommunications play a significant role in everyday life, allowing the sharing of information in our society to be seamless and less cumbersome in most cases. Ultimately, the usefulness of a communication system is its ability to deliver information from one point to another as intended. The common challenge in transmitting over high frequency bands is the effects of attenuation. Among others, precipitation effects are identified as the most dominant over radio links in the form of rain, mist, fog, ice, hail and snow. Overall, rain attenuation is the most problematic phenomenon over radio links because of water particles having a higher dielectric constant capable of scattering electromagnetic waves [Murrell *et al*, 1994 and Nemarich *et al*, 1988]. Thus, rainfall causes more degradation to the performance of a radio link than ice. Moreover, water particles have a higher dielectric loss and attenuation due to thermal dissipation [Ishimaru, 1978 and Jonathan, 2004]. Radio waves transmitted through a rainy medium may be absorbed or scattered and hence may never reach the receiver. Scattering and absorption phenomena are the two most dominant causes of attenuation. When the signal wavelength is large relative to the raindrop size, scattering has a dominant effect on the attenuation. Conversely, when the wavelength is small relative to the raindrop size, absorption is considered a dominant cause of attenuation [Ivanovs, 2006].

### 1.2 Problem Statement

The extent of attenuation of a transmitted signal is a consequence of a combination of many factors such as frequency of the signal, rain rate, raindrop size distribution and many more [Alonge, 2014]. However, it is possible for the signal to be transmitted through a rainy medium without noticeable absorption and/or scattering for lower rain rates and raindrop sizes. In the case of higher rain rates and raindrop sizes, there is a significant amount of attenuation on the transmitted signal and as such a thorough understanding of the rain behavior and its effects on radio links is vital. Owing to this, there has been an extensive amount of research conducted in Durban, South Africa which has produced valuable and meaningful contributions with regards to the effects of rainfall attenuation as found in [Fashuy *et al*, 2006; Odedina and Afullo, 2008;

*Odedina and Afullo, 2010 and Owolawi, 2011*]. Some of the group's research work has been conducted by utilizing measured rainfall rates, rainfall drop-size distributions (DSD), seasonal and regime-based effects of rainfall attenuation on microwave links in Durban and other areas [*Odedina and Afullo, 2008; Odedina and Afullo, 2010 and Owolawi, 2011, J*]. Recently, *Alonge and Afullo (2014a)*, determined that rainfall rate spikes follow a particular queue discipline as the clouds move during a rainfall event. Accordingly, with the knowledge of rainfall rate, rainfall DSD, rainfall growth and rainfall cell behavior; they applied queueing theory to model the rainfall behavior in subtropical and equatorial regions in Africa. Moreover, *Alonge and Afullo (2014b)*, compared the rainfall queue parameters for two African locations (Butare and Durban) and investigated the occurrences of the rainfall rate peaks. Most recently, *Alonge and Afullo (2014a)*, developed a Queueing Theory Technique (QTT) in order to understand the probabilistic complexities of rainfall microphysics. The QTT was found to be very useful in determining rain attenuation statistical information relevant for planning, design and implementation of radio links for both terrestrial and satellite applications. However, the influence of the sampling time during data acquisition on QTT results has not been investigated. In this view, this study specifically aims to investigate the effect of sampling time on rainfall queues by comparing queue generated data sets modeled from two differently sampled measurements. This will be accomplished by using the approach of *Alonge and Afullo (2014a)* with rain datasets at 30-second and 1-minute sampling times.

### **1.3 Objectives**

The objectives of this work are:

- 1) To investigate the queueing attributes of rain events toward microwave and millimeter wave in Durban at 30-second sampling time and determine the queue discipline.
- 2) To investigate the queueing characteristics of rainfall at two different sampling times in the same location.
- 3) To determine the relationship between the 30-second and 1-minute sampling time queue parameters.
- 4) To investigate the long-term behavior of rainfall queues for long-term modeling in Durban.
- 5) To compare rain attenuation over radio links determined from both the 30-second and 1-minute sampling time data.

### **1.4 Methodological Approach**

Measurement data for this research is retrieved from the Joss-Waldvögel RD-80 distrometer installed on the roof top of the Electrical, Electronic and Computer Engineering building, Howard College Campus of the University of KwaZulu-Natal with the processing units housed inside the microwave laboratory, located

in Durban, South Africa (29°52'S, 30°58'E). Since the previous work of [Alonge, 2014a] utilized the 1-minute data, this research will focus on rainfall data acquired at 30-second sampling time over a period of 42 months between April 2013 and June 2016.

## **1.5 Organization of the Dissertation**

This work is arranged according to six chapters in total. Chapter one provides the introduction to the subject matter of the research arranged as follows: The introduction and challenges experienced by radio links, problem formulation, objectives of the research, methodological approach, summary of the thesis and publications.

Chapter two provides the background on the study arranged as follows: The chapter is introduced followed by a review of rainfall specific attenuation, review of rainfall attenuation models, review of rain rate models, review of rain drop Size Distribution (DSD) models, review of the Markov chain as applied to model rainfall behavior, review of rainfall attenuation studies in South Africa and finally the chapter summary.

Chapter three deals with rainfall as a queueing process for two sampling times of 30-seconds and 1-minute in Durban, presented as follows: Chapter introduction, determination of time bounds within which the majority of rainfall rate spikes' service time belongs at 30-second sampling time, modeling and analysis of rainfall queue parameters at 30-second sampling time, determination of the minimum number of servers required for the rainfall queues at 30-second sampling time to reach the steady-state, determination of the relationship between the number of rain spikes and the duration of rain events, comparison between the rainfall queue parameters at 30-second and 1-minute sampling time, and the chapter summary.

Chapter four presents the investigation of long-term rainfall behavior at 30-second sampling time in Durban, structured as follows: Chapter introduction, determination of the relationship between the 30-second and 1-minute sampling time datasets, conversion of 1-minute dataset to the 30-second dataset and modeling the converted rainfall dataset, error analysis between the modeled converted dataset and the measured one through their respective queue parameters, validation of the conversion method, long-term rainfall data modeling and chapter summary

Chapter Five presents the effect of sampling time on rainfall attenuation arranged as follows: Chapter introduction, predicted rainfall rate exceeded for different percentages of time at 30-second and 1-minute sampling time, prediction and comparison of specific attenuation at 30-second and 1-minute sampling time, prediction of path attenuation in Durban, determination of rain attenuation exceeded for different

percentages of time, conclusion on the significance of the sampling time on rainfall attenuation prediction and the summary of the chapter.

Chapter six presents the applications and conclusions of this research work, structured as follows: Chapter introduction, chapter three conclusions, chapter four conclusions, chapter five conclusions and future work.

## **1.6 Publication**

**Godfrey N. Mazibuko, Thomas J. Afullo and Akintunde A. Alonge**, “Effects of Lower Sampling Interval on Rainfall Queue Characteristics over Radio Links in South Africa”, presented in the 2017 *IEEE AFRICON Conference*, Cape Town, South Africa, 18 – 20 September, 2017.

# CHAPTER TWO

## Literature Review

### 2.1 Introduction

The attractiveness of utilizing millimeter and microwave frequency bands cannot be overstated due to the ability to re-use frequencies for short distance communications. However, signals transmitted at these bands suffer a great deal of degradation as they propagate through the air. At the lower level of the atmosphere, the propagating wave experiences high attenuation because of the random atmospheric conditions that change from time to time [Crane, 2003]. There are several attenuation agents that contribute towards the signal loss such as vegetation, obstacles like mountains, hills and tall buildings, varying terrain structures, solar flares, ionospheric disturbances and above all, precipitation [Seybold, 2005; Ajayi et al., 1996]. Signal loss due to precipitation comes in the form of rain, mist, fog, ice, hail and snow. Of these factors, the component that causes significant attenuation on communication links operating at about 7 GHz and beyond is rainfall [Islam et al., 1997; Crane, 2003]. Accordingly, a lot of effort has been directed towards an understanding of the statistical behavior of the rainfall process which is an essential component of radio link design. In this light, this chapter aims to review some of the research works provided in literature which deals with rain attenuation and related subjects.

### 2.2 Specific Rain Attenuation

The following three assumptions are assumed to be valid: (1) the intensity of an electromagnetic wave exponentially decays as the wave travels through a rain cell, (2) the raindrops are assumed to have a spherical shape and (3) the contributions from each raindrop are additive and independent of one another. The electromagnetic wave propagating through a rain cell with an extent,  $d$ , in the direction of propagation is expressed as [Ippolito, 1996; Ippolito, 2008]:

$$A_{dB} = \int_0^d A_S dx \quad (2.1)$$

where  $A_S$  and  $d$  are the specific attenuation of the rain cell and extent of the propagation path from  $x = 0$  to  $x = d$  respectively.

Using assumption (1), the received power is given as [Ippolito, 2008]:

$$P_r = P_t e^{-kd} \quad (2.2)$$

where  $P_t$  and  $P_r$  are transmitted and received power respectively,  $k$  is the attenuation coefficient for the rain cell.

The simplest way to express the electromagnetic wave attenuation is [Ippolito, 2008]:

$$A_{dB} = 10 \log_{10} \left( \frac{P_t}{P_r} \right) \quad (2.3)$$

By using (2.2) and (2.3), the attenuation in general can be expressed as:

$$A_{dB} = 4.343kd \quad [dB] \quad (2.4a)$$

where

$$k = \rho Q_t \quad (2.4b)$$

and

$$Q_t(r, \lambda, m) = Q_s + Q_a \quad [mm^2] \quad (2.4c)$$

where  $Q_t$ ,  $Q_s$  and  $Q_a$  are the attenuation, scattering and absorption cross section of the raindrop respectively, and  $\rho$  is the drop density.

By using (2.1) and (2.4), then specific attenuation can be given as:

$$A_{dB} = 4.343 \int Q_t(r, \lambda, m) \eta(r) dr \quad (2.5)$$

Furthermore, it was identified that there is a power-law relationship that exists between specific attenuation,  $A_s$ , and rain rate,  $R$ , in mm/h given as [ITU-R P.838-3, 2005; Freeman, 2007]:

$$A_s = zR^\alpha \quad (2.6)$$

where  $z$  and  $\alpha$  are frequency and temperature dependent regression coefficients respectively.

When using (2.6), ITU-R P.838-5 (2005) provides the values of  $z$  and  $\alpha$  as  $k_H$  and  $\alpha_H$  for horizontal polarization,  $k_V$  and  $\alpha_V$  for vertical polarization. These values are given in Appendix A.

## 2.3 Rain Attenuation Models

### 2.3.1 ITU-R Model

ITU-R P.530-10 provides a method that can be used for long-term attenuation prediction. Path attenuation at 0.01% of the time is given as follows [ITU-R, 2001].

$$A_{0.01} = A_S d_{eff} = A_S r d \quad dB \quad (2.7a)$$

where the effective path length,  $d_{eff}$ , is presented as the product of the actual path length,  $d$ , and a distance factor,  $r$ , given respectively as follows:

$$d_{eff} = r d \quad (2.7b)$$

and

$$r = \frac{1}{1 + d/d_0} \quad (2.7c)$$

$d_0$  is called a rainfall rate dependence factor given as follows:

$$d_0 = 35e^{-0.015} R_{0.01} \quad (2.7d)$$

This is valid for  $R_{0.01} \leq 100 \text{ mm/h}$  and  $R_{0.01}$  is accepted as  $100 \text{ mm/h}$  if it is found to be  $R_{0.01} \geq 100 \text{ mm/h}$ . The ITU-R rain attenuation model is considered to be valid in all parts of the world for frequencies up to 40 GHz and path length up to 60 km.

### 2.3.2 Moupfouma Model

Moupfouma 1984, proposed a rain attenuation prediction model for terrestrial paths given 1-minute data rain rates and the percentage of time for which these rain rates are exceeded. The rain attenuation along the link path is given as [Moupfouma, 1984].

$$A(dB) = A_S d_{eff} \quad (2.8a)$$

where the effective path length,  $d_{eff}$ , is presented as the product of the actual path length,  $d$ , and a distance factor,  $r$ , given respectively as follows:

$$d_{eff} = r d \quad (2.8b)$$

and

$$r = \frac{1}{1 + Cd^m} \quad (2.8c)$$

Attenuation  $A(dB)$  and rain rates sampled at 1-minute intervals must be calculated at the same percentage. From the experimental data  $C$  and  $m$  were obtained. From the results,  $C$  was found to depend on the percentage ( $p$ ) of interest on the available data; whereas  $m$  was found to depend on the link path length and the corresponding frequency. Therefore, the path length reduction factor is modified to:

$$r = \frac{1}{1 + 0.03 \left(\frac{p}{0.01}\right)^{-\beta} d^m} \quad (2.8d)$$

where

$$m(F, d) = 1 + \Upsilon(F) \log_e d \quad (2.8e)$$

$$m(F, d) = 1.4 \times 10^{-4} F^{1.76} \quad (2.8f)$$

$F$  is the frequency in GHz and the  $\beta$  coefficient is obtained as a result of a best fit by:

$$\left. \begin{array}{ll} d < 50 \text{ km} & \\ \beta = 0.45 & \text{for } 0.001 \leq p \leq 0.01 \\ \beta = 0.6 & \text{for } 0.01 \leq p \leq 0.1 \\ d \geq 50 \text{ km} & \\ \beta = 0.36 & \text{for } 0.001 \leq p \leq 0.01 \\ \beta = 0.6 & \text{for } 0.01 \leq p \leq 0.1 \end{array} \right\} \quad (2.8g)$$

### 2.3.3 Crane's Global Model

Crane global attenuation prediction model was proposed for both satellite and terrestrial paths. The model depends on the vertical variations of temperature in the atmosphere, rain rate and rain structure [Crane, 1996 and 2003]. Crane presented the path profile piecewise by an exponential function in order to accomplish the model. The resultant attenuation model is given as follows [Crane, 1996]:

$$A_T(R, d) = A_S \left( \frac{e^{y\delta(R)} - 1}{y} + \frac{e^{zd} - e^{y\delta(R)}}{z} e^{\alpha B} \right) \quad \delta(R) < d < 22.5 \quad (2.9a)$$

$$A_T(R, d) = A_S \left( \frac{e^{y\delta(R)} - 1}{y} \right) \quad 0 < d < \delta(R) \quad (2.9b)$$

where

$A_T$  = horizontal path attenuation (dB);

$R$  = Rain Rate (mm/hr);

$A_S$  = specific attenuation (dB).

The other coefficients are given as:

$$\left. \begin{aligned} B &= \ln(b) = 0.83 - 0.17 \ln(R) \\ c &= 0.026 - 0.03 \ln(R) \\ \delta(R) &= 3.8 - 0.6 \ln(R) \\ u &= \frac{B}{\delta(R)} + c \\ y &= \alpha u \\ z &= \alpha c \end{aligned} \right\} \quad (2.9c)$$

## 2.4 Rain Rate Models

### 2.4.1 Rice-Holmberg (R-H) Rain Rate

*Rice and Holmberg (1973)* developed the R-H model by using extensive long term statistics from 150 locations all over the world. This model assembles a rainfall rate distribution from thunderstorm events (mode 1) and “other rain” (mode 2). The total distribution is the sum of the two models:

$$M = \text{Model 1} + \text{Model 2} \quad [mm] \quad (2.10)$$

The percentage of an average year for which the rain rate exceeds  $R$  mm/h at a medium location is given by [*Dissanayake et al., 1997; Dissanayake et al., 2002*],

$$P(R)\% = \frac{M}{87.6} \{0.03\beta e^{-0.03R} + 0.2(1 - \beta)[e^{-0.258R} + 1.86e^{-1.63R}]\} \quad (2.11)$$

where  $M$ ,  $\beta$  and  $R$  are the average annual accumulations of rainfall [ $mm$ ], the thunderstorm component of  $M$  and clock minute rain rate in  $mm/h$  respectively.

Values of  $\beta$  and  $M$  are provided in the world maps as provided in *Rice and Holmberg (1973)*, or also calculated as [*Rice and Holmberg, 1973; Dissanayake et al., 2002*],

$$\beta = \frac{M_1}{M} \quad (2.12a)$$

where  $M_1$  is the average annual accumulation of thunderstorm rain [mm].

Additionally,  $\beta$  can be calculated as:

$$\beta = \beta_0 \left[ 0.25 + \frac{2e^{-0.35}(1 + 0.125M)}{U} \right] \quad (2.12b)$$

$$\beta_0 = 0.03 + 0.97e^{-5 \exp(-0.004M_m)} \quad (2.12c)$$

where  $U$  is the average number of thunderstorm days anticipated throughout an average year and  $M_m$  is the biggest monthly precipitation received during the time of the experiment.

The R-H model was later improved by *Dutton and Dougherty (1974)* to include the attenuation prediction property, which was missing in the earlier R-H (1973) model. The modified model is given as:

$$P(R) = \begin{cases} 0.0114(T_{11} + T_{12})e^{-\frac{R}{R_1}}, & R < 5\text{mm/h} \\ 0.0114T_{21}\exp\left(-\sqrt[4]{\frac{R}{R_{21}}}\right) & 5 \leq R \leq 30 \\ 0.0114T_{11}\exp\left(-\frac{R}{R_{11}}\right) & R > 30 \end{cases} \quad (2.13)$$

where  $T_{11}$ ,  $T_{21}$ ,  $R_1'$  and  $\bar{R}$  are linear combinations of  $M$ ,  $\beta$  and  $D = 24 + 3M$ , determined from regression equations.

The R-H model, when compared with measured data, suffers a drawback in underestimating rainfall rates at 0.01% and lower [*Crane, 1996*].

#### **2.4.2 Crane Rain Rate Model**

The model popularly known as the Crane Global model is the first model that was developed by [*Crane, 1980*]. His second model is the 2-Component *Crane (1982)* model, where he used a path integrated technique in which a link calculation resulted from the sum of separately computed volume cell contribution and debris contribution. This is a closed-form probability distribution model that, separately, handles the

input of the volume cells and debris during the prediction of rainfall rate cumulative distribution functions (CDFs). This model was established to determine the probability that a specified attenuation level is exceeded and this probability is the sum of probabilities associated with each component. The empirical rain rate distribution function is given by [Crane, 1996] as:

$$P(r \geq R) = P_C(r \geq R) + P_D(r \geq R) - P_{CD}(r \geq R) \quad (2.14a)$$

with

$$P_C(r \geq R) = P_C e^{-\frac{R}{R_C}} \quad (2.14b)$$

$$P_D(r \geq R) = P_N N\left(\frac{\ln R - \ln R_D}{S_D}\right) \quad (2.14c)$$

$$= \frac{P_N}{\sqrt{2\pi}S_D} \int_R^\infty \exp\left[-\frac{1}{2}\left(\frac{\ln R}{S_D}\right)^2\right] \quad (2.14d)$$

$$P_{CD}(r \geq R) = P_C(r \geq R)P_D(r \geq R) \quad (2.14e)$$

where  $P(r \geq R)$  is the probability that an observed rainfall rate  $r$  exceeds the specified rainfall rate  $R$ .  $P_C(r \geq R)$ ,  $P_D(r \geq R)$  and  $P_{CD}(r \geq R)$  represent the CDF's of the volume cells, debris and joint CDF for volume cells and debris respectively.  $P_C$  &  $P_D$  are probability of cell and debris respectively.  $R_C$  and  $R_D$  represent average rain rate in a cell and median rain rate in debris respectively.  $N$  is the normal distribution function and  $S_D$  is the standard deviation of natural logarithm of rainfall rate. The revised 2-Component model was later introduced in 1989 and included other features such as spatial correlation and statistical variations of rain within a cell.

### 2.4.3 The Moupfouma I Model

This three-parameter model was developed by [Moupfouma, 1987], at higher rain rates it bears a resemblance to an exponential distribution and lognormal distribution at lower rain rates. This model accepts rainfall rates as inputs and produce probabilities that correspond to those rainfall rates. The Moupfouma I model is given as:

$$P(r \geq R) = 10^{-4} \left(\frac{R_{0.01}}{r}\right)^b e^{(\lambda 10^{1-s}[(\frac{R_{0.01}}{r})-1])} \quad (2.15a)$$

where  $r$  and  $R$  are rain rates in mm/h and,

$$b = 8.22(R_{0.01})^{-0.584} \quad (2.15b)$$

$$\mu = \lambda r^{-s} \quad (2.15c)$$

In the *Moupfouma (1987)* model, the values of  $\lambda$  and  $s$  are given by ITU-R according to climatic zones *Moupfouma (1987)* as shown in Table 2.1.

**TABLE 2.1:** ITU-R PARAMETERS FOR MOUPFOUMA MODELS [ITU-R P.837-1, 1994].

Param.	Climatic Zone										
	D	E	F	G	H	J	K	L	M	N	P
$\lambda$	0.18	0.05	0.07	0.14	0.06	0.07	0.05	0.05	0.05	0.033	0.035
$s$	0.33	0.29	0.32	0.28	0.19	0.18	0.17	0.22	0.09	0.06	0.1

#### 2.4.4 The *Moupfouma and Martin Model*

This model was developed by *Moupfouma and Martin (1995)* for empirical rainfall rate prediction to overcome the shortcomings of the *Moupfouma I* model. It has proven to work better for both tropical and temperate climates, and it is given as:

$$P(r \geq R) = 10^{-4} \left( \frac{R_{0.01}}{r+1} \right)^b \exp[\mu(R_{0.01} - r)] \quad (2.16a)$$

where  $r$  in mm/h and  $R_{0.01}$  are the rain rate exceeded for a fraction of the time and rainfall rate exceeded for 0.01% of time respectively. Then  $b$  is approximated by the following expression:

$$b = \left( \frac{r - R_{0.01}}{R_{0.01}} \right) \ln \left( 1 + \frac{r}{R_{0.01}} \right) \quad (2.16b)$$

and  $\mu$  in equation (2.16a) is given as:

$$\mu = \left( \frac{4 \ln 10}{R_{0.01}} \right) \exp \left( -\lambda \left( \frac{r}{R_{0.01}} \right) \right) \quad (2.16c)$$

where  $\lambda = 1.066$  and  $\gamma = 0.214$

## 2.5 Rain Drop Size Distribution (DSD) Models

The knowledge of the rain drop size distribution (DSD) is essential for the prediction of rainfall attenuation. Rain DSD depends on various factors including rainfall intensity, precipitation type, wind share, cloud type and circulation system [Das et al., 2010]. It is therefore not an easy task to describe rain DSD by a universal, simple and precise model due to the spatial, temporal variability and complexity involved in the formation of rainfall [Rodgers et al., 1976; Medeiros et al., 1986; Das et al., 2010]. In spite of this difficulty, it is essential to determine the rain DSD at a given rain rate for the calculation and modeling of rainfall attenuation. A number of DSD models exist in literature such as the lognormal DSD model, exponential DSD model, modified gamma model, Erlang DSD model and Weibull DSD model. Parameters for these models are generally estimated using method of moment's technique and the maximum likelihood method [Das et al., 2010; Alonge, 2011].

### 2.5.1 Lognormal Rainfall DSD Model

The Lognormal rainfall drop size distribution function is given by [Feingold and Levin, 1986; Kozu and Nakamura, 1991; Timothy et al., 2002]:

$$N(D_i) = \frac{N_T}{\sigma D_i \sqrt{2\pi}} \exp \left\{ -\frac{1}{2} \left[ \frac{\ln D_i - \mu}{\sigma} \right]^2 \right\} [m^{-3} mm^{-1}] \quad (2.17)$$

where  $N_T$ ,  $D_i$ ,  $\mu$  and  $\sigma$  are the total number of rain drops, mean drop diameter in mm, mean and standard deviation of drop sizes respectively.

Previous research has shown that the DSDs in tropical and sub-tropical regions are lognormal distributed [Das and Maitra, 2010; Alonge and Afullo, 2011]. The studies of Moupfouma and Tiffon (1982), Ajayi and Olsen (1985), Massambani and Morales (1988), Massambani and Rodriguez (1990) showed that Laws and Parsons (L-P) model, and Marshall and Palmer (M-P) model overestimates the number of rain drops in the small and large diameter regions. Ajayi and Olsen (1985), using a method of regression and rain rates ranging from 0.25mm/h to 150 mm/h with data obtained from Ile-Ife, developed a two-parameter lognormal model with parameters  $\mu$  and  $\sigma$  and an additional parameter  $N_T$  for measurement fittings.

### 2.5.2 Modified Gamma Rainfall DSD Model

The modified Gamma is a three-parameter rainfall drop size distribution model which can be expressed as [Atlas and Ulbrich, 1974; Ulbrich, 1983; Kozu and Nakamura 1991]:

$$N(D_i) = N_m(D_i)^\mu \exp(-\lambda D_i) \quad (2.18)$$

According to *Ulbrich (1983)*, at both low and high rain rates this statistical DSD model captures well the rainfall DSDs. It has previously been applied in tropical and sub-tropical rain climates of Taiwan and Singapore [*Tseng et al, 2005; Lakshmi et al., 2010; Kumar et al., 2010*], South Africa [*Afullo, 2011; Alonge and Afullo, 2011; Owolawi, 2011; Alonge and Afullo, 2012*], India [*Das and Maitra, 2010*], Malaysia [*Yakubu et al., 2014; Lam et al., 2015*], Nigeria [*Ajayi and Olsen, 1985;* ], USA [*Zheng et al., 2000*], among others.

## **2.6 Markov chain Model on Rainfall Process**

There are many stochastic techniques that have been explored by different researchers for modeling the rain process. Among those techniques is the Markov chain, which is characterized as a stochastic process with a limited number of states and its future state depends on the current state. *Feyisa et al 2016*, modeled rain rate spikes in all rain regimes at Jimma, Ethiopia, by applying both the Markov chain and queueing models. It was found that the spikes average lifespan increases with the rain rate. Its then follows that rainfall spikes from the thunderstorm regime will last longer than any other rainfall spikes from other regimes. *Heder and Bitos 2008*, generated rainfall attenuation time series using the N-state Markov Chain model for a microwave channel. It was found that the first and second order rainfall attenuation statistics can be derived directly from the Markov model parameters. Therefore, at early stages of the planning of a suggested link, the N-state Markov model can be useful for rainfall attenuation predictions [*Heder and Bitos 2008*]. *Alasseur et al 2005*, proposed two useful methods suitable for generating synthetic rainfall rate time-series; which can be used for the simulation of the performance of radio communication systems at frequencies beyond 10 GHz. The proposed models were based on hierarchic Markov chains. *Vucetic and Du 1992*, proposed an analog model that can describe signal amplitude and phase variations on shadowed satellite mobile channels. An N-state Markov chain was used to represent environment parameter variations, the results agreed with the experimental measurements.

## **2.7 Rainfall Studies in South Africa**

### **2.7.1 Rainfall DSD Studies**

A remarkable effort on rainfall DSD study has been done associated with the rainfall microstructural properties and microphysics for an accurate prediction of rainfall attenuation on microwave Line-of-sight (LOS) links on South Africa, specifically in Durban [*Owolawi et al., 2009; Owolawi, 2011; Akuon and Afullo, 2011; Afullo, 2011; Alonge and Afullo, 2012; Odedina and Afullo, 2012; Malinga et al., 2013; Alonge and Afullo, 2014*]. For example, *Alonge and Afullo (2014)* investigated the microphysics of rainfall based on four different regimes for two climatic regions, one tropical and the other sub-tropical. *Odedina and Afullo (2008)* proposed rainfall zones for attenuation prediction based on International

Telecommunication Union (ITU) recommendation P.837-4 nomenclature [ITU-R P.837-4, 2003]. In their work, *Odedina and Afullo (2012)* also asserted that rain fading is extreme in the north eastern areas of South Africa compared to the western areas. Furthermore, *Owolawi (2011)* developed the contour maps based on rainfall rate at 0.01% percentage of exceedence; and re-classified the ITU-R and Crane rain zones for the Southern Africa area. The study was based on 5-minute rainfall data converted to 1-minute using a proposed hybrid method. This study supports the earlier investigations of *Odedina and Afullo (2008)*. The DSD approach in [Afullo, 2011] represents the initial efforts on rain rate measurement campaign over Durban.

### 2.7.2 Rainfall Queueing Theory

*Alonge and Afullo (2014a)* investigated the rainfall process by considering the arrival of clouds as a first come first served (FCFS) process over radio links as shown in Figure 2.1. The rainfall events were identified as a queueing process of rain clouds/spikes parallel to the cloud motion. The speed of clouds is called advection speed, which is responsible for maintaining the clouds motion. The advection speed changes with different kinds of rainfall structure and cell size [Alonge, 2014 and Pawlina, 2002]. The identified spikes' queueing pattern has three relevant parameters namely the inter-arrival time ( $t_a$ ), service time ( $t_s$ ) and overlap time ( $t_o$ ). The inter-arrival time ( $t_a$ ) of the rainfall spikes is the time between two successive arrivals of the rain spikes/cloud at a point of observation. The service time ( $t_s$ ) of a spike is the life span of the rainfall spike. The overlap time ( $t_o$ ) of the spikes, is the intersection period between the arriving and the dying cloud. The average inter-arrival time ( $\bar{t}_a$ ), average service time ( $\bar{t}_s$ ) and average overlap time ( $\bar{t}_o$ ) expressions are given respectively as follows [Alonge and Afullo, 2014a and Hillier and Lieberman, 2010]:

$$\bar{t}_a = \frac{1}{N_a} \sum_{k=1}^{N_a} t_{a,k} = \frac{1}{\lambda_a} \quad \forall t_a \in \mathbb{R} \quad (2.19a)$$

$$\bar{t}_s = \frac{1}{N_s} \sum_{k=1}^{N_s} t_{s,k} = \frac{1}{\mu_s} \quad \forall t_s \in \mathbb{R} \quad (2.19b)$$

$$\bar{t}_o = \frac{1}{N_o} \sum_{k=1}^{N_o} t_{o,k} = \frac{1}{\sigma_o} \quad \forall t_o \in \mathbb{R} \quad (2.19c)$$

where  $N_a, N_s, N_o$  are the total sampled number of the inter-arrival times, service times and overlap times, respectively. Parameters  $\bar{\lambda}_a, \bar{\mu}_s$  and  $\bar{\sigma}_o$  denote the average arrival rate, service rate and overlap rate respectively.

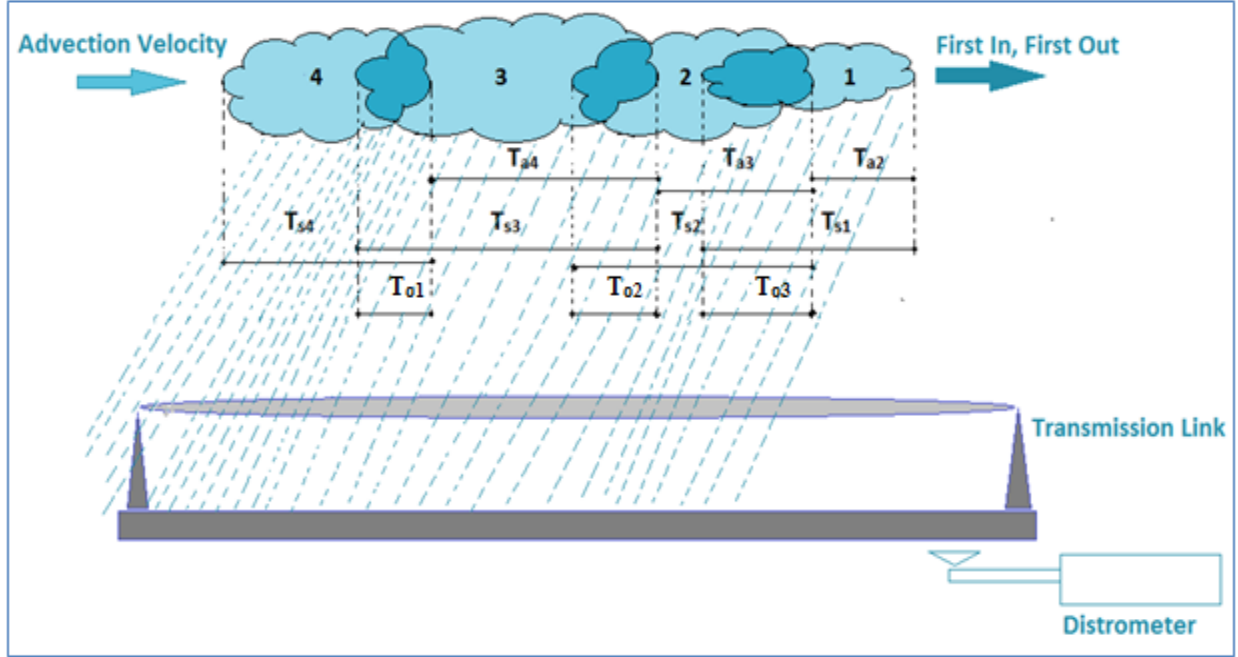


**Figure 2.1:** The Process of Rainfall Spikes Delivering Rain Droplets over Radio Links.

### 2.7.2.1 Data Collection

The rainfall measurements were carried out by a Joss-Waldvogel (JW) RD-80 distrometer. This equipment is installed in South Africa, Durban (29°52'S, 30°58'E) with an adjustable sampling time parameter. The measurements were taken from January 2009 to December 2010 (24 months) at 1-minute sampling time. The equipment is installed at University of KwaZulu-Natal, Howard College Campus. It consists of two basic parts connected via RS-232c communication standard. The equipment's outdoor part consists of the sensor that converts the rainfall drops into electronic pulse trains as shown in Figure 2.2. The sampled pulses are grouped into twenty specified diameter channels ranging between 0.359 and 5.373 depending on the intensity of the rainfall [Alonge and Afullo, 2014a and Prasanna, 2008].

### 2.7.2.2 Rainfall Spikes Queue Analysis

In determining the rainfall queue parameters in Durban, the service and overlap times were found to be Erlang-k distributed as given by [Alonge and Afullo 2014a]:

$$f(t_s; k, \mu_s) = \frac{(k\mu_s)^k k^{k-1} \exp(-k\mu_s t_s)}{\Gamma(k)} [\text{minute}]^{-1} \text{ for } t > 0; t_s \forall \mathbb{R} \quad (2.20)$$

where  $k$  represents the number of stages and  $\mu_s$  denotes the service rate. For the overlap time,  $\mu_s$  is replaced by  $\sigma_o$  (overlap rate) and  $t_s$  by  $t_o$  (overlap time) in (2.20).

It is found that the average spikes service time is less than 21 minutes regardless of the rain regime as shown in Table 2.2. On the other hand the average overlap time is less than 11 minute irrespective of the rainfall regime. The number of stages for the Erlang-k function for both these queue parameters is less than 5 regardless of the regime. The inter-arrival time was found to follow an exponential distribution ( $M$ ) which can be defined as [Alonge and Afullo 2014a]:

$$a(t_a; \lambda_a) = \lambda_a \exp(-\lambda_a t_a) [\text{minute}]^{-1} \text{ for } t_a > 0; t \forall \mathbb{R} \quad (2.21)$$

where  $\lambda_a$  represents the arrival rate and  $t_a$  for the inter-arrival time in minutes.

The obtained rainfall spikes' queue discipline in Durban at 1-minute sampling time was found to be a semi-Markovian process ( $M/E_k/s/FCFS/\infty$ ). It was also found that the peak attained by each generated spike is random and has a positive power-law relationship with its corresponding service time. Furthermore, there was a comparative study between the rainfall queues obtained from measured data in Durban and that in Butare (2°36'S, 29°44'E). It was found that a large number of collected rainfall data in Butare is characterized as either shower or thunderstorm, while that which was collected in Durban is

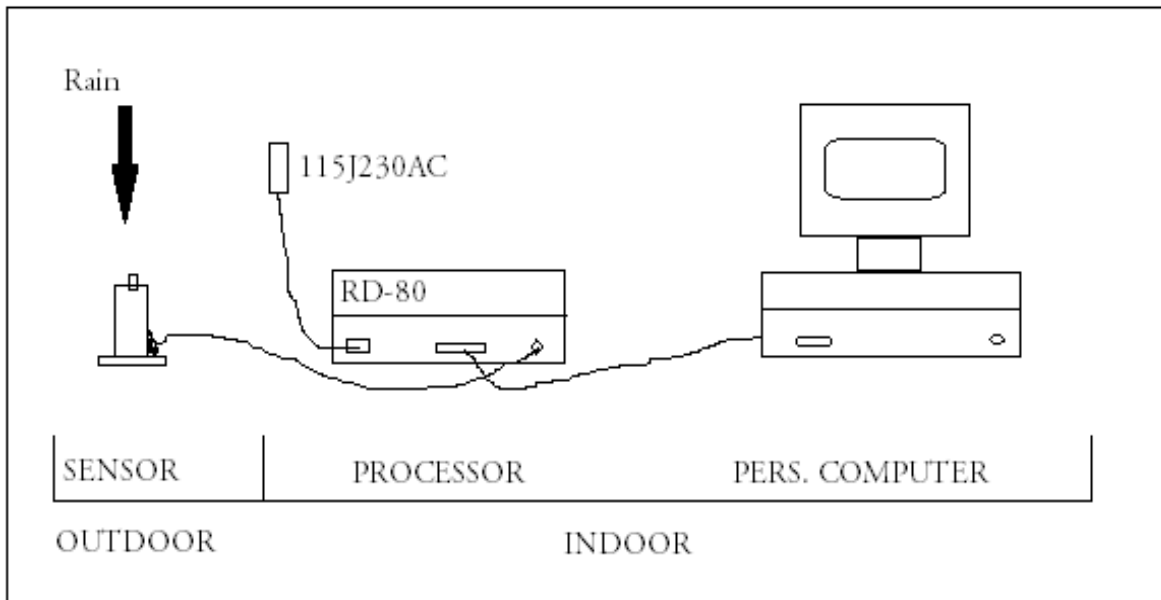


**Figure 2.2:** Rainfall measurement equipment setup (Joss-Waldvogel RD-80 distrometer) [Alonge, 2014].

**TABLE 2.2: RAINFALL QUEUE PARAMETERS STATISTICAL INFORMATION AT 1-MINUTE SAMPLING TIME IN DURBAN**

<b>SERVICE TIME</b>				
<b>SAMPLING TIME</b>	<b>REGIME</b>	<b>RATE (<math>\mu_s</math>)</b>	<b>AVERAGE (<math>\bar{t}_s</math>)</b>	<b>NUMBER OF STAGES (<math>k</math>)</b>
1-minute	Drizzle	0.0808	12.3755	5
	Widespread	0.0729	13.7095	5
	Shower	0.0615	16.2556	4
	Thunderstorm	0.0489	20.4409	3
<b>INTER-ARRIVAL TIME</b>				
<b>SAMPLING TIME</b>	<b>REGIME</b>	<b>RATE (<math>\lambda_a</math>)</b>	<b>AVERAGE (<math>\bar{t}_a</math>)</b>	<b>NUMBER OF STAGES (<math>k</math>)</b>
1-minute	Drizzle	0.1921	5.2065	1
	Widespread	0.1533	6.5242	1
	Shower	0.1486	6.7312	1
	Thunderstorm	0.0922	10.8475	1
<b>OVERLAP TIME</b>				
<b>SAMPLING TIME</b>	<b>REGIME</b>	<b>RATE (<math>\sigma_o</math>)</b>	<b>AVERAGE (<math>\bar{t}_o</math>)</b>	<b>NUMBER OF STAGES (<math>k</math>)</b>
1-minute	Drizzle	0.2506	3.9906	3
	Widespread	0.2331	4.2899	3
	Shower	0.1705	5.8667	3
	Thunderstorm	0.1739	5.7509	2

characterized mainly by drizzle and widespread type of rainfall [Alonge and Afullo, 2014b]. As it was the case with Durban, the rain rate time series was found to follow a semi-Markovian process,  $M/E_k/s/FCFS/\infty$ , in Butare. The rainfall spike traffic as a single queue entity of rainfall process was found to be aperiodically generated. Rainfall spikes' service time in Durban was found to be increasing as the rain rates increases. This implies that rain attenuation growth processes in Durban is slower with a high chance of prolonged network outage window, especially for intense rainfall conditions with high rainfall rates. Alonge and Afullo (2015) explored the probabilistic nature and underlying behavior of rainfall. They presented a peculiar method of generating rainfall rates by a queueing scheduling technique for regions where rain data may be unavailable or insufficient. A bit of this applies the queueing characteristics of rain to generate

instantaneously distinct time-varying rainfall events. In their investigation, they presented a synthesis technique for rainfall queues with rainfall spikes at subtropical and equatorial locations. The error analysis between the queue generated rainfall distributions and measured data validated the model suitability at both locations. It is therefore reasonable to suggest that the stochastic nature of rainfall may be captured and ultimately synthesized through a queue scheduling process for rain fade prediction and mitigation thereof. In this approach, the availability of the queue parameters at a location remains the key input model parameters towards a successful prediction of rainfall attenuation.

## **2.8 Chapter Summary**

This chapter presented a review of rainfall attenuation models, rainfall rate models and rainfall drop size distribution models. These models are based on empirical, analytical and statistical approaches and thus form a good basis for rainfall attenuation prediction. Moreover, the accomplished work on rainfall queues in South Africa is reviewed. It is shown that the arrival pattern of rain clouds at 5-minute sampling time in Durban follows exponential distribution. While the service times of arriving rainfall clouds is discovered to be Erlang- $k$  distributed. This information of rain queue theory is essential for the future development of countermeasure paradigm for dynamic rain fade mitigation, as this will complement the current ITU-R approach.

## CHAPTER THREE

### Impact of the Sampling Time on the Rainfall Queues in Durban

#### 3.1 Introduction

The overall behavior of the rainfall queues strongly depend on the three relevant rainfall queue parameters namely the inter-arrival, service and overlap time. However, these parameters may be influenced by many factors during the process of rainfall measurements; among those factors is sampling time. A rainfall event may be considered a continuous process and such an event is characterized by a numerous content of raindrop sizes and rain rates. The rainfall measurement process, as is the case with many continuous processes, is such that data it is obtained by discrete-time sampling. It would then follow that the expected rain rate time series depend on the sampling rate. The basic idea is that a process that changes rapidly will need to be sampled much faster than that which changes slowly. In signal processing, the Shannon sampling theorem formalizes the required sampling rate in a clean and elegant way. This is primarily because more often the information regarding the sampled process (signal) is available in terms of its frequency components. However, in terms of changes in rain behavior and content, such information is not available and one can only speculate as to the amount of time (which informs frequency) which needs to be considered adequate to capture changes in rain behavior. Most of the devices in the market today provide for adjustment in terms of sampling time but the question still remains: what is the suitable sampling time with which resources are not wasted while accurate process reconstruction remains a possibility? Most of the research globally, Duran included, have analyzed and proposed different models for different climatic conditions derived from empirical data. As recommended by the ITU, rainfall measurements are often conducted at 1-minute sampling time. Nevertheless, one would argue that the dynamics of rainfall may not be well captured at 1-minute intervals and as such this may lead to under-representation of the rain process. However, the type of rain that dominates a location may also have an influence on the choice of sampling time e.g. in areas dominated by drizzle-type rainfall it may be sufficient to sample at 1-minute as this type of rain tends to maintain a steady intensity over longer periods of time. The determination of an optimum sampling time may well be an analytical problem the solution of which may have little use practically since it is common practice to use commercially available instruments which have pre-determined sampling times. In this study, we examine the influence of sampling time on rain-induced attenuation by re-modeling the statistical behavior of rainfall with data obtained at twice the previous sampling rate over the same location. The same system setup discussed in chapter 2, subsection 2.7.2.1, was used to acquire rainfall data over a period of 42 months (3.5 years) from April 2013 up to June 2016 at 30-second (2 S/min) sampling time. At this sampling rate we have doubled the previous rate of 1S/min which was previously used by

[Alonge and Afullo, 2014a]. In order to fully appreciate the effect of sampling time on rainfall queue parameters, a comparison is made between the two datasets. Before one performs standard tests such as error analysis, a much more relevant comparison is made in terms of the quantities of the obtained queue parameters. For example, it is expected that under the doubled sampling rate there should be a higher arrival rate just as there should be higher service rate. Even though there is no benchmark for comparison, the usefulness of such a comparison remains in that the queue parameters provide an early indication of the effect of sampling time. The distributions for the queue parameters are then determined to establish the overall queue system and compare the results with those previously obtained under half the sampling rate. Accordingly, error analysis is performed between the two queue-generated datasets to quantify the difference that arises due to sampling.

### **3.2 Sampled Rain Spikes**

Of the total collected rainfall data at 30-second sampling time, most of the sampled rain spikes have a service time that falls within the range  $0 \leq t < 20$  minutes and  $20 \leq t < 40$  minutes as shown in Table 3.1. In the drizzle regime, 89.6% and 9.3% of the rain spikes service time lies within  $0 \leq t < 20$  minutes and  $20 \leq t < 40$  minutes, respectively. Widespread rainfall has 85.3% and 13.8% of the rainfall spikes service time that is within  $0 \leq t < 20$  minutes and  $20 \leq t < 40$  minutes, respectively. The shower regime has 79.5% and 14.9% of the rain spikes service time in the range  $0 \leq t < 20$  minutes and  $20 \leq t < 40$  minutes, respectively. In the thunderstorm regime 80.1% and 12.4% of the sampled rain spikes service time lies within  $0 \leq t < 20$  minutes and  $20 \leq t < 40$  minutes respectively. It is observed that the drizzle regime has the highest percentage of sampled rain spikes with service time in the range  $0 \leq t < 20$  minutes, whereas in the range  $20 \leq t < 40$  minutes the dominant number of rain spikes belongs to the shower regime. A similar trend is observable for other queue parameters as can be deduced from Table 3.1.

### **3.3 Rainfall Queue Parameters Modeling and Results Analysis at 30-second sampling**

#### **3.3.1 Service Time**

The rainfall spikes service time is one of the key parameters in the determination of the queue system for any given process. This parameter directly translates to the length of time during transmission within which the radio link is affected by moments of continuous precipitation at a certain rain rate. Prolonged service time of certain rain rates may lead to failure of the communication system to recover lost or corrupted transmissions due to rainfall ultimately causing network outage. Since service time is a statistical parameter, its variation is therefore captured by statistical tools and it has been determined that it is Erlang-k distributed, with  $k = 2$  for all regimes except thunderstorm regime where  $k = 3$  as presented

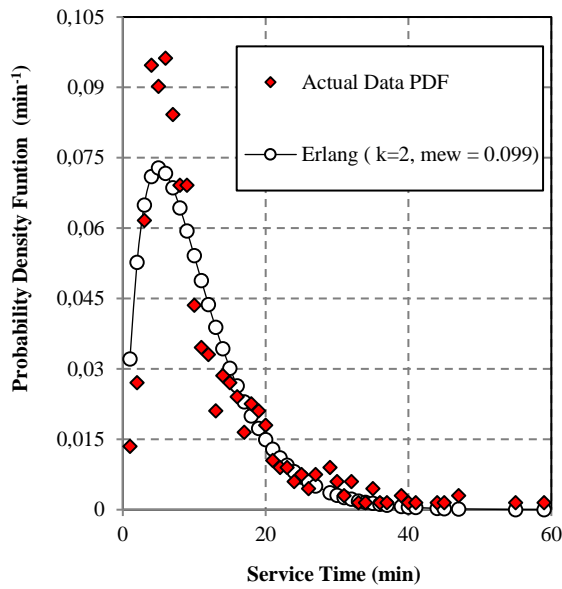
**TABLE 3.1:** NUMBER OF SAMPLED RAINFALL SPIKES ACCORDING TO THEIR TIME BOUNDS AND QUEUE PARAMETERS AT 30- SECOND SAMPLING TIME

<i>SERVICE TIME (minutes)</i>				
<b><i>TIME BOUNDS</i></b> <i>(minutes)</i>	<b><u>30 Seconds Integration time</u></b>			
	<i>Drizzle</i>	<i>Widespread</i>	<i>Shower</i>	<i>Thunderstorm</i>
$0 \leq t < 20$	596	506	442	149
$20 \leq t < 40$	62	82	83	23
$40 \leq t < 60$	7	3	18	10
$t \geq 60$	0	2	13	4
$\Sigma$	665	593	556	186
<i>INTER-ARRIVAL TIME (minutes)</i>				
<b><i>TIME BOUNDS</i></b> <i>(minutes)</i>	<b><u>30 Seconds Integration time</u></b>			
	<i>Drizzle</i>	<i>Widespread</i>	<i>Shower</i>	<i>Thunderstorm</i>
$0 \leq t < 20$	488	464	453	130
$20 \leq t < 40$	24	31	37	16
$40 \leq t < 60$	4	3	12	3
$t \geq 60$	0	2	2	1
$\Sigma$	516	500	504	150
<i>OVERLAP TIME (minutes)</i>				
<b><i>TIME BOUNDS</i></b> <i>(minutes)</i>	<b><u>30 Seconds Integration time</u></b>			
	<i>Drizzle</i>	<i>Widespread</i>	<i>Shower</i>	<i>Thunderstorm</i>
$0 \leq t < 20$	516	500	498	149
$20 \leq t < 40$	0	0	3	1
$40 \leq t < 60$	0	0	2	0
$t \geq 60$	0	0	1	0
$\Sigma$	516	500	504	150

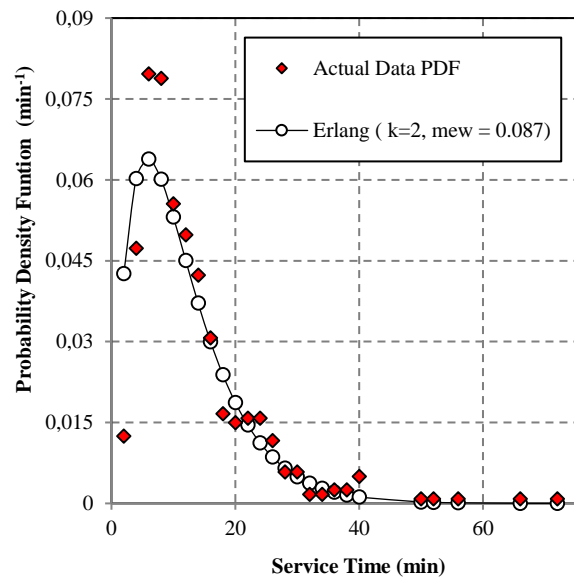
in Table 3.2 and Figure 3.1. Rainfall spikes in the shower regime are observed to have the longest average service time (lifespan) of approximately 15 minutes. In summary, rain spikes' average service time is within the range  $10 < t < 15$  minutes for all regimes in Durban at 30-second sampling time. On the other hand drizzle is characterized by higher service rates compared to all other regimes, thus it is more likely that the lower service rates under shower-type rainfall will be responsible for most of the network outages due to their prolonged service time.

**Table 3.2:** RAINFALL QUEUE PARAMETERS MODELING RESULTS AT 30-SECOND SAMPLING TIME

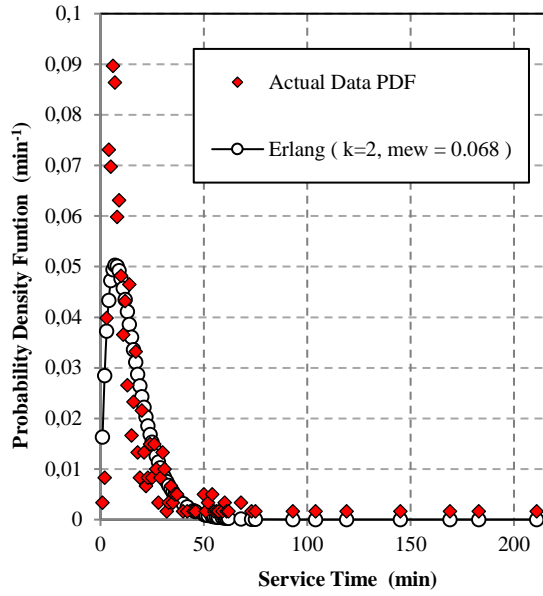
QUEUE PARAMETER	REGIME	AVERAGE TIME ( $\bar{t}_s$ )	RATE PARAMETER ( $\mu_s$ )	NUMBER OF STAGES (k)
SERVICE TIME	Drizzle	10.103	0.099	2
	Widespread	11.517	0.087	2
	Shower	14.618	0.068	2
	Thunderstorm	14.331	0.070	3
QUEUE PARAMETER	REGIME	AVERAGE TIME ( $\bar{t}_a$ )	RATE PARAMETER ( $\lambda_a$ )	NUMBER OF STAGES (k)
INTER-ARRIVAL TIME	Drizzle	4.805	0.208	4
	Widespread	5.791	0.173	2
	Shower	5.745	0.174	2
	Thunderstorm	9.105	0.110	2
QUEUE PARAMETER	REGIME	AVERAGE TIME ( $\bar{t}_o$ )	RATE PARAMETER ( $\sigma_o$ )	NUMBER OF STAGES (k)
OVERLAP TIME	Drizzle	1.435	0.697	1
	Widespread	1.750	0.571	1
	Shower	2.474	0.404	1
	Thunderstorm	1.844	0.542	1



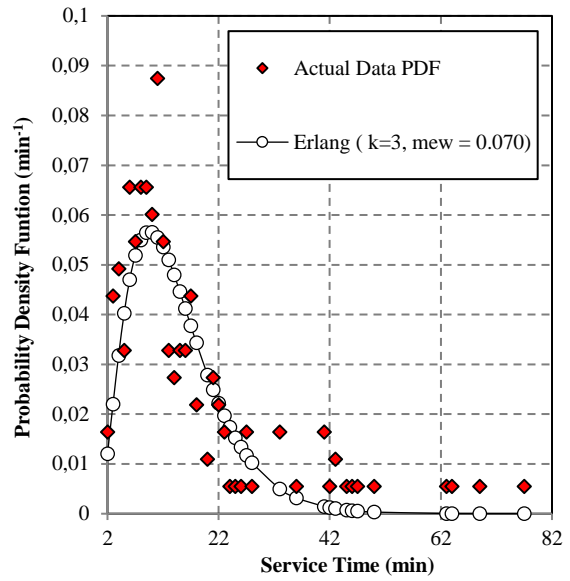
a) Drizzle



b) Widespread



c) Shower

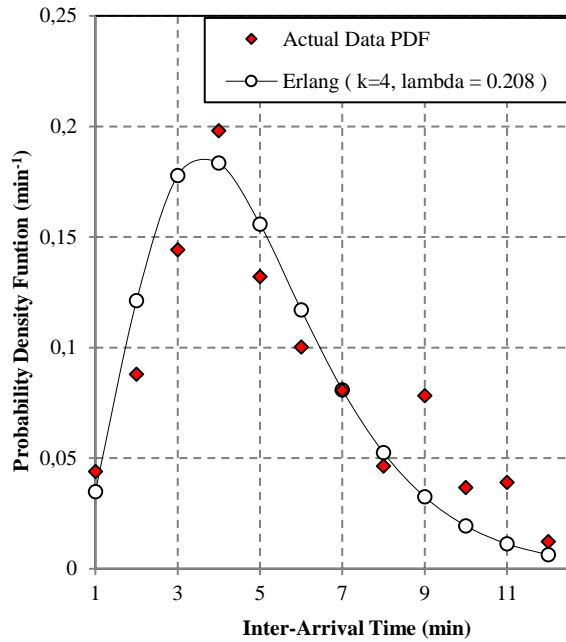


d) Thunderstorm

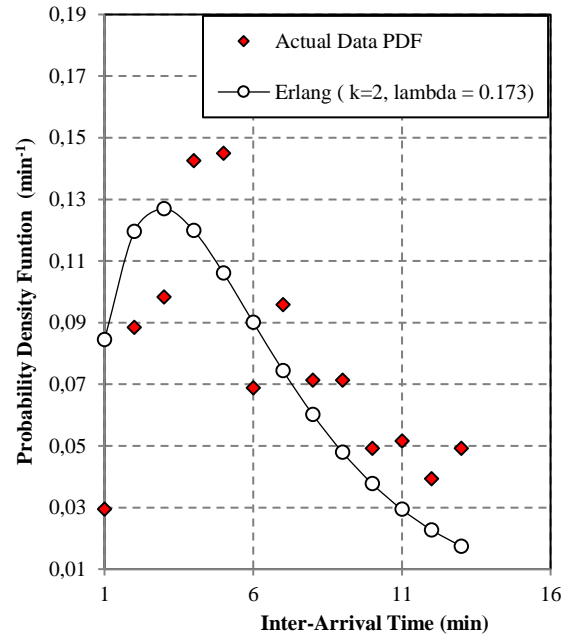
**Figure 3.1:** Service Time PDFs of Actual and Simulated Rainfall Data in Durban at 30-second Sampling Time.

### 3.3.2 Inter-Arrival Time

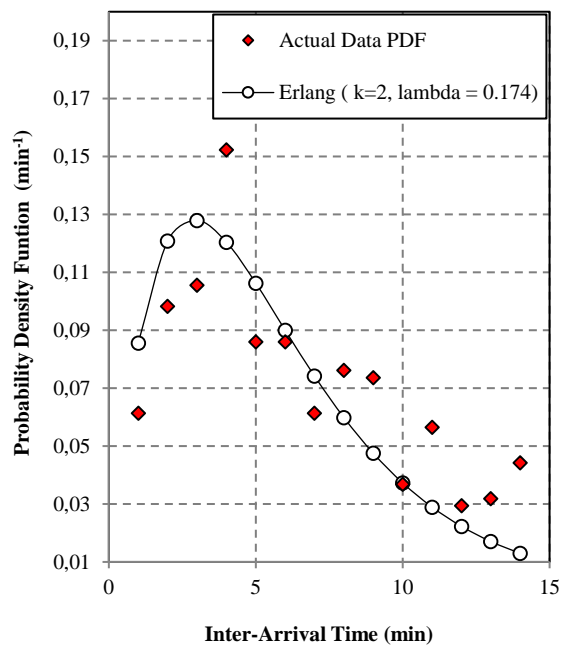
The time difference between successive arrivals of the rainfall spikes is called the inter-arrival time. It is one of the parameters required for a complete specification of the queue system of the rain rate time series as a queue process. The properties of the inter-arrival distribution are discussed and modeled. It was established that the rain spikes inter-arrival time follows an Erlang- $k$  distribution with  $k = 2$  for all rainfall regimes except drizzle where  $k = 4$ . It is observed that there is an increase in the average inter-arrival time from drizzle to thunderstorm. Thus, the average time between thunderstorm rain spikes is the longest compared to all other regimes; it takes approximately 10 minutes on average for another spike to arrive during thunderstorm events. In general, the average rainfall spike inter-arrival time in Durban at 30-second sampling time is between  $4 < t < 10$  minutes across all the rainfall regimes. Accordingly, there is a decrease in rainfall spike arrival rates from drizzle to thunderstorm. Thus the frequency of rainfall spike arrivals is highest during drizzle events where the rain rate is between  $1 \leq t < 5$  mm/h. All the inter-arrival times modeled and simulation results are presented in Table 3.2 and Figure 3.2 for all rainfall regimes.



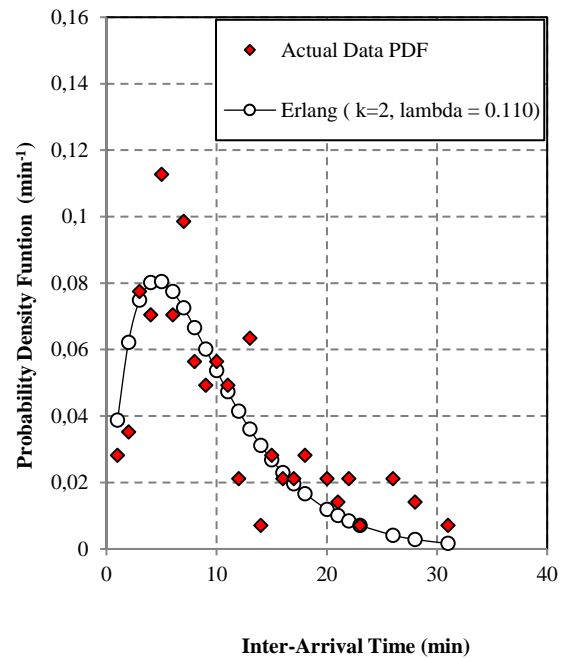
a) Drizzle



b) Widespread



c) Shower

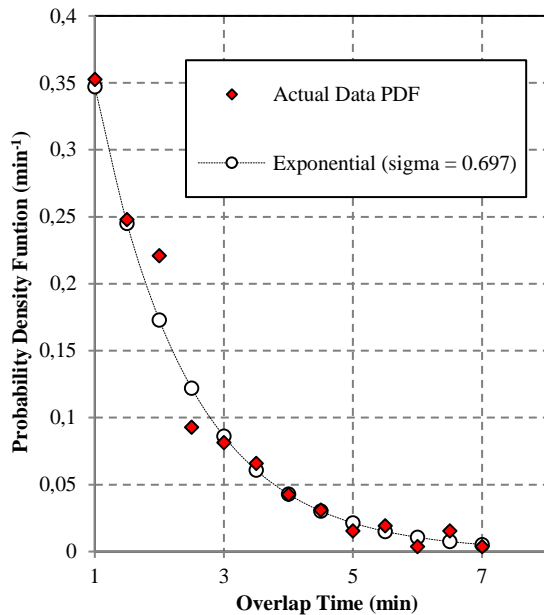


d) Thunderstorm

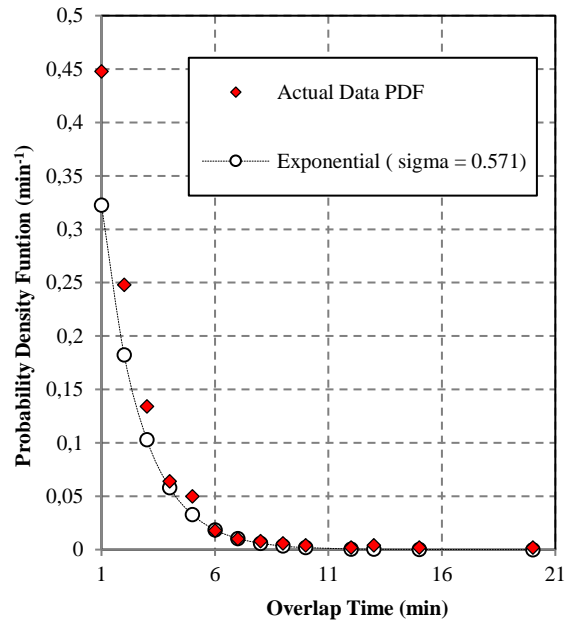
**Figure 3.2:** Inter-Arrival Time PDFs of Actual and Simulated Rainfall Data in Durban at 30-second Sampling Time.

### 3.3.3 Overlap Time

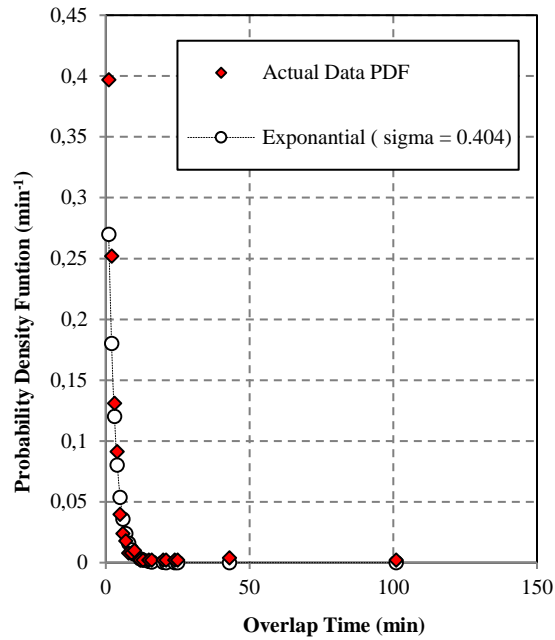
The natural arrangement of clouds and possible continuous growth of droplets advected by turbulent flow of clouds tends to cause overlap in the measured rain time series at a station. It is common in queueing systems to experience overlap and it should duly be taken into consideration for accurate characterization of the underlying process. In the presence of overlap, the arrival time of the next event encroaches into the time service of the current event. Though this does not change the service time of the current event, it does however imply that there are times of parallel service in the system. The nature of the overlap time parameter is analogous to that of the service time, since it is regarded as a subset of the service time. It is therefore expected to exhibit similar probabilistic characteristics as the service time parameter. Table 3.2 and Figure 3.3 present both the modeled and measured probabilistic results for the overlap time distribution for different regimes in Durban at 30-second sampling time. The overlap time parameter is found to be exponentially distributed, which is a special case of the Erlang- $k$  distribution with  $k = 1$ . The shower regime is observed to have the longest average overlap time. Drizzle, as expected, has the highest overlap rate compared to other regimes. This stems from the earlier observation under service time, where drizzle was found to have the highest service rate and it logical to conclude that the higher the service rate in the regime, the higher the overlap rate in the same regime.



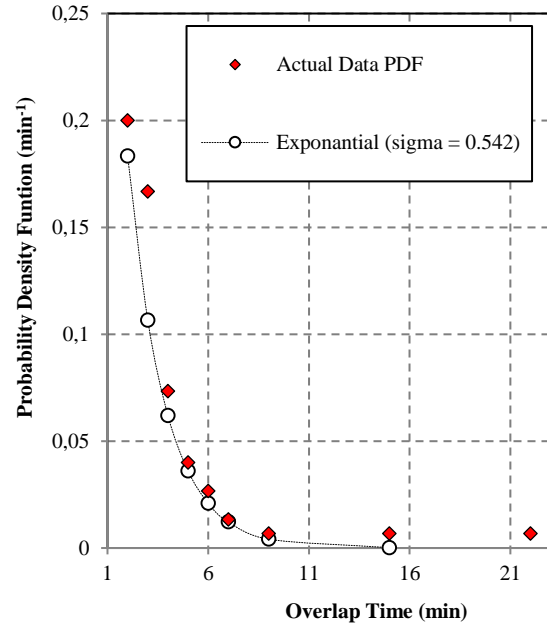
a) Drizzle



b) Widespread



c) Shower



d) Thunderstorm

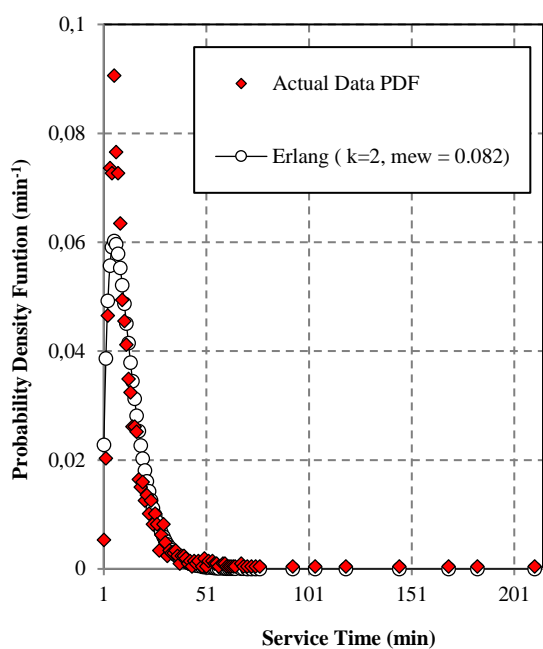
**Figure 3.3:** Overlap Time PDFs of Actual and Simulated Rainfall Data in Durban at 30-second Sampling Time.

**TABLE 3.3:** OVERALL QUEUE PARAMETERS AT 30-SECOND SAMPLING TIME IN DURBAN

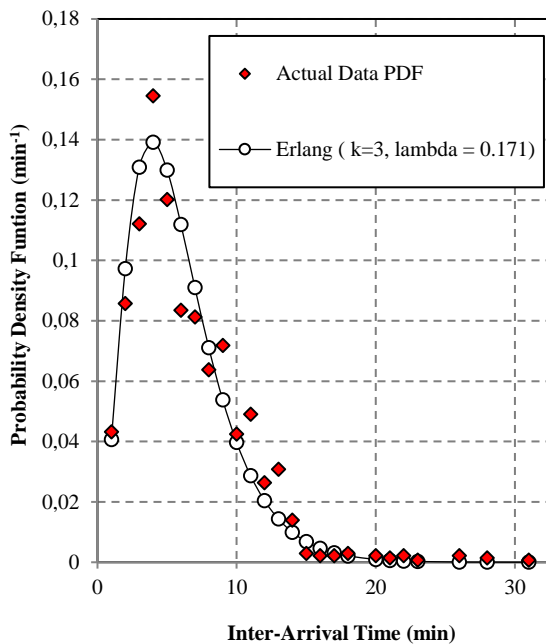
QUEUE PARAMETER	AVERAGE TIME	RATE PARAMETER	NUMBER OF STAGES
	$\bar{t}_s$	$\mu$	<b>k</b>
Service Time	12.210	0.082	2
	$\bar{t}_a$	$\lambda$	<b>k</b>
Inter-Arrival Time	5.832	0.171	3
	$\bar{t}_o$	$\sigma$	<b>k</b>
Overlap Time	1.872	0.534	1

### 3.3.4 Overall Queue Parameters

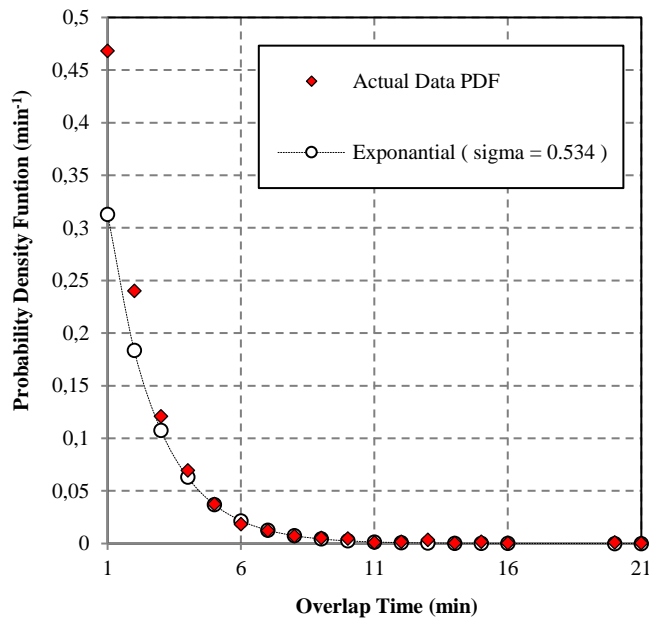
Over the years, the study of rainfall behavior has been carried out in two of ways: 1) as a regime-based process and different researchers have used different regime margins in their respective classifications 2) as a unified process where the statistical analysis is derived from the entirety of measured rainfall data



a) Overall Service Time



b) Overall Inter-Arrival Time



(c) Overall Overlap Time

**Figure 3.4:** Overall Queue Parameter's PDFs of Actual and Simulated Rainfall Data in Durban at 30-second Sampling Time.

without any rain rate classification. The type of rain at a location may influence the choice of approach and this also applies to regime classifications. In this work, both approaches are considered and thus the overall rain queue system is also determined. Both approaches serve a meaningful purpose in terms of application. The availability of a communication link is usually derived from the overall annual rain statistics at a location. On the other hand, a regime-based rain fade prediction will improve dynamic fade countermeasure processes a great deal as it offers specific details about the variability of rain behavior for individual events. The 30-second sampled data collected over 3.5 years is used again to establish the overall queue parameters. The obtained results are presented in Table 3.3 and Figure 3.4 which show the actual data as well as the modeled behavior. The overall service time is Erlang-k distributed, with  $k = 2$ , the same number of stages obtained under regime-based modeling except for thunderstorm regime. The overall average service time is 12.21 minutes, which is very close to that of the widespread regime (11.517 minutes). The overall service rate is 0.08 spikes per second which is between the lower and upper bounds obtained under regime-based service rates. The overall inter-arrival time parameter follows an Erlang-k distribution, where the arrival process is a three-stage process ( $k = 3$ ). The overall average inter-arrival time is approximately 6 minutes and lies between the lower and upper values obtained under the regime-based inter-arrival times and notably closer to the widespread average inter-arrival time presented in Table 3.2. A similar observation can be made in terms of the overall arrival rate of 0.17 spikes every 30-second in comparison with 0.173 under the widespread regime. Conversely, the overall overlap time follows the exponential distribution. The overall average overlap time is 1.9 minutes and likewise, is very close to that of the widespread regime. In general, the average values of the overall queue parameters are within the bounds of the regime-based queue parameters and it may be concluded that the general probabilistic characteristic of rainfall in Durban is of widespread nature.

### ***3.3.5 Error Analysis of the Suggested Distributions***

There are numerous statistical tools used to test the suitability of a proposed model as to whether it captures the underlying process adequately. Such techniques include Anderson-Darling, Shapiro –Wilk, Kolmogorov- Smirnov, Hosmer-Lemeshow test and many more. In this work only the Root Mean Square Error (RMSE) and Chi-square statistics ( $\chi^2$ ) are used to test the suitability of the proposed models. RMSE and  $\chi^2$  are presented in (3.1) and (3.2) respectively [*Alonge and Afullo, 2014a*]:

$$\text{RMSE} = \left[ \frac{1}{n} \sum_{i=1}^n (x_i - x'_i)^2 \right]^{\frac{1}{2}} \quad (3.1)$$

$$\chi^2 = \sum_{i=1}^n \frac{(x_i - x'_i)^2}{x_i} \quad (3.2)$$

where  $x_i$ ,  $x'_i$  and  $n$  are the actual dataset, proposed model dataset and sampled population respectively.

The error analysis results produced by equation (3.1) and (3.2) are displayed in Table 3.4 obtained for all the queue parameters and rainfall regimes accordingly. The 5% significant level is chosen as a rejection region. If the null hypothesis is accepted, then 95% of the data generated by the proposed distribution may be considered to be drawn from the actual data. For the service time parameter, the RMSE ranges between 0.7% and 1.1% for all the rainfall regimes, hence the null hypothesis is not rejected as 5% significant level. Additionally, under the  $\chi^2$  test the null hypothesis is not rejected. The standard  $\chi^2$  table of values can be accessed in [1]. In this consideration, the service time for rain rate is proven to be Erlang-k distributed. The inter-arrival time parameter is Erlang-k distributed with a RMSE that varies between 1.4% and 2.4% for all the rainfall regimes. Hence at 5% significant level the null hypothesis is not rejected. Therefore, the arrival process of rainfall rate spikes in Durban at 30-second sampling time is best described by an Erlang-k distribution. The overlap time exponential distribution error analysis shows that its RMSE varies between 1.2% and 3.9% regardless of the rain regime. Also, the  $\chi^2$  values are less than 5% significant threshold. Thus, the null hypothesis is accepted. Conclusively, the Erlang-k distribution best describes the behavior of the service and inter-arrival of the actual rainfall data, whereas the exponential distribution describes the overlap time parameter at 30-second sampling time in Durban.

Lastly, the overall queue parameters' RMSE ranges between 0.6% and 3.5%, which makes the null hypothesis acceptable at 5% significant level. Also by applying  $\chi^2$ , the null hypothesis is not rejected at 5% significant level. Therefore, the overall service and inter-arrival times are Erlang-k distributed, whereas the overall overlap time is exponential distributed. Hence, all the three overall queue parameters belong to the same family of distributions. In conclusion, at 30-second sampling the rainfall process follows a non-Markovian process ( $E_k/E_k/s/\infty/FCFS$ ) in Durban.

### 3.4 Investigation of the Number of Servers

The queue system performance is highly dependent on one of the queue parameters called number of servers. This parameter is vital for the analysis of the steady state stability of the queue system. For the system to reach stability, it is required to satisfy steady-state criterion [Bolch et. al, 1998; Hillier and Lieberman, 2001]:

$$\rho = \left( \frac{\lambda_a}{S\mu_s} \right) \leq 1 \quad (3.3)$$

where  $\rho$  is called the utilization factor.

**TABLE 3.4:** PROPOSED QUEUE PARAMETERS DISTRIBUTION ERROR INVESTIGATION

QUEUE PARAMETER	RAINFALL REGIME	PROPOSED MODEL	REGIME RMSE	REGIME $\chi^2$	DEGREE OF FREEDOM (DF)	SIGNIFICANT LEVEL (SL)
SERVICE TIME	DRIZZLE	<i>Erlang-k</i>	0.009	0.1264	664	762.66
	WIDESPREAD	<i>Erlang-k</i>	0.007	0.102	592	658.09
	SHOWER	<i>Erlang-k</i>	0.011	0.392	555	658.09
	T/STORM	<i>Erlang-k</i>	0.008	0.166	185	217.74
INTER-ARRIVAL TIME	DRIZZLE	<i>Erlang-k</i>	0.024	0.089	515	553.13
	WIDESPREAD	<i>Erlang-k</i>	0.016	0.196	499	553.13
	SHOWER	<i>Erlang-k</i>	0.021	0.091	503	605.67
	T/STORM	<i>Erlang-k</i>	0.014	0.206	149	178.49
OVERLAP TIME	DRIZZLE	<i>Exponential</i>	0.012	0.074	515	605.67
	WIDESPREAD	<i>Exponential</i>	0.039	0.077	499	553.13
	SHOWER	<i>Exponential</i>	0.033	0.102	503	605.67
	T/STORM	<i>Exponential</i>	0.020	0.041	149	178.49

**TABLE 3.5:** PROPOSED OVERALL QUEUE PARAMETERS DISTRIBUTION ERROR INVESTIGATION

PARAMETERS	PROPOSED MODEL	OVERALL RMSE	OVERALL $\chi^2$	DF	SL
SERVICE TIME	<i>Erlang-k</i>	0.006	0.147	1999	1074.8
INTER-ARRIVAL TIME	<i>Erlang-k</i>	0.021	0.800	1669	1074.8
OVERLAP TIME	<i>Exponential</i>	0.035	0.079	1669	1074.8

**TABLE 3.6: THE MINIMUM NUMBER OF SERVERS FOR THE FOUR  
RAINFALL REGIMES**

<i>MINIMUM NUMBER OF SERVERS</i>				
<b>Sampling Time</b>	<b>Drizzle</b>	<b>Widespread</b>	<b>Showers</b>	<b>Thunderstorm</b>
30 Seconds	3	2	3	2

Applying (3.3) on the rainfall queue discipline at 30-second sampling ( $E_k/E_k/s/\infty/FCFS$ ) for each regime, it is found that the system will not reach the stability ( $\rho > 1$ ) under a single server. However, the system can still be investigated in terms of the number of servers required for to reach stability. Therefore, the minimum number of servers ( $s_{min}$ ) required for a queue system to reach stability must satisfy the following condition [Alonge and Afullo, 2014b]:

$$s_{min} \geq \text{ceil} \left( \frac{\lambda_a}{\mu_s} \right) \quad (3.4)$$

where  $\text{ceil}$ ,  $\lambda_a$  and  $\mu_s$  denote the smallest integer returned greater or equal to the expression in the brackets, arrival and service rate respectively.

For each regime the minimum number of servers required is presented in Table 3.6. It is found that the produced queue system only needs two servers for widespread and thunderstorm, and three servers for drizzle and shower to reach system stability.

### **3.5 Investigation of the Relationship between the Overall Number of Spikes and Event Duration**

The overall number of rainfall spikes collected for this study is 2000, extracted from 378 rainfall events. Results from fitting provide clear evidence of the relationship between the number of rainfall spikes ( $N$ ) and rainfall events duration ( $T_S$ ) as shown in Figure 3.5. This relationship can be interpreted by a power law as follows

$$T_S = \alpha N^\beta \quad (3.4)$$

where  $\alpha$  and  $\beta$  are the power law coefficients.

By collecting all the rainfall spikes across all rainfall events and fitting the event count against their corresponding event duration using the power law relationship in EXCEL, the power law coefficients in equation (3.4) are obtained. Table 3.7 and Figure 3.5 presents the fitted power law relationship which exists

between the overall number of rainfall spikes and their respective event durations, where the convergent coefficients ( $\alpha$ ,  $\beta$ ) are (6.7915, 1.1369) respectively.

**TABLE 3.7:** RELATIONSHIP BETWEEN THE NUMBER OF RAINFALL SPIKES AND RAINFALL EVENTS  
DURATION

Rainfall Regimes	$\alpha$	$\beta$	Average Events Duration (minutes)	Number of Events	Number of Spikes
Drizzle	6.4664	1.0917	40.61	151	665
Widespread	6.9996	1.149	60.98	104	593
Shower	9.1652	1.0583	82.92	92	556
Thunderstorm	7.8793	1.1268	70.83	34	186
Overall	6.7915	1.1369	59.03	378	2000

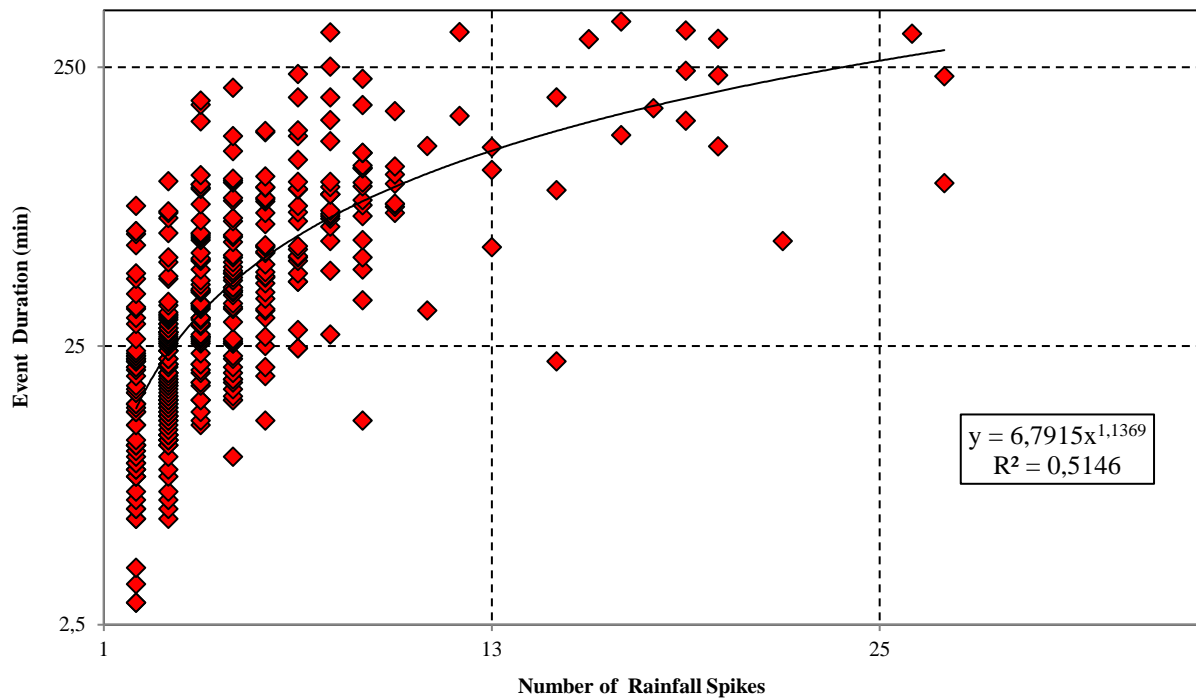


*Figure 3.5: Relationship between the Overall Number of Rainfall Spikes and Rainfall Duration.*

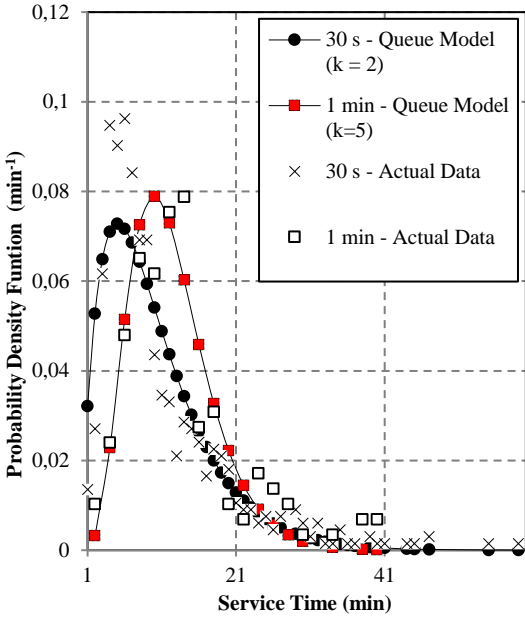
Additionally, Table 3.7 also presents the regime-based results. The average events duration results indicate that the shower regime is characterized by prolonged events compared to other rainfall regimes, which corroborates the results found earlier under the service time queue parameter.

### **3.6 Comparison of the Rainfall Queue Parameters at 30-second and 1 minute Sampling Time**

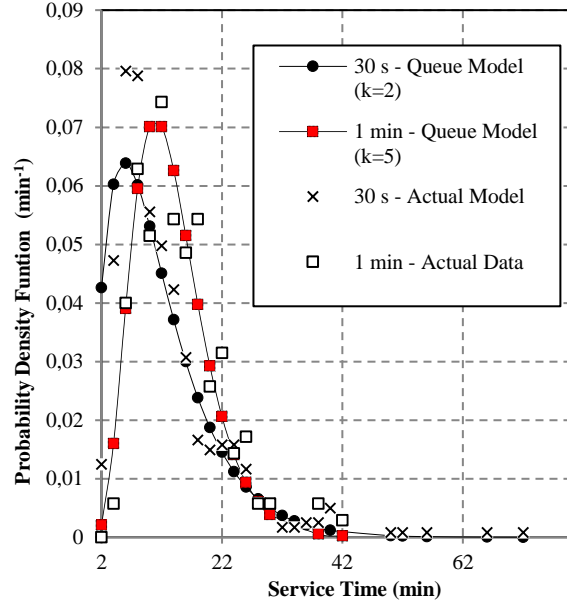
The queueing theory approach in modeling of the rainfall behavior at 1-minute sampling time over radio links in Durban was pioneered by [Alonge and Afullo, 2014a]. Similarly, by applying the queueing theory approach on the 30-second sampled data in Durban, improved results have been obtained in this current work. This presents an opportunity to study the effects of sampling time on rainfall queues by comparing queue parameters at 30-second and 1-minute sampling.

#### **3.6.1 Service Times**

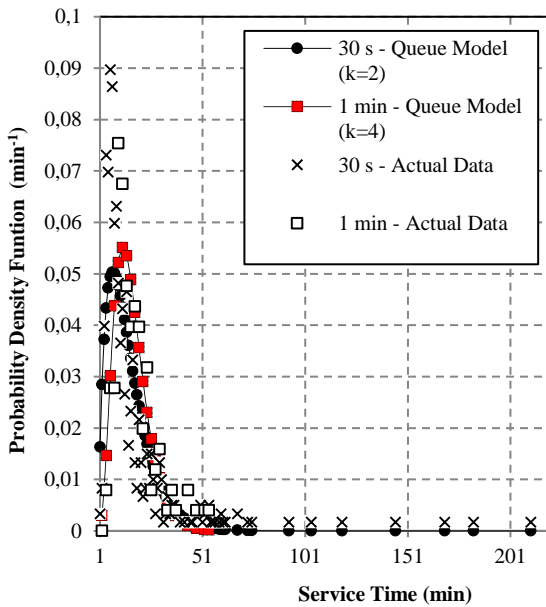
The simulation and modeling results of the rainfall queue parameters at 30-second and 1 minute sampling times in Durban are shown in Table 3.2 and Table 2.2 respectively. The results show that the service time parameter at both 30-second and 1-minute is Erlang-k distributed, as also seen graphically in Figure 3.6. The number of stages increases as the rain rate increases from drizzle to thunderstorm at 30-second sampling while the opposite is true at 1-minute sampling. Distinctly, the thunderstorm regime at 30-second and 1-minute sampling has the same number of stages. The average service time at 30-second sampling gradually increases from drizzle to shower regime, hence the shower regime possesses the highest average service time,  $\bar{t}_s = 14.6 \text{ min}$ , compared to all other regimes. At 1-minute sampling, the regime which possesses the highest average service time,  $\bar{t}_s = 20.4 \text{ min}$ , is the thunderstorm regime. The spikes service rates at 30-second sampling gradually decreases from drizzle to shower regime. Therefore, the drizzle regime has the highest service rate,  $\mu_s = 0.099 \text{ spikes/min}$ , compared to all other regimes. Also at 1-minute sampling, service rates were found to be gradually decreasing from drizzle to thunderstorm regime. Drizzle has the highest service rate of  $\mu_s = 0.081 \text{ spikes/min}$ . For both the 30-second and 1-minute sampling, drizzle rainfall has the highest service rates. In general, drizzle rainfall spikes are the most frequent in Durban regardless of the sampling time employed. Moreover, it is observed that each rainfall regime at 30-second sampling is characterized by higher service rates compared to their counterparts at 1-minute sampling. Hence at 30-second sampling more rainfall spikes are identified.



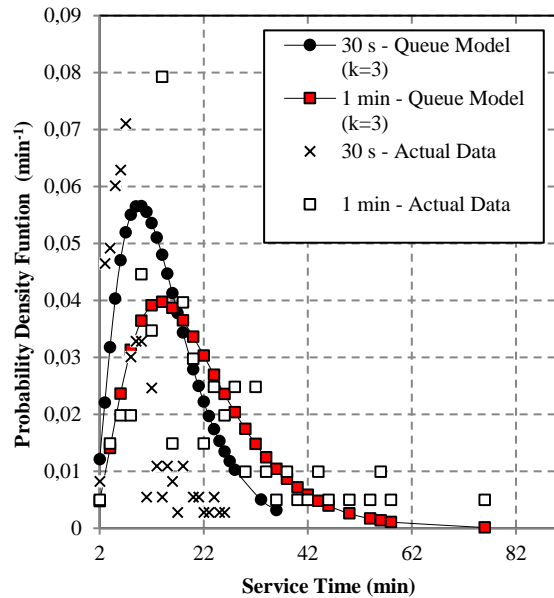
a) Drizzle



b) Widespread



c) Shower



d) Thunderstorm

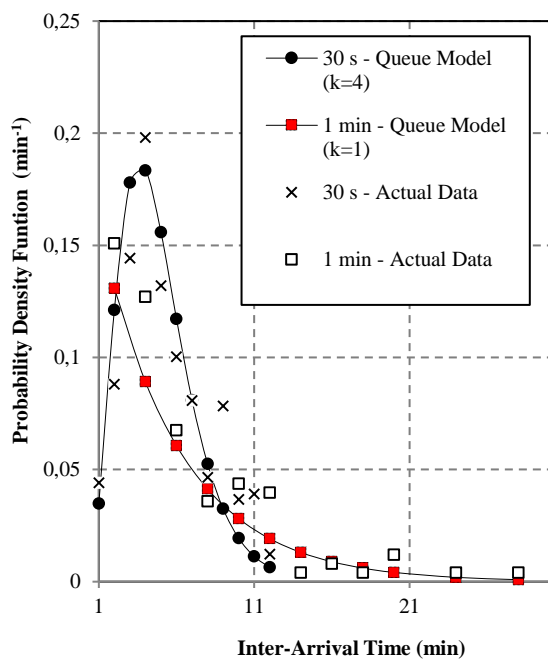
**Figure 3.6:** Plots of the Proposed Queue Models and Actual Data Sets for the Service Time at 30-Second and 1-min Sampling Time According to the Regimes.

1) 30 s Queue Model  $\rightarrow$  Erlang- $k$  Distribution.

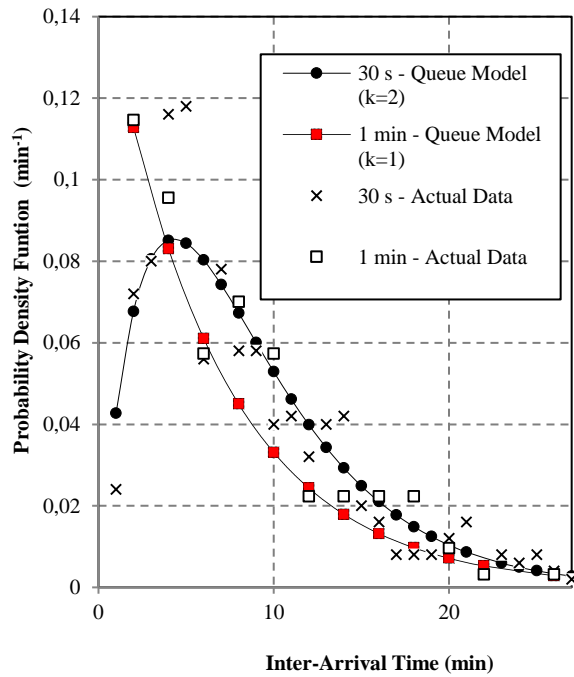
2) 1-min Queue Model  $\rightarrow$  Erlang- $k$  Distribution.

### 3.6.2 Inter-Arrival Times

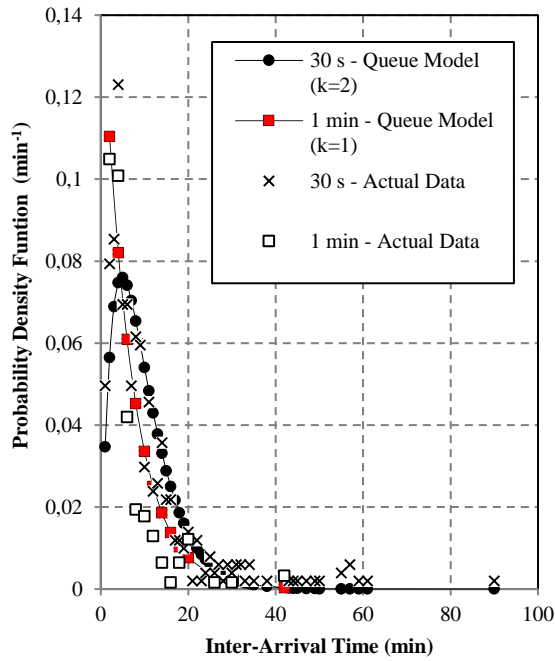
The inter-arrival time is Erlang-k distributed at 30-second sampling, where  $k = 2$  for all the rainfall regimes except drizzle where  $k = 4$  as shown in Table 3.2 and Figure 3.7. Conversely, at 1-minute sampling the inter-arrival times follow the exponential distribution, which is the special case of Erlang-k distribution, with  $k = 1$ . Thus, the inter-arrival times for both sampling times are of the same probability distribution family with different number of stages. The thunderstorm regime at 30-second sampling has the highest average inter-arrival time,  $\bar{t}_a = 9.1 \text{ min}$ , compared to all other regimes. At 1-minute sampling the average inter-arrival time is gradually increasing from drizzle to thunderstorm regime. Therefore, the thunderstorm regime has the highest average inter-arrival time,  $\bar{t}_a = 10.8 \text{ min}$ , compared to all other regimes. Arrival rates results at 30-second sampling show that during drizzle events there are more rainfall spike arrivals,  $\lambda_a = 0.192 \text{ spikes/min}$ , compared to all other regimes. Similarly, at 1-minute sampling the arrival rate results show that during drizzle events more spike arrivals are expected since it has the highest arrival rate,  $\lambda_a = 0.208$ , compared to all other regimes. Based on the arrival rate results from both sampling times, it is evident that each regime at 30-second sampling has more rainfall spike arrivals compared to their counterparts at 1-minute sampling. This further confirms the results found under the service time parameter that at lower sampling times more rainfall spikes are resolved.



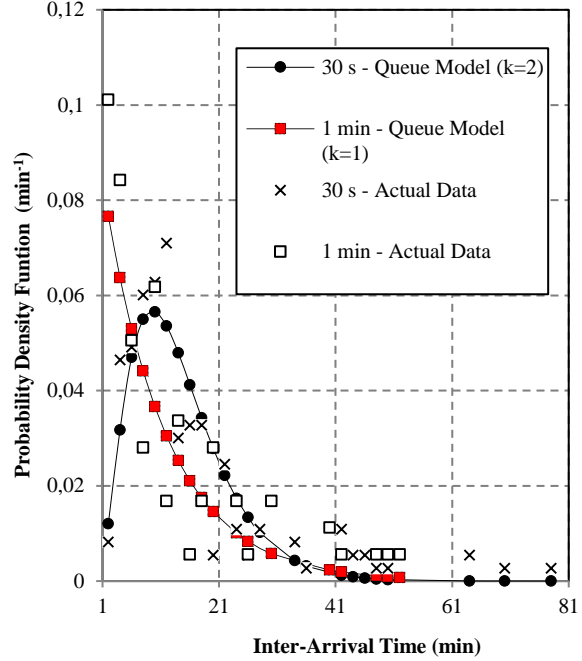
a) Drizzle



b) Widespread



c) Shower



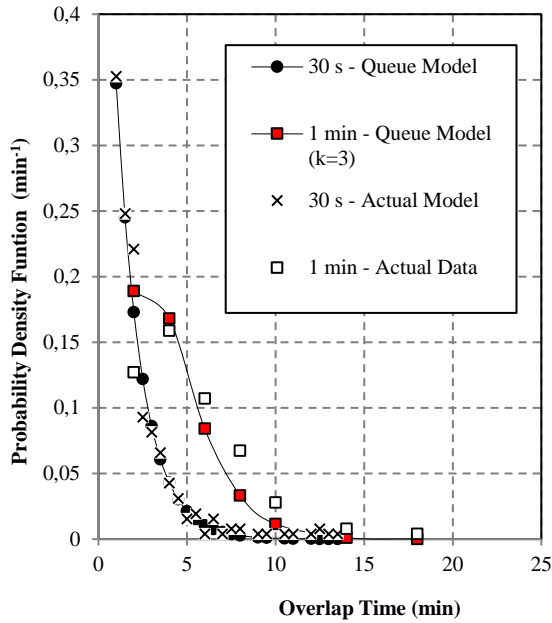
d) Thunderstorm

**Figure 3.7:** Plots of the Proposed Queue Models and Actual Data Sets for the Inter-Arrival Time at 30-Second and 1- min Sampling Time According to the Regimes.

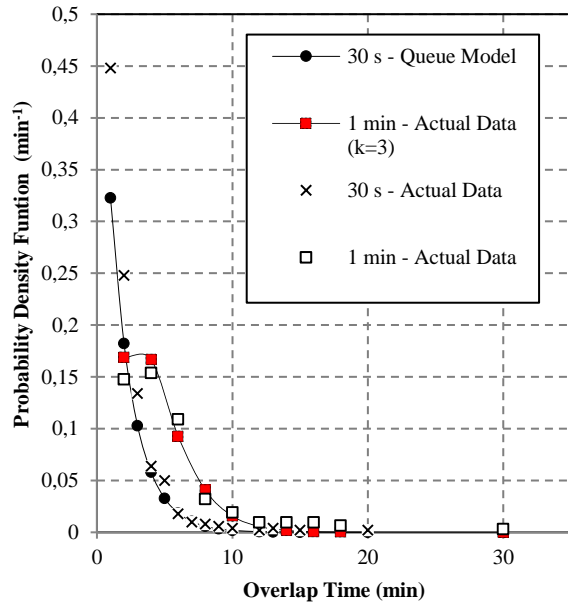
- 1) 30 s Queue Model  $\rightarrow$  Erlang- $k$  Distribution.      2) 1-min Queue Model  $\rightarrow$  Exponential Distribution.

### 3.6.3 Overlap Times

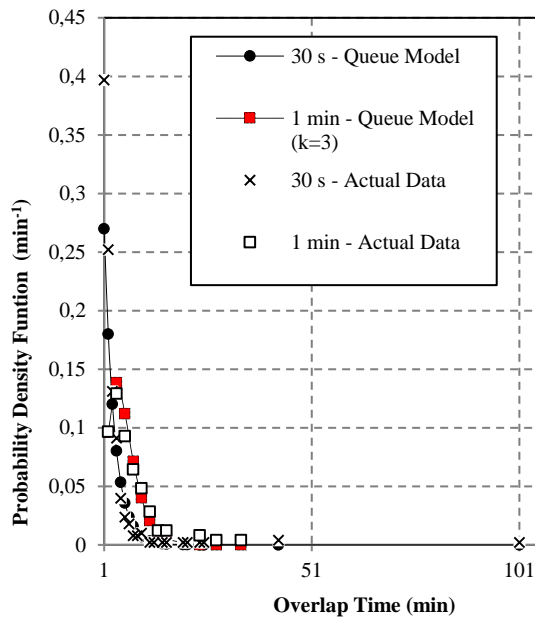
At 30-second sampling, the rainfall spikes overlap time follows an exponential distribution for all the rainfall regimes as shown in Table 3.2 and Figure 3.8. Comparatively, at 1-minute sampling the overlap time parameter follows an Erlang- $k$  distribution with the number of stages,  $k = 3$ . The number of stages is the same for all regimes except thunderstorm regime where  $k = 2$ . At 30-second sampling, the shower regime has the highest average overlap time,  $\bar{t}_o = 2.474 \text{ min}$ , compared to all other regimes. At 1-minute sampling, the spikes average overlap time behavior is similar to that at 30-second sampling in that the shower regime has the highest average overlap time,  $\bar{t}_o = 5.867 \text{ min}$ , compared to other regimes. The results at 30-second sampling show that there is higher overlap rate,  $\delta_o = 0.697 \text{ spikes/min}$ , during the drizzle events. Therefore this corroborates the results found under the 30-second service time parameter where there are more observable rainfall spikes under the drizzle regime, which effectively results in more overlapping spikes. At 1-minute sampling, the overlap rates behave similarly to those at 30-second sampling, the highest overlap rate,  $\delta_o = 0.251 \text{ spikes/min}$ , is found during the drizzle events. Conclusively, the assertion that more rainfall spikes are identified as sampling time decreases still holds,



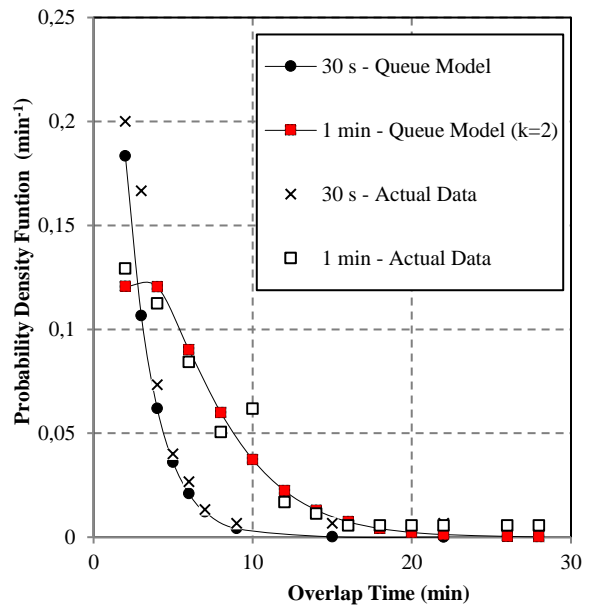
a) Drizzle



c) Widespread



c) Shower



d) Thunderstorm

**Figure 3.8:** Plots of the Proposed Queue Models and Actual Data Sets for the Overlap Time at 30-Second and 1-min Sampling Time According to the Regimes.

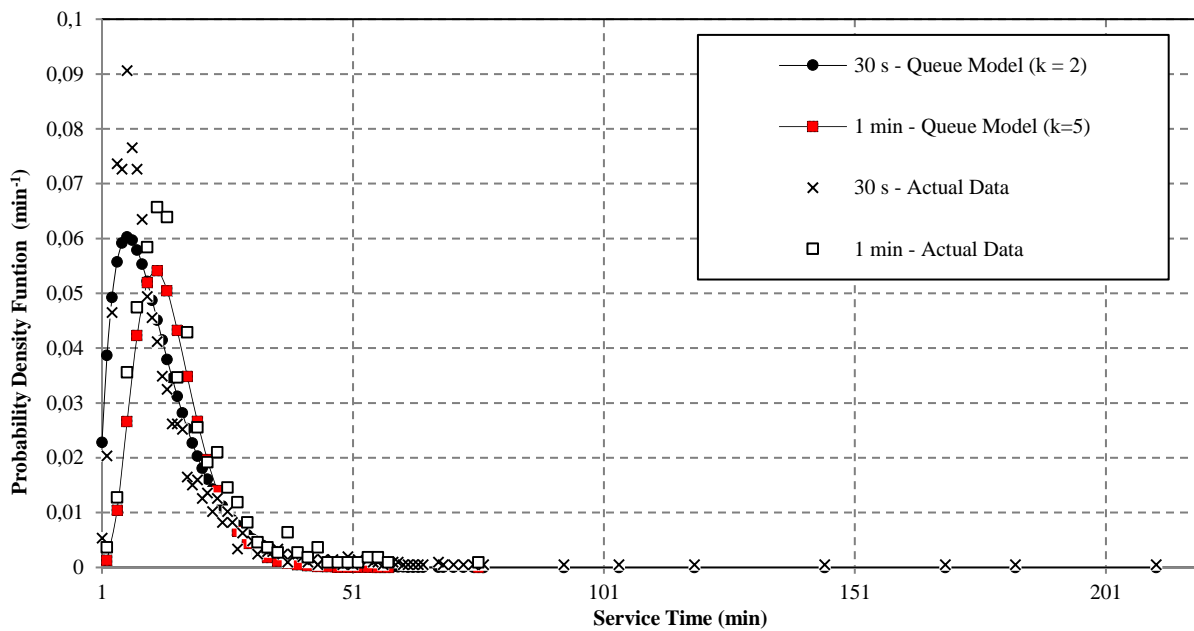
1) 30 s Queue Model  $\rightarrow$  Exponential Distribution.

2) 1-min Queue Model  $\rightarrow$  Erlang-k Distribution.

since more overlapping rain spikes are found at 30-second than at 1-minute sampling. Therefore, all the queue parameter statistics confirm that at lower sampling time more significant rainfall spikes are resolved.

### 3.6.4 Overall Queue Parameters

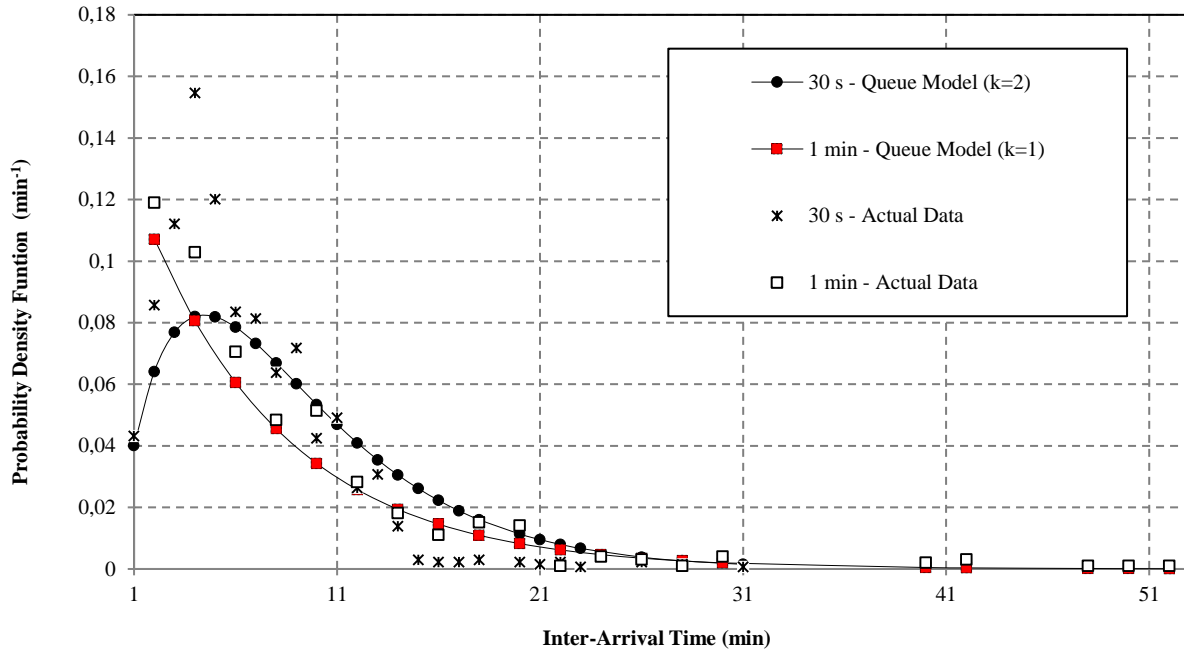
The overall service and inter-arrival times at 30-second sampling are Erlang-k distributed where the number of stages is 2 and 3, respectively; whereas the overall overlap time is exponentially distributed as presented in Table 3.3 and Figure 3.9. With regards to 1-minute sampling, the overall service time and overlap time follow the Erlang-k distribution where the number of stages are 5 and 3, respectively. Conversely, the overall inter-arrival time was found to be exponential distributed [Alonge and Afullo, 2014b]. Therefore, all the overall queue parameters at both sampling times belong to the same family of probability distributions. It is observed that at 30-second sampling the overall average service, inter-arrival and overlap times are lower compared to those at 1-minute sampling. It then follows that the rate parameters for these queue parameters at 30-seconds sampling are higher compared to those at 1-minute sampling. This means that there are more observable rainfall spikes at 30-second sampling than at 1-minute sampling.



a) Overall Service Time

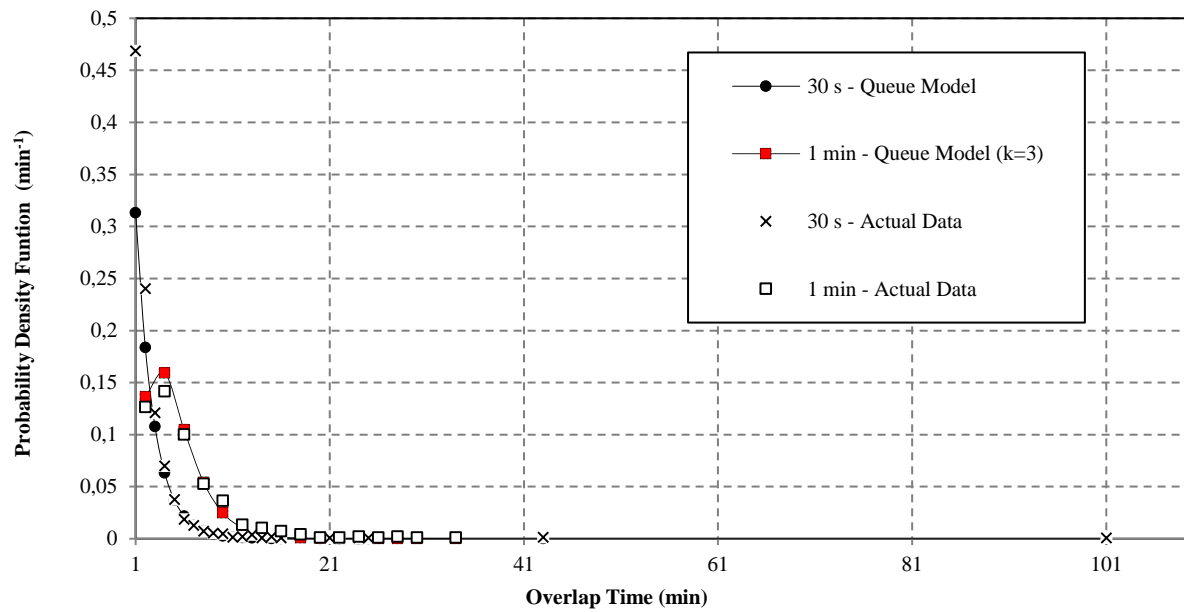
1) 30 s Queue Model → Erlang-k Distribution.

2) 1-min Queue Model → Erlang-k Distribution



b) Overall Inter-Arrival Time

1) 30 s Queue Model  $\rightarrow$  Erlang-k Distribution.    2) 1-min Queue Model  $\rightarrow$  Exponential Distribution



c) Overall Overlap Times

1) 30 s Queue Model  $\rightarrow$  Exponential Distribution.    2) 1-min Queue Model  $\rightarrow$  Erlang-k Distribution

**Figure 3.9:** Plots of the Proposed Queue Models and Actual Data Sets for the Overall Queue Parameters at 30-Second and 1- min Sampling Time According to the Regimes.

### 3.7 Chapter Summary

This chapter shows that in Durban at 30-second sampling rainfall events follow a particular queue pattern, which is a non-Markovian process ( $E_k/E_k/s/\infty/FCFS$ ). The service and inter-arrival times are found to be Erlang-k distributed, whereas the overlap times are exponentially distributed. The inter-arrival time parameter is found to be characterized by the longest average time during thunderstorm events. Drizzle events are found to have many rainfall spike arrivals compared to all other rainfall regimes. However, the average service time parameter has been found to be the longest under the shower regime. This may imply that shower events are more likely to cause network outage at 30-second sampling due to sustained perturbation of the propagation path. The highest average overlap time is found under the shower regime, whereas the highest overlap rate is found under the drizzle regime. The Erlang-k distribution is also found to be the best fit for all the overall queue parameters, except the overall overlap time which is exponentially distributed. When comparing the 30-second and 1-minute data, it is found that the average service time of the rainfall spikes in Durban is between  $10 < t < 21$  minutes regardless of the sampling time. All the queue parameter rates (service, inter-arrival and overlap) at 30-second sampling are higher than those at 1-minute sampling. Thus, more rainfall spikes are identified at 30-second sampling as compared to 1-minute sampling. Conclusively, the 30-second sampling gives more detailed statistical information about rainfall spikes than at 1-minute sampling. Therefore based on these results, we strongly recommend that for better predictions, 30-second sampling must be used as opposed to 1-minute sampling for rainfall data acquisition.

## CHAPTER FOUR

### Long Term Modeling of the Rainfall Spikes at 30-second Sampling Time in Durban

#### 4.1 Introduction

It has been shown in chapter 3 that at 30-second sampling a great deal of detail is achieved as compared to the 1-minute sampling enabling more rainfall rate spikes to be revealed. However, the data obtained from the measurement campaign using 1-minute sampling remains relevant. This work takes advantage of the availability of the two datasets and implements a conversion strategy to map one dataset into the other, thereby expanding the data volume. In this manner, the long term probabilistic characteristics of rainfall may be predicted with improved accuracy at a location. Essentially, the combined data will represent a measurement period spanning sixty six (66) months. It is therefore preferable to convert the 1-minute sampled data to 30-second data primarily because of the variations in detail observed in chapter 3. The significance of long-term modeling is two-fold: 1) network planning requires availability statistics as accurately as possible in order to determine realistic link margins under rainy conditions, 2) many natural processes tend to exhibit self-similarity characteristics, and this property will be assessed herein. The advantage of dealing with self-similar processes emanates from the fact that the fractals of the process may be used to infer the underlying process. Rainfall measurement is a long process that span years with specialized equipment required. Moreover, a suitable location is required for placement of such equipment with ample care necessary for the sensing units as well as safe housing of processing units. Such requirements may prove prohibitive for adequate measurement campaigns over extended periods of time. However, self-similar processes require only a fraction of the time and long-term behavior may subsequently be inferred without long-term measurement which is both time and resource intensive. Therefore, the aim of this chapter is to determine the long-term behavior of rainfall queues at 30-second sampling in Durban.

#### 4.2 Investigation of the Typical Relationship between the 30-second and 1-minute Data

It is generally correct to assume that each and every location is characterized by common weather conditions; hence a relationship will exist between all rainfall datasets obtained from the same location irrespective of the sampling time. Thus, the two datasets used in this study are expected to have some sort of a relationship which can be used to mimic one data generating process given the other. The cumulative distribution function (CDF) is observed as a better tool to use for comparing two data sets, since at each point of the CDF more data population is found than in probability distribution function (PDF). Therefore, this section presents the methodology used to determine the existing relationship between the 30-second and 1-minute data by comparing their CDFs.

**Table 4.1:** COEFFICIENT OF DETERMINATION VALUES ( $R^2$ ) BETWEEN THE 1-MINUTE AND 30-SECOND RAINFALL QUEUE PARAMETERS

REGIME	FUNCTION	SERVICE TIME ( $R^2$ )	INTER-ARRIVAL TIME ( $R^2$ )	OVERLAP TIME ( $R^2$ )
Drizzle	<i>polynomial</i>	0.9914*	0.9914*	0.9354*
	<i>linear</i>	0.9714	0.9037	0.4909
Widespread	<i>polynomial</i>	0.9989*	0.9805*	<b>0.9997*</b>
	<i>linear</i>	0.9582	0.9304	0.9939
Shower	<i>polynomial</i>	<b>0.9997*</b>	0.9933*	0.9982*
	<i>linear</i>	0.9581	0.7467	0.9075
Thunderstorm	<i>polynomial</i>	0.9992*	<b>0.9975*</b>	0.9992*
	<i>linear</i>	0.9674	0.9893	0.9481
<b>OVERALL PARAMETERS</b>	<i>polynomial</i>	<b>0.999*</b>	<b>0.9974*</b>	<b>0.9998*</b>
	<i>linear</i>	0.9563	0.9964	0.9679

{\* denote the lowest error statistics} and {Bold - denote the lowest error statistics amongst the queue parameters}

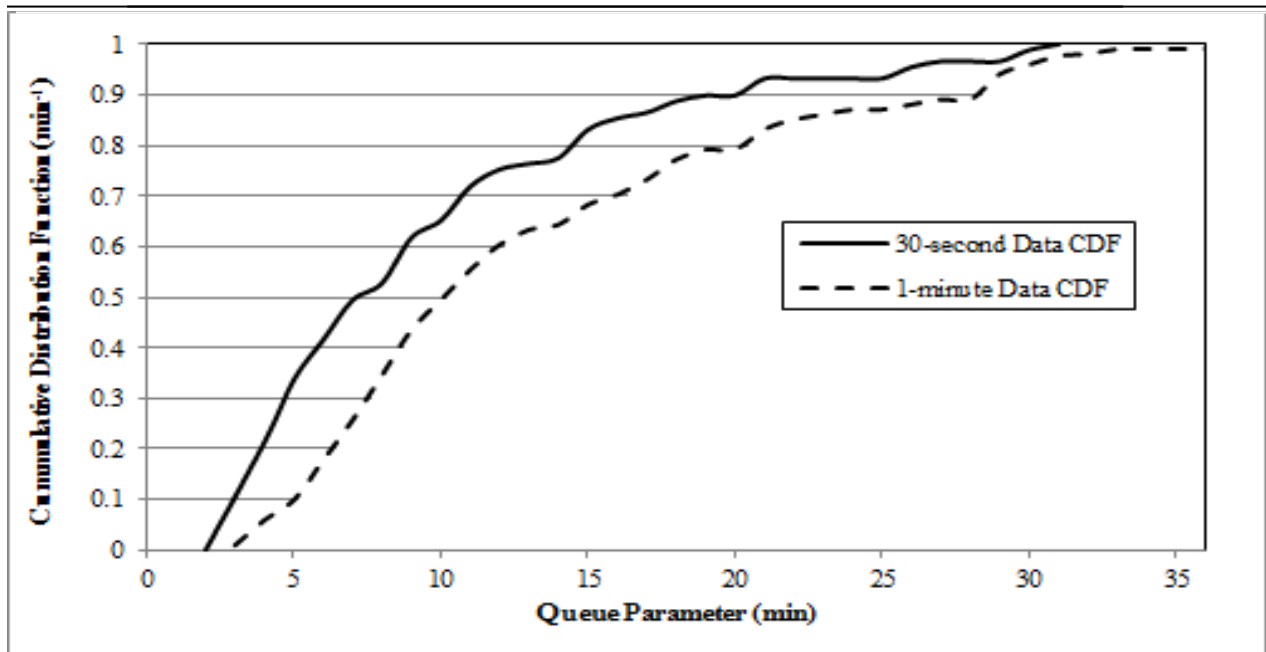


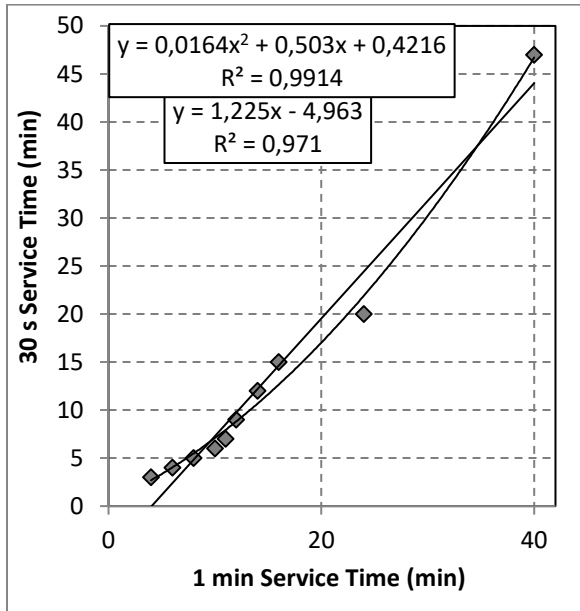
*Figure 4.1: Comparison Procedure of the 30-second and 1-minute Cumulative Distribution Functions (CDFs)*

The procedure used for developing the relationship between the two rainfall datasets is as follows: For each queue parameter for both the 30-second and 1-minute sampled data in each rainfall regime, the CDFs are compared. The comparison is made for 10 corresponding equally spaced percentage points of the CDFs as demonstrated in Figure 4.1. Obviously the accuracy can be improved by choosing a fine discretization of the percentage values but the chosen step-size is adequate. The datasets sampled from the two CDFs are then plotted against each other, with the 1-minute data on the x-axis and the 30-second data on the y-axis as shown in Figure 4.2 through 4.5. In this way, a pairwise plot is obtained and the relationship between the two datasets may be determined. Microsoft Excel is used to plot the data points and its trend line feature is used to find the best fit relationship that exists between the 30-second and the 1-minute queue parameters. It turns out that, at a glance, the polynomial and linear functions are best suited to describe the relationship between these two data sets. However, by evaluating the coefficient of determination ( $R^2$ ) in each case, it was found that the polynomial function best describes the existing relationship between the 30-second and 1-minute queue parameters as shown in Table 4.1. The identified polynomial is of second order and its general representation may be given as:

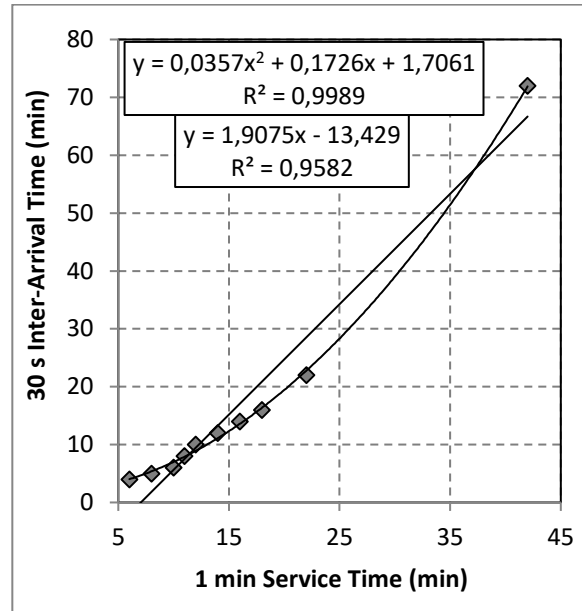
$$T_{30s} = a_1 T_{1min}^2 + a_2 T_{1min} + a_3 \quad \text{where } (a_1, a_2, a_3) \in \mathbb{R}, \quad (4.1)$$

where  $T_{1min}$ ,  $T_{30s}$  and  $(a_1, a_2, a_3)$  are 1 minute data, 30 second data and polynomial coefficients respectively.

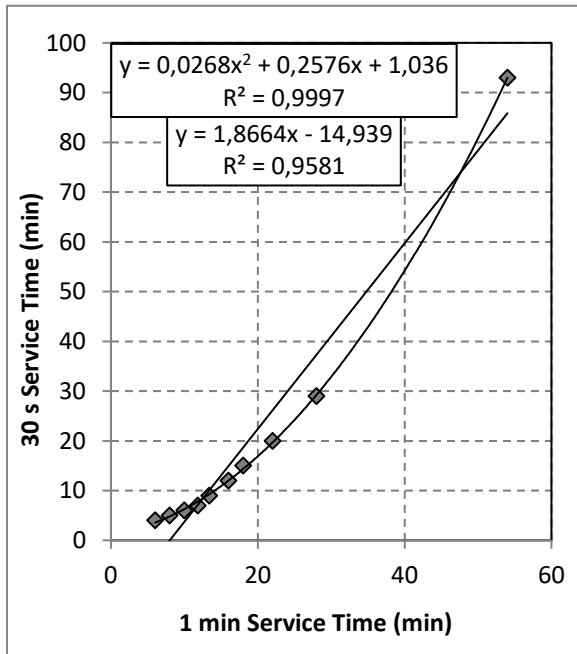
It is noticeable that a linear fit also results in a high correlation coefficient in most cases but it is still outperformed by the polynomial fit in all cases without exception. In fact the linear fit performs rather poorly in the case of inter-arrival time for both drizzle and shower regimes. We take interest in the linear function because the polynomial function has a relatively slow curvature due to the small values of the  $a_1$  coefficients. In some cases this coefficient approaches zero and thus may be approximated as a first order polynomial (linear). Considering the inherent errors introduced by the discretization of the CDFs, the slight curvatures introduced by the second order polynomial will be considered significant. The highest  $R^2$  obtained for each queue parameter across all rainfall regimes is shown in Table 4.1 in bold font. This translates into greater confidence in terms of the modeled relationship between the two datasets for the corresponding rain regimes. However, the validity of the relationship for other rain regimes is by no means poor as the minimum correlation coefficient recorded across all rain regimes and for all queue parameters is 0.9354. The relationship between the queue parameters is also evaluated for the overall case (regime-independent), and again, the polynomial fit performs better than the linear fit as shown in Figure 4.5 and Table 4.1. The lowest correlation coefficient of 0.9974 across all queue parameters is observed



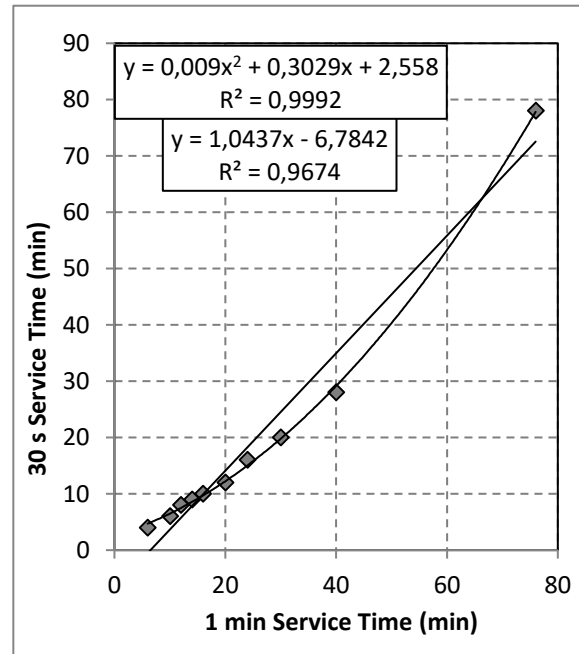
a) Drizzle



b) Widespread

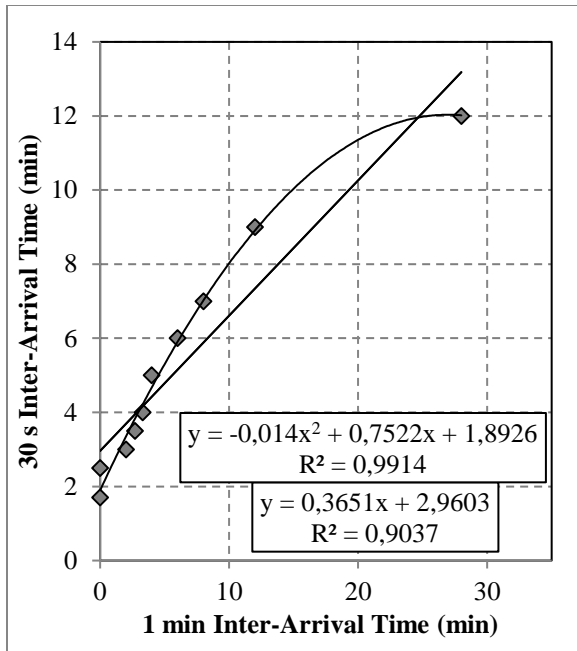


c) Shower

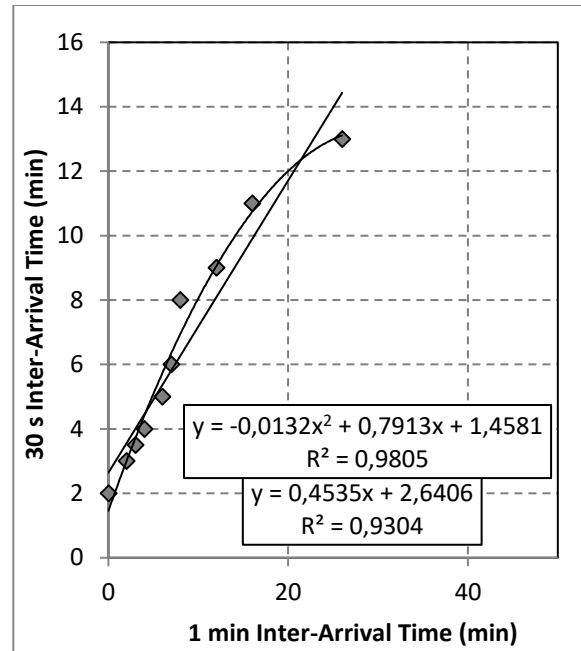


d) Thunderstorm

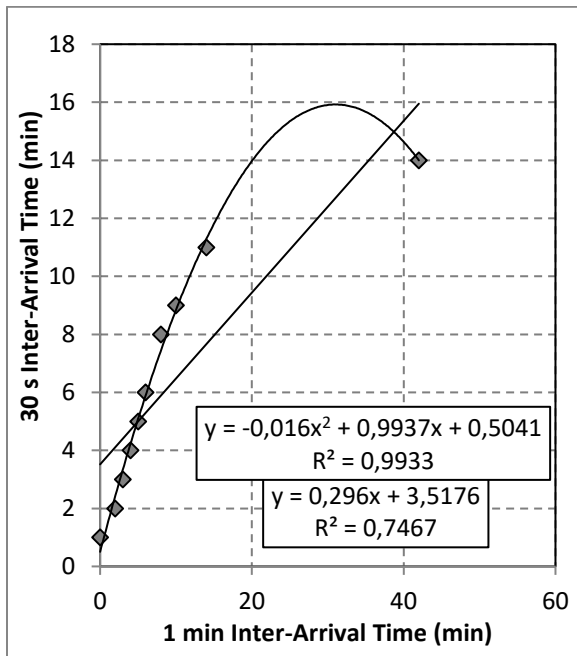
Figure 4.2: Relationship between the Regime Service Times of the 1-minute and 30-second Data.



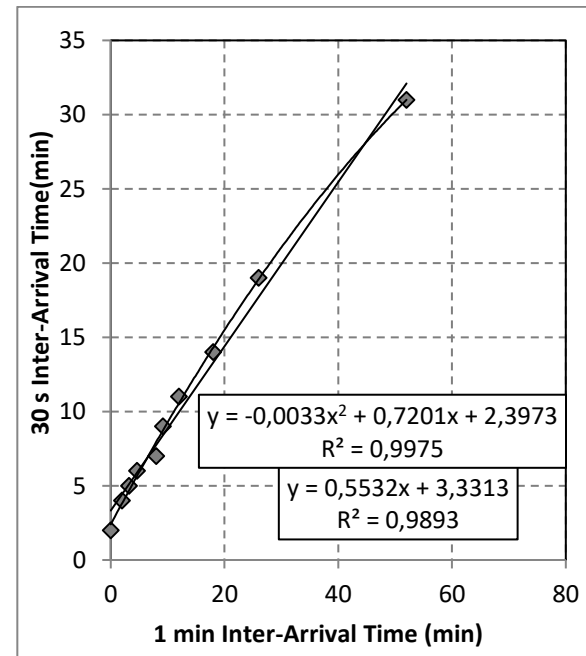
a) Drizzle



b) Widespread

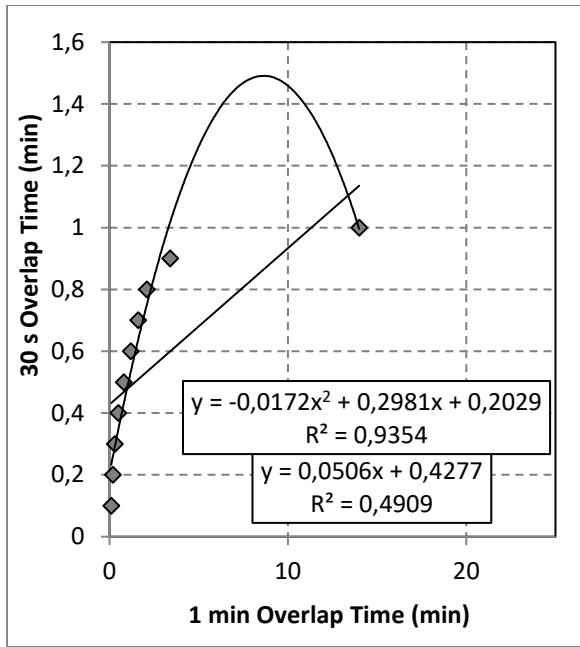


c) Shower

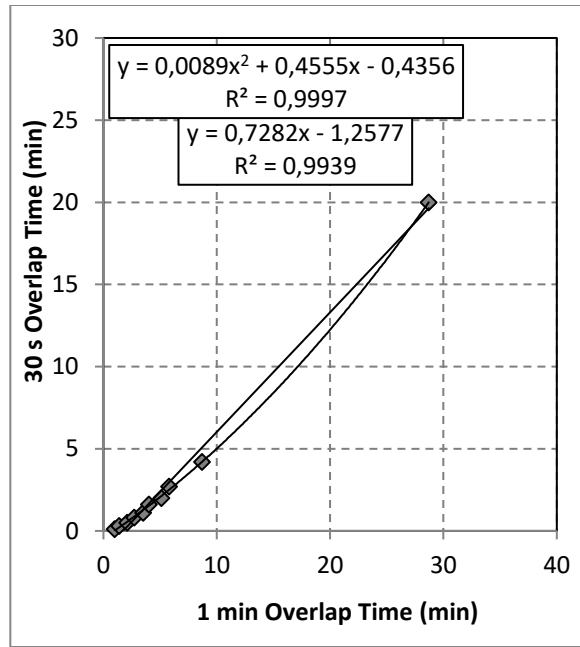


d) Thunderstorm

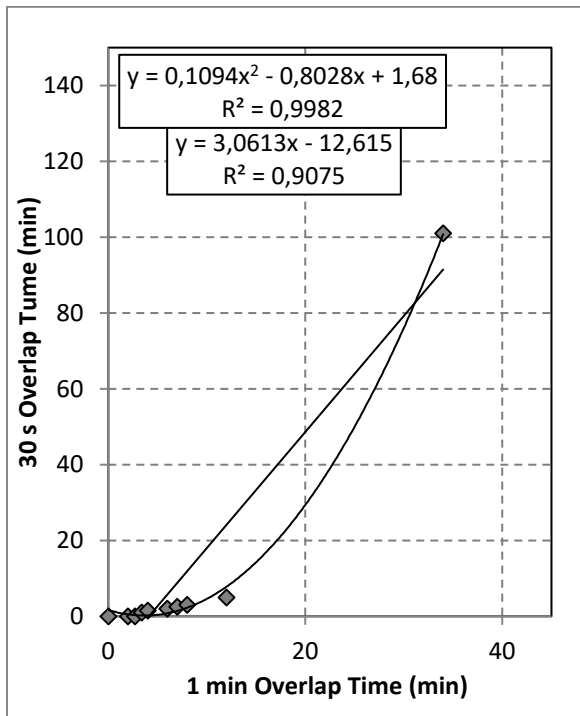
Figure 4.3: Relationship between the Regime Inter-Arrival Times of the 1-minute and 30-second Data.



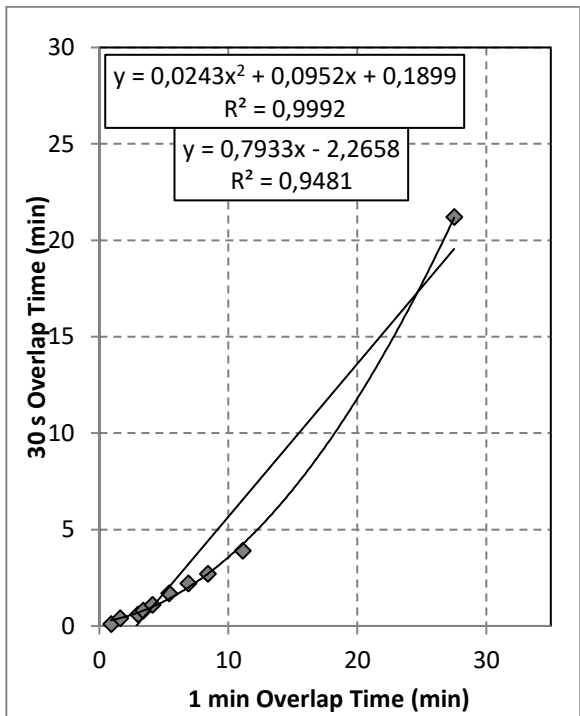
a) Drizzle



b) Widespread



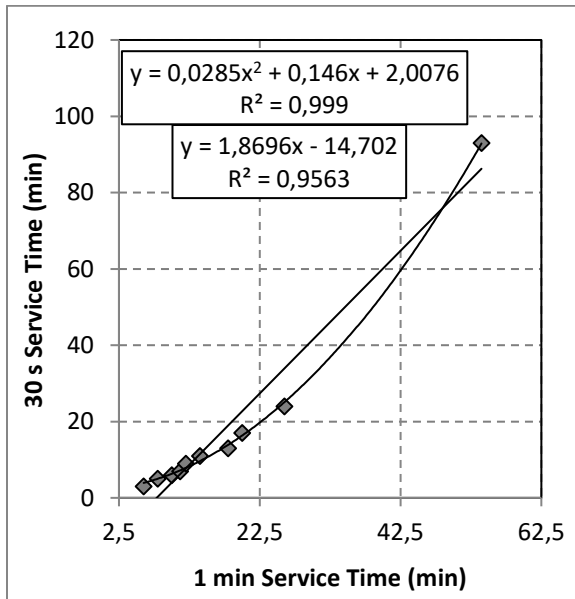
c) Shower



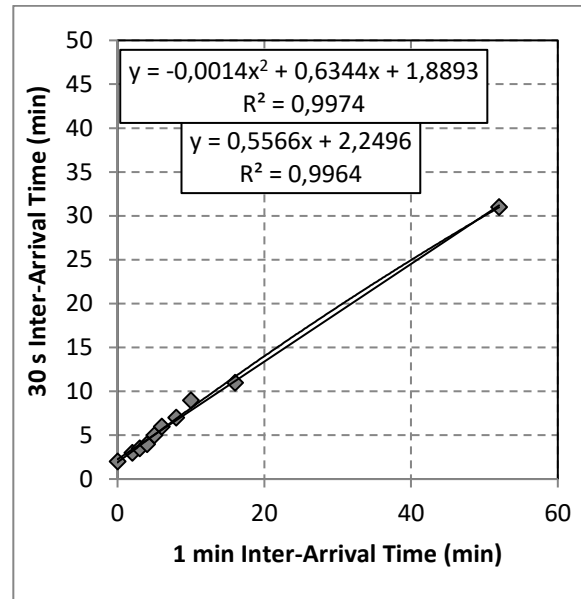
d) Thunderstorm

**Figure 4.4:** Relationship between the Regime Overlap Times of the 1-minute and 30-second Data.

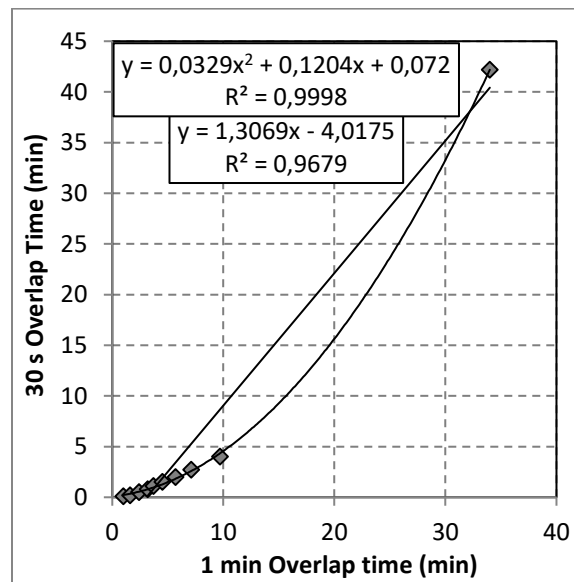
under the inter-arrival time. With such high correlation coefficients, it is reasonable to conclude that the conversion between the 1-minute and 30-second sampled data in Durban may be achieved by employing a univariate second-order polynomial function.



a) Overall Service Times



b) Overall Inter-Arrival Times



a) Overall Overlap Times

**Figure 4.5:** Relationship between the Overall Queue parameters of the 1-minute and 30-second Data.

**Table 4.2:** MODELING RESULTS OF THE CONVERTED RAINFALL QUEUE PARAMETERS FROM 1-MINUTE TO 30-SECOND SAMPLING TIME

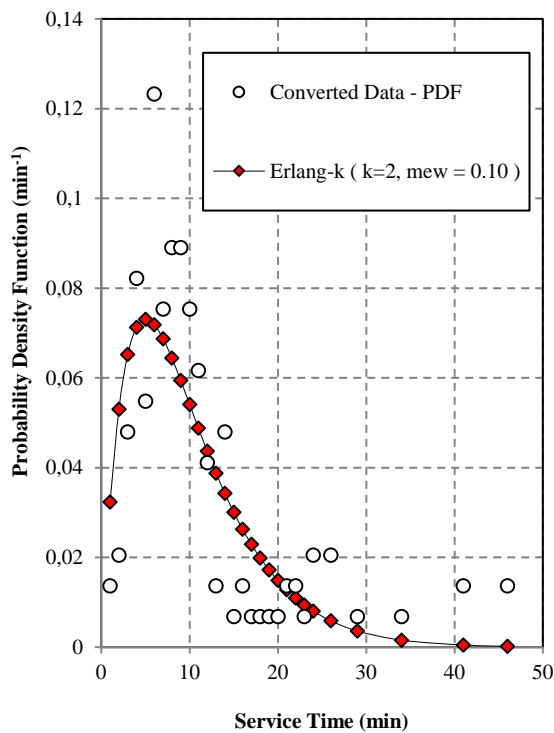
QUEUE PARAMETER	REGIME	AVERAGE TIME ( $\bar{t}_s$ )	RATE PARAMETER ( $\mu_s$ )	NUMBER OF STAGES ( $k$ )
SERVICE TIME	Drizzle	10.07	0.10	2
	Widespread	12.36	0.08	3
	Shower	14.72	0.07	2
	Thunderstorm	14.20	0.07	3
QUEUE PARAMETER	REGIME	AVERAGE TIME ( $\bar{t}_a$ )	RATE PARAMETER ( $\lambda_a$ )	NUMBER OF STAGES ( $k$ )
INTER-ARRIVAL TIME	Drizzle	5.08	0.20	5
	Widespread	5.55	0.18	3
	Shower	5.71	0.18	3
	Thunderstorm	9.38	0.11	2
QUEUE PARAMETER	REGIME	AVERAGE TIME ( $\bar{t}_o$ )	RATE PARAMETER ( $\sigma_o$ )	NUMBER OF STAGES ( $k$ )
OVERLAP TIME	Drizzle	1.80	0.56	1
	Widespread	2.10	0.48	1
	Shower	3.72	0.27	1
	Thunderstorm	2.91	0.34	1

### 4.3 Modeling Results of the Converted Queue Parameters

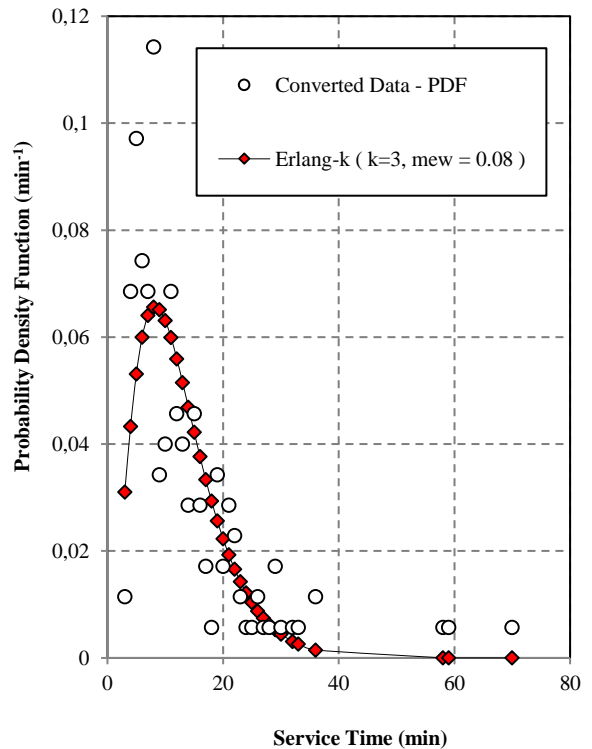
In the event that the 1-minute data has successfully been converted into the 30-second data, it is necessary to validate the conversion technique itself. High correlation coefficients do not prove that the conversion methodology is appropriate but rather provide information about the closeness of a quantity to a model function. In a top-down manner, the idea is to work backwards and prove that the resultant relationship is indeed capable of reproducing the statistical behavior of the 30-second data given the 1-minute data. The polynomial coefficients,  $(a_1, a_2, a_3)$ , in (4.1) have been determined for all the queue parameters under different rain regimes. By substituting these coefficients accordingly, the second-order polynomial becomes the data generating function for which the ‘new’ 30-second sampled data is generated. The goodness of this ‘new’ generated data lies in its statistical characteristics in comparison with those of the measured data. Accordingly, a statistical error test will be performed to confirm the validity of the conversion technique. As previously done, the validity of the conversion will be assessed on both regime-based and overall queue parameters.

### 4.3.1 Service Time

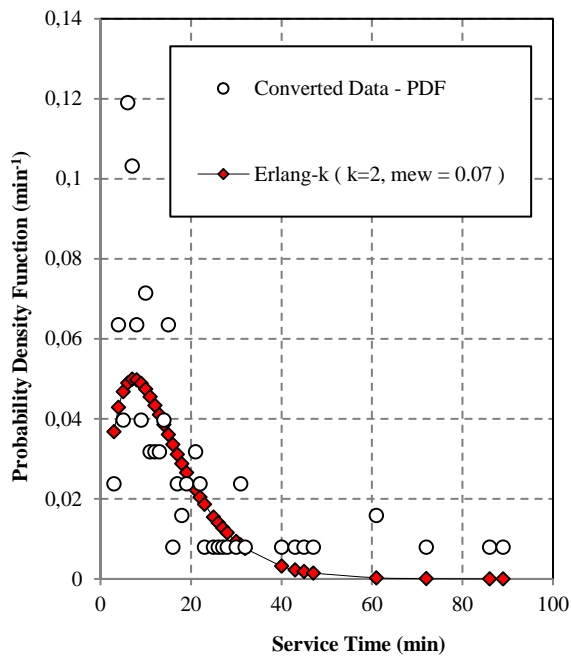
The 30-second sampling data obtained by conversion follows the Erlang-k distribution with either 2 or 3 number of stages across all rainfall regimes as shown in figure 4.6. The shower regime is characterized by the longest average service time,  $\bar{t}_s = 14.72 \text{ min}$ , while the drizzle regime has the highest service rate,  $\mu_s = 0.10 \text{ spikes/min}$ , compared to all other regimes. In the original 1-minute data the average service times are 12.38, 13.71, 16.26 and 20.44 for drizzle, widespread, shower and thunderstorm respectively [Alonge and Afullo, 2014a]. In comparison, it is evident that the average service time has reduced in the converted data e.g. from 16.26 min to 14.72 min for the shower regime. The same is true for all the rainfall regimes as shown in Table 4.2. This can be attributed to the fact that there is now more clarity in terms of distinguishing between rainfall spikes, resolving ambiguous portions of the rain rate time series which was previously not possible. The benefit of a higher sampling rate is evident and thus an improved accuracy in the modeling process is expected.



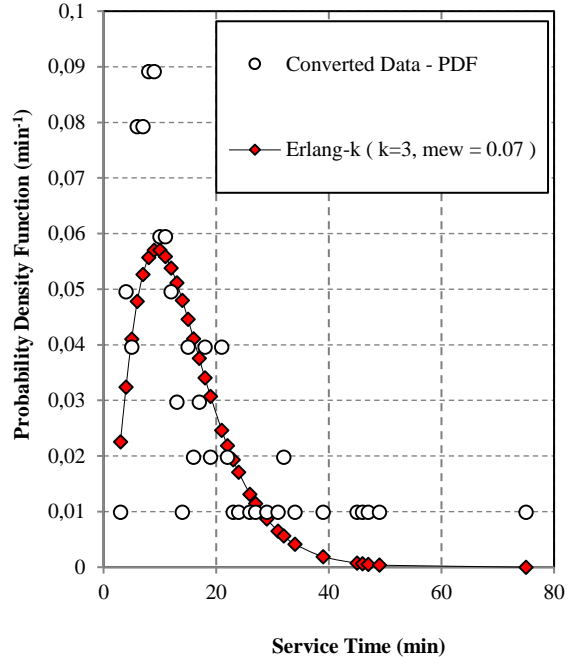
a) Drizzle



b) Widespread



c) Shower

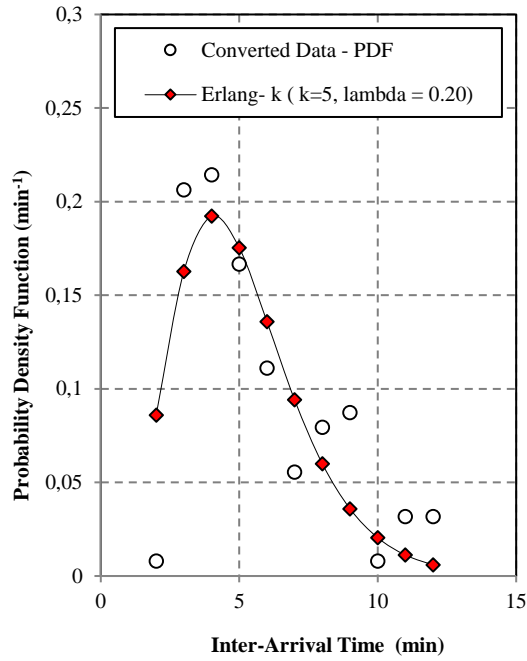


d) Thunderstorm

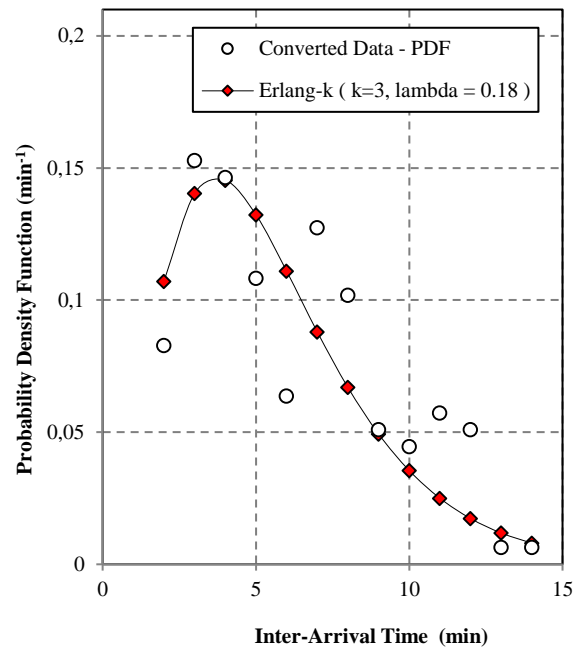
**Figure 4.6:** Converted regime service time PDFs of the actual and simulated data.

### 4.3.2 Inter-Arrival Time

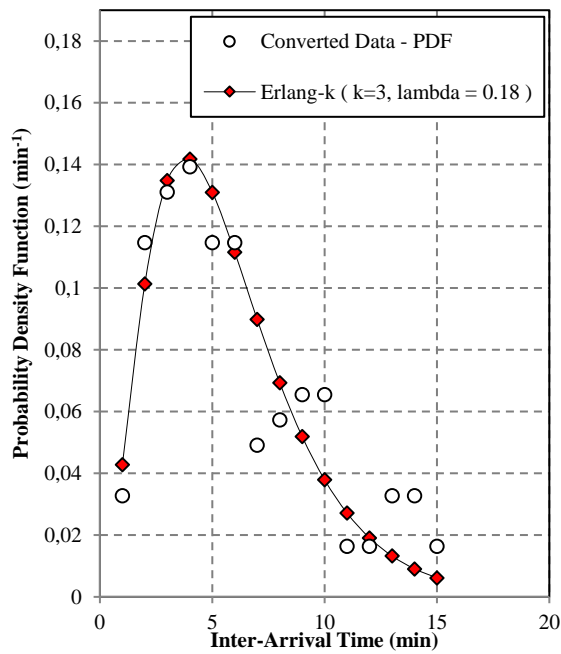
Figure 4.7 and Table 4.2 present the simulation and modeling results of the converted inter-arrival time data. The results show that the inter-arrival time is Erlang- $k$  distributed, where the number of stages is in the range  $2 \leq k \leq 5$  for all the rainfall regimes. The longest average inter-arrival time,  $\bar{t}_a = 9.38 \text{ min}$ , is found under the thunderstorm regime. Drizzle is found to have the highest arrival rate,  $\lambda_a = 0.20 \text{ spikes/min}$ , compared to all other rainfall regimes. Hence more rainfall spikes are expected during the drizzle events as compared to other regimes over a fixed period of time. In the original 1-minute data, the average inter-arrival times were found to be 5.08, 6.52, 6.73 and 10.85 for drizzle, widespread, shower and thunderstorm respectively [Alonge and Afullo, 2014a]. The lower average inter-arrival times found using the converted data imply higher arrival rates. Thus, over a fixed period of time more arrivals will be recorded as compared to that under the 1-minute sampled data. The lack of good resolution in the 1-minute sampling makes it difficult to tell some of the spikes apart if their arrival is separated by small amount of time. Such spikes are often considered as a single spike during data processing, which reduces the number of spikes recorded and results in increased average service time as seen under sub-section 4.3.1.



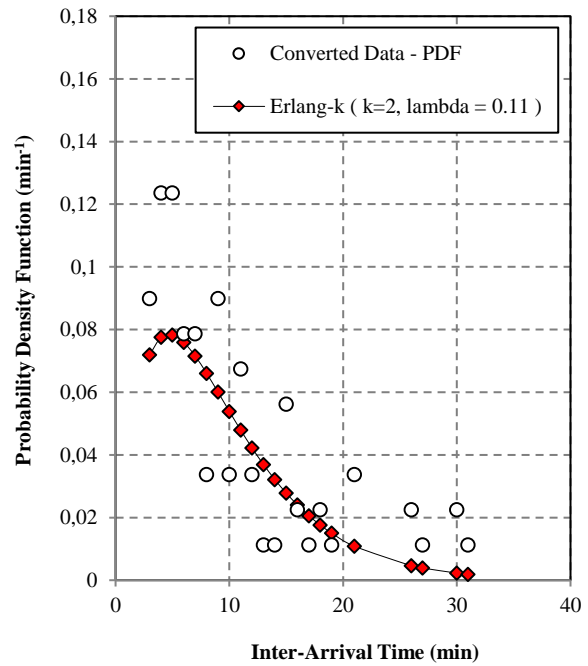
a) Drizzle



b) Widespread



c) Shower



d) Thunderstorm

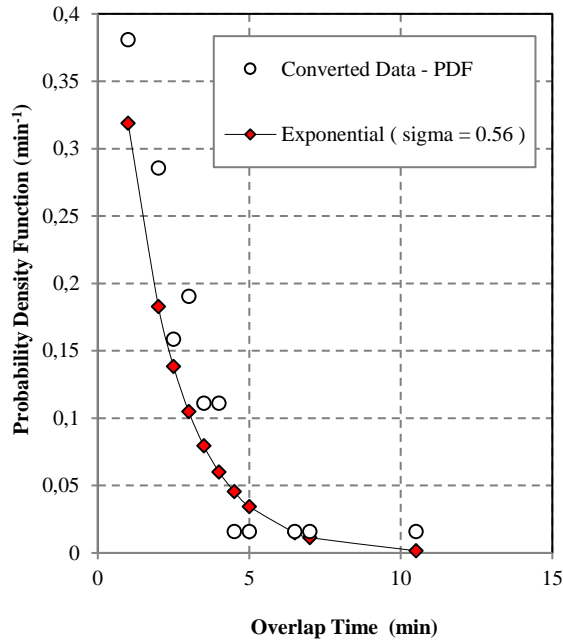
**Figure 4.7:** Converted regime inter-arrival time PDFs of the actual and simulated data.

### 4.3.3 Overlap Time

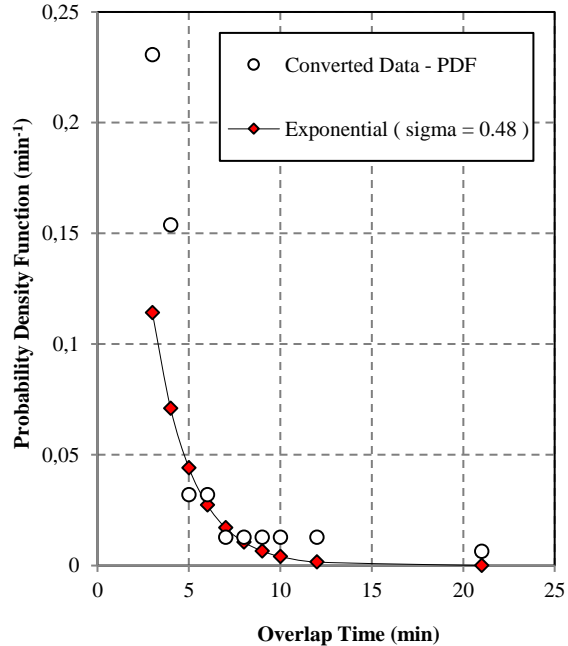
The converted overlap time data is Exponentially distributed as shown in Figure 4.8 and Table 4.2. The longest average overlap time,  $\bar{t}_o = 3.72 \text{ min}$ , is found in the shower regime. The highest overlap rate,  $\delta_o = 0.56 \text{ spikes/min}$ , is found in drizzle rainfall regime. In the original 1-minute data the average overlap times are 3.99, 4.29, 5.87 and 5.75 for drizzle, widespread, shower and thunderstorm respectively [Alonge and Afullo, 2014a]. The same trend observed for the service time parameter is evident for the overlap time as well. In the 1-minute data, the overlap areas are poorly resolved and their time span is often exaggerated which leads to longer average overlap times.

### 4.3.4 Overall Queue Parameters

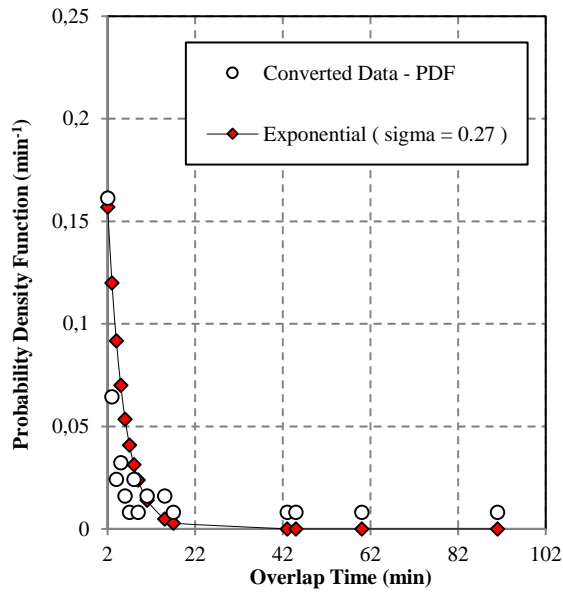
The regime-based queue parameters have been determined and compared for both the converted 30-second and measured 1-minute datasets. Consistently, it is evident across all regimes that the converted data provides more insight into the characteristic behavior of the queue parameters. In a general sense, the overall queue parameters are also examined and the results are presented in Figure 4.9 and Table 4.3 where both the modeling and simulation results of the overall queue parameters are shown. It is observed



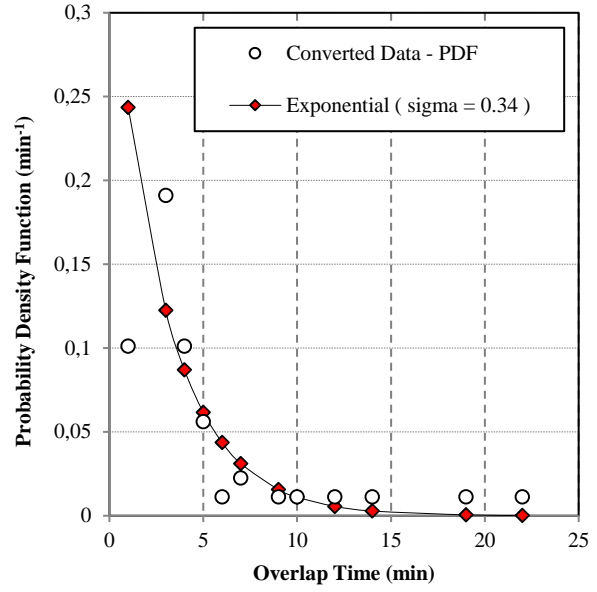
a) Drizzle



b) Widespread



c) Shower



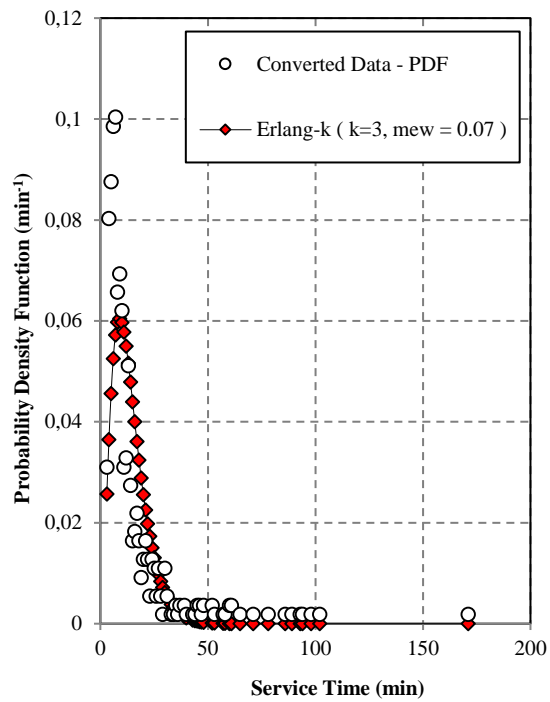
d) Thunderstorm

**Figure 4.8:** Converted regime overlap time PDFs of the actual and simulated data.

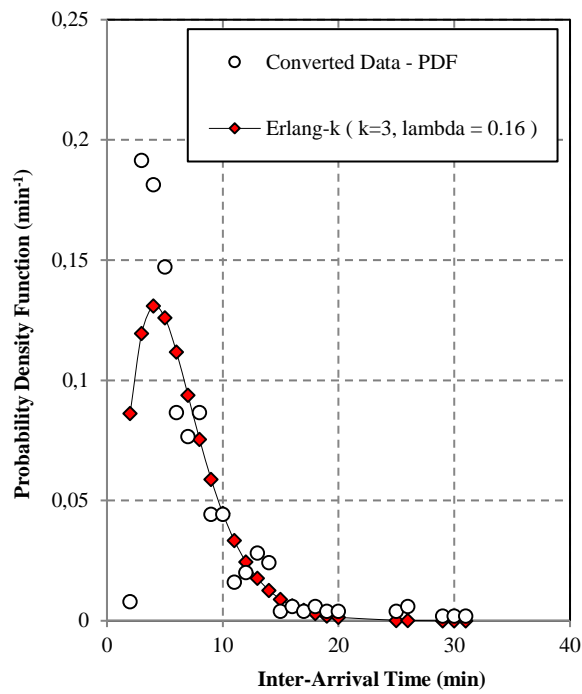
**TABLE 4.3:** MODELING RESULTS OF THE CONVERTED OVERALL QUEUE PARAMETERS FROM 1-MINUTE TO 30-SECOND SAMPLING TIME.

QUEUE PARAMETER	AVERAGE TIME	RATE PARAMETER	NUMBER OF STAGES
Service Time	$\bar{t}_s$ 13.43	$\mu_s$ 0.07	<b>k</b> 3
Inter-Arrival Time	$\bar{t}_a$ 6.20	$\lambda_a$ 0.16	<b>k</b> 3
Overlap Time	$\bar{t}_o$ 2.58	$\sigma_o$ 0.39	<b>k</b> 1

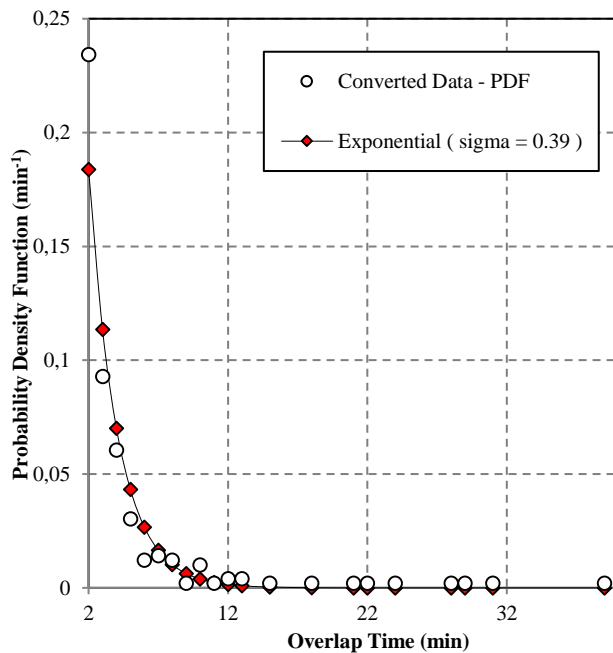
that the overall service and inter-arrival times are Erlang-k distributed with 3 number of stages. Conversely, the overall overlap time follows an exponential distribution. The original 1-minute data overall average service, inter-arrival and overlap time are 15.18, 7.02 and 4.87 respectively [Alonge and Afullo, 2014b]. In comparison to the queue parameters shown in Table 4.3, it is evident that the overall 1-minute sampled data has less detail.



a) Overall Service Time



b) Overall Inter-Arrival Time



b) Overall Overlap Time

**Figure 4.9:** *Converted Overall Queue Parameters PDFs of Actual and Simulated Data.*

#### 4.4 Error Analysis of the Proposed Distributions

The validity of the proposed distributions in adequately modeling the queue parameters of the converted data is examined by performing error analysis through the RMSE and  $\chi^2$  statistics. The results are presented in Table 4.4. Once again the 5% significant level is chosen as the rejection region, thus if the null hypothesis is accepted, then 95% of the data obtained from the proposed distribution may be assumed to be drawn from the converted dataset. The error analysis results show that the regime service and inter-arrival times are indeed Erlang-k distributed, with RMSE between 0.6 and 3.7% for all rainfall regimes. Therefore the null hypothesis is not rejected. Also by applying the  $\chi^2$ , the null hypothesis is not rejected. The overlap time RMSE is between 2.9 and 4.6% across all rainfall regimes, hence the null hypothesis is not rejected at 5% significant level. Therefore, the overlap time parameter is exponential distributed.

With regards to the overall queue parameters, the RMSE is between 1.2 and 2.6% as shown in Table 4.5. Hence the null hypothesis is accepted at 5% significant level. Also by evaluating the  $\chi^2$ , the null hypothesis is not rejected at 5% significant level. The proposed models for the queue parameters are therefore accepted and will thus be used as their data generating processes (DGP) henceforth.

**TABLE 4.4:** ERROR ANALYSIS OF THE PROPOSED DISTRIBUTIONS FOR THE CONVERTED QUEUE PARAMETERS

QUEUE PARAMETER	RAINFALL REGIME	PROPOSED MODEL	REGIME RMSE	REGIME $\chi^2$	DF	SL
SERVICE TIME	DRIZZLE	Erlang-k	0.006	0.417	145	174.10
	WIDESPREAD	Erlang-k	0.017	0.321	174	205.78
	SHOWER	Erlang-k	0.019	0.318	125	152.09
	T/STORM	Erlang-k	0.021	0.256	100	124.34
INTER-ARRIVAL TIME	DRIZZLE	Erlang-k	0.037	0.901	125	152.09
	WIDESPREAD	Erlang-k	0.026	0.120	156	186.15
	SHOWER	Erlang-k	0.017	0.100	123	149.89
	T/STORM	Erlang-k	0.022	0.282	88	110.89
OVERLAP TIME	DRIZZLE	Exponential	0.046	0.212	125	152.09
	WIDESPREAD	Exponential	0.044	0.136	155	185.05
	SHOWER	Exponential	0.029	0.579	123	149.89
	T/STORM	Exponential	0.045	0.357	88	110.89

**TABLE 4.5: ERROR ANALYSIS OF THE PROPOSED DISTRIBUTIONS FOR THE OVERALL CONVERTED QUEUE PARAMETERS**

QUEUE PARAMETERS	OVERALL RMSE	OVERALL $\chi^2$	DF	SL
SERVICE TIME	0.014	0.402	543	605.67
INTER-ARRIVAL TIME	0.026	0.873	491	553.13
OVERLAP TIME	0.012	0.075	491	553.13

#### 4.5 Validation of the Conversion Method

At this point the conversion method has been successfully developed and the converted data behaves differently to the original 1-minute data. Both the service and inter-arrival times are Erlang-k distributed, whereas the overlap time follows the exponential distribution. Also in the converted data more rainfall spikes are identified as opposed to when using the original data (1-minute). As seen previously in Chapter 3, lowering the sampling time provides more detail in the rain rate time series. In order to validate the conversion process, it is straightforward to compare the distribution of the 30-second data generated by the conversion process with that of the measured 30-second data at the same location. The two datasets are generated by their respective distributions which were determined earlier. The PDFs are preferred as opposed to the modeled datasets themselves primarily because they have different lengths, which make for a difficult comparison. Utilizing the time range (time bounds) for each queue parameter, data is generated in that range by the respective PDFs for all regimes as well as the overall case. In this way, datasets of the same length are obtained and standard error analysis tools are used for comparison. The error analysis will be performed in terms of the Chi-square ( $\chi^2$ ) and Kolmogorov-Smirnov (KS) test statistics.

The Chi-square ( $\chi^2$ ) test statistics is well explained in chapter 3 section 3.3.5; hence only the Kolmogorov-Smirnov (KS) test will be elaborated in this section. The test statistics for the Kolmogorov-Smirnov is given as [3].

$$D_{n,m} = \max_x |F_{1,n}(x) - F_{2,m}(x)| \quad (4.2a)$$

where  $F_{1,n}(x)$  and  $F_{2,m}(x)$  are the cumulative distribution functions of the proposed PDFs for the actual and converted 30-second data. In this case, the data samples are Erlang-k distributed and from the obtained PDFs the cumulative distribution data is obtained as follows:

$$F(x) = 1 - \sum_{p=0}^{k-1} \frac{1}{p!} e^{-\lambda x} (\lambda x)^p \quad (4.2b)$$

where  $k$  and  $\lambda$  are the Erlang- $k$  stages and rate respectively.

The Kolmogorov-Smirnov null and alternative hypotheses are as follows, respectively [5]:

$H_0$ : The two distributions are the same,

$H_a$ : The two distributions are not the same.

The critical value is defined as follows:

$$D_{n,m,\alpha} = c(\alpha) \sqrt{\frac{n+m}{nm}} \quad (4.2c)$$

**TABLE 4.6:** ERROR ANALYSIS BETWEEN THE QUEUE PARAMETERS PROPOSED PDFS OF THE 30-SECOND ACTUAL DATA AND CONVERTED DATA

QUEUE PARAMETER	RAINFALL REGIME	COMPARED MODELS	$\chi^2$	DF	SL		$D_{n,m}$	$D_{n,m,\alpha}$
<b>SERVICE TIME</b>	DRIZZLE	<i>Erlang-k</i>	0.0002	49	74.919		0.005	0.39
	WIDESPREAD	<i>Erlang-k</i>	0.109	49	74.919		0.316	0.39
	SHOWER	<i>Erlang-k</i>	0.00003	49	74.919		0.004	0.39
	T/STORM	<i>Erlang-k</i>	0.00005	49	74.919		0.003	0.39
<b>INTER-ARRIVAL TIME</b>	DRIZZLE	<i>Erlang-k</i>	0.179	49	74.919		0.195	0.39
	WIDESPREAD	<i>Erlang-k</i>	0.133	49	74.919		0.250	0.39
	SHOWER	<i>Erlang-k</i>	0.185	49	74.919		0.252	0.39
	T/STORM	<i>Erlang-k</i>	0.00001	49	74.919		0.001	0.39
<b>OVERLAP TIME</b>	DRIZZLE	<i>Exponential</i>	0.228	49	74.919		0.080	0.39
	WIDESPREAD	<i>Exponential</i>	0.128	49	74.919		0.064	0.39
	SHOWER	<i>Exponential</i>	0.573	49	74.919		0.147	0.39
	T/STORM	<i>Exponential</i>	1.184	49	74.919		0.170	0.39

where  $n$  and  $m$  are the sample sizes of the first and second sample respectively. The value of  $c(\alpha)$  can be found in the Kolmogorov-Smirnov Table for the most common significant levels of  $\alpha$  or else given as [3 and 4].

$$c(\alpha) = \sqrt{-\frac{1}{2} \ln \left( \frac{\alpha}{2} \right)} \quad (4.2d)$$

The null hypothesis is rejected at the significant level,  $\alpha$ , if

$$D_{n,m} > D_{n,m,\alpha} \quad (4.2e)$$

The chosen significant level is 0.1% and both PDFs are mapped into 50 points, therefore

$$n = m = 50 \quad (4.2f)$$

hence,

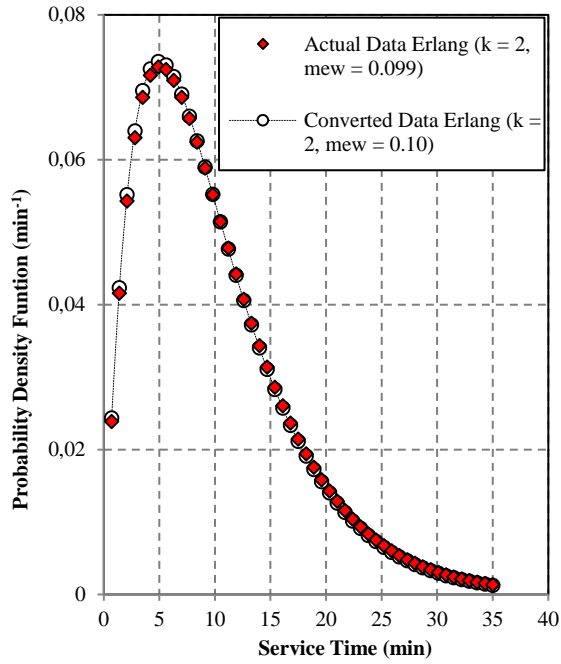
$$D_{n,m,\alpha} = 0.39 \quad (4.2g)$$

#### 4.5.1 Service Times Comparison

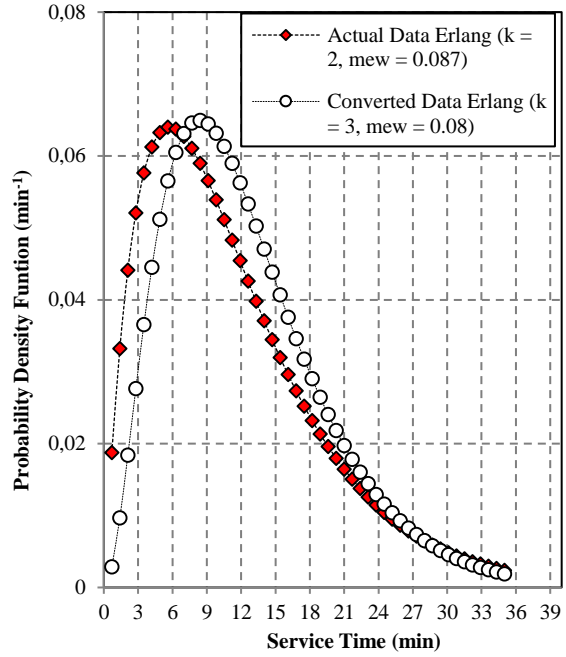
Both service times of the converted and actual 30-second data are Erlang-k distributed as shown in Figure 4.10. The Error analysis results between the converted and actual 30-second data proposed PDFs are presented on Table 4.6. At 0.1% significant level, the Chi-square error test does not reject the null hypothesis. Hence the difference between the two PDFs is insignificant. Moreover, the Kolmogorov-Smirnov error test does not reject the null hypothesis at 0.1% significant level as well. This means that the difference between the converted and actual 30-second data proposed PDFs is not significant; hence the two PDFs may be considered representative of the same process. Therefore, if the service times of both datasets are the same, then the conversion method may be considered valid for the service time parameter.

#### 4.5.2 Inter-Arrival Times Comparison

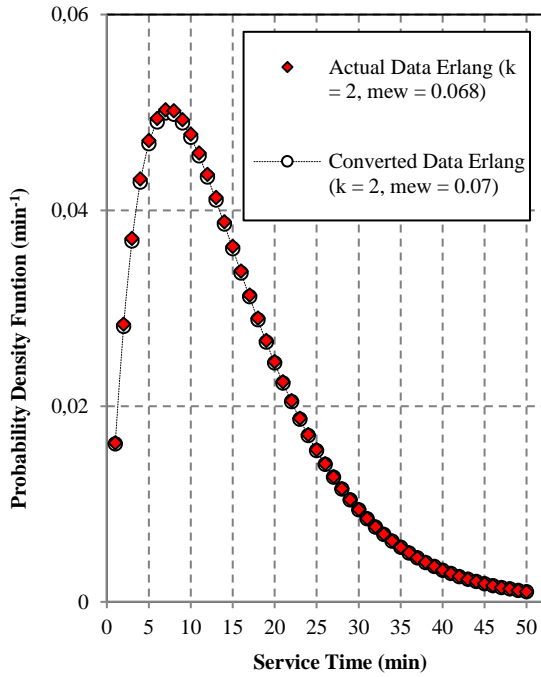
Likewise, the inter-arrival times of the converted and measured 30-second data both follow an Erlang-k distribution as shown in Figure 4.11. The null hypothesis is not rejected at 0.1% significant level with the Chi-square error test as shown in Table 4.6; thus the two PDFs are similar. Also, the Kolmogorov-Smirnov error test does not reject the null hypothesis at 0.1% significant level. Therefore, the CDFs prove to have insignificant differences. This implies that the inter-arrival times of the converted and measured 30-second data are the same. In this regard, the conversion method is also valid for the inter-arrival time parameter.



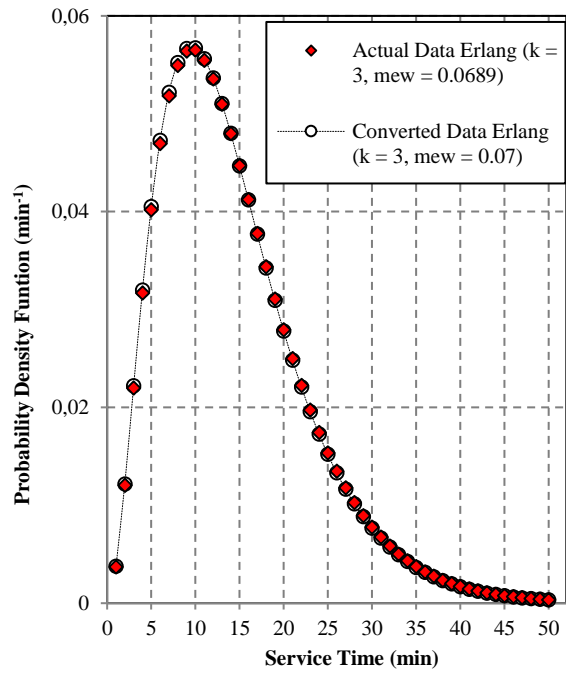
a) Drizzle



b) Widespread

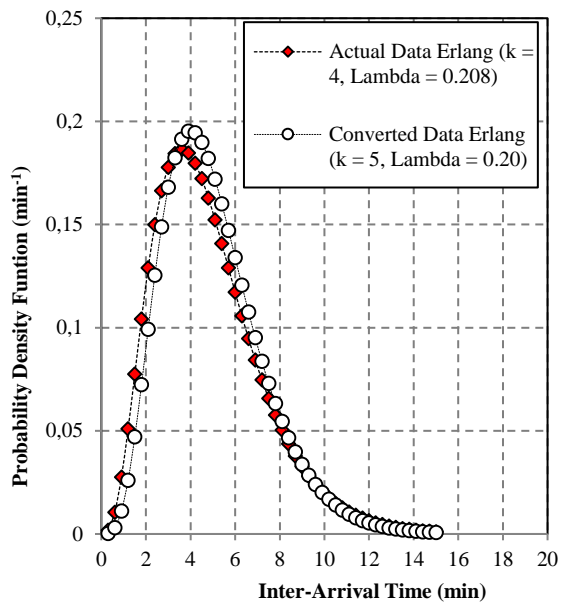


c) Shower

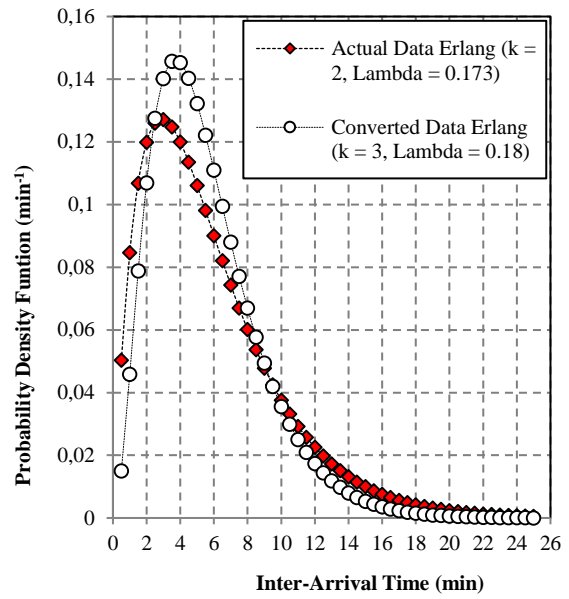


d) Thunderstorm

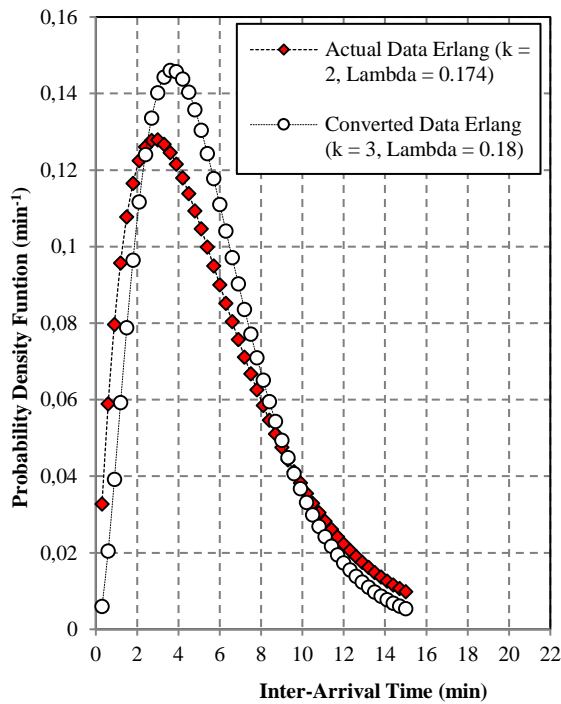
*Figure 4.10: Comparison of the Service Times Proposed Models for the 30-second Actual Data and Converted Data.*



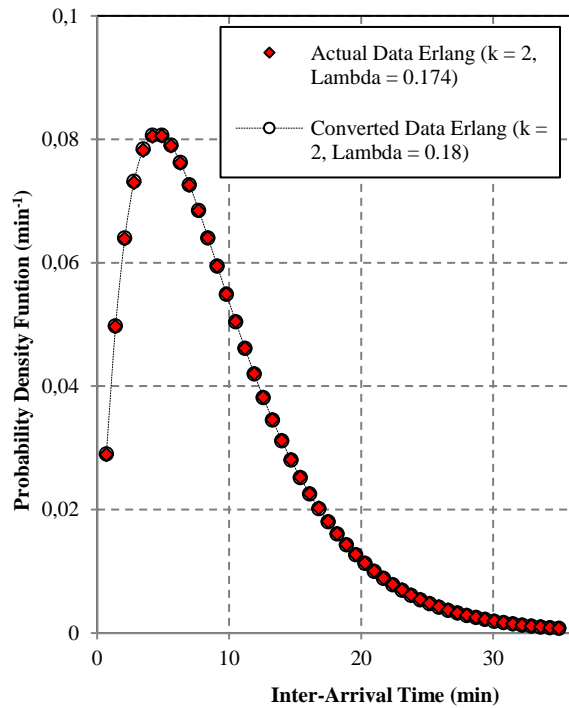
a) Drizzle



b) Widespread



c) Shower



d) Thunderstorm

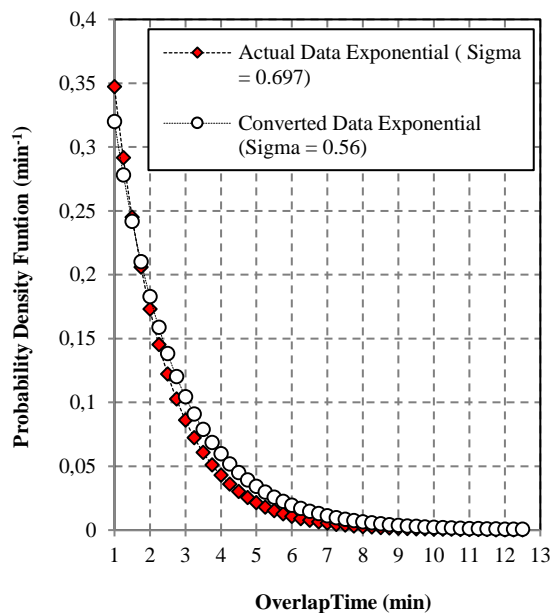
**Figure 4.11:** Comparison of the Inter-Arrival Times Proposed Models for the 30-second Actual Data and Converted Data.

**TABLE 4.7:** ERROR ANALYSIS BETWEEN THE OVERALL QUEUE PARAMETERS PROPOSED PDFS OF THE 30-SECOND ACTUAL DATA AND CONVERTED DATA

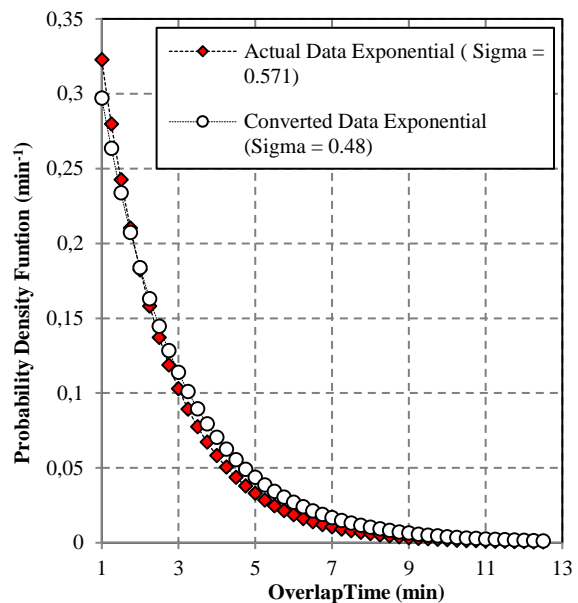
PARAMETERS	PROPOSED DISTRIBUTION	$\chi^2$	DF	SL	$D_{n,m}$	$D_{n,m,\alpha}$
SERVICE TIME	<i>Erlang-k</i>	0.1601	49	74.919	0.356	0.39
INTER-ARRIVAL TIME	<i>Erlang-k</i>	0.1595	49	74.919	0.307	0.39
OVERLAP TIME	<i>Exponential</i>	0.0440	49	74.919	0.040	0.39

### 4.5.3 Overlap Times Comparison

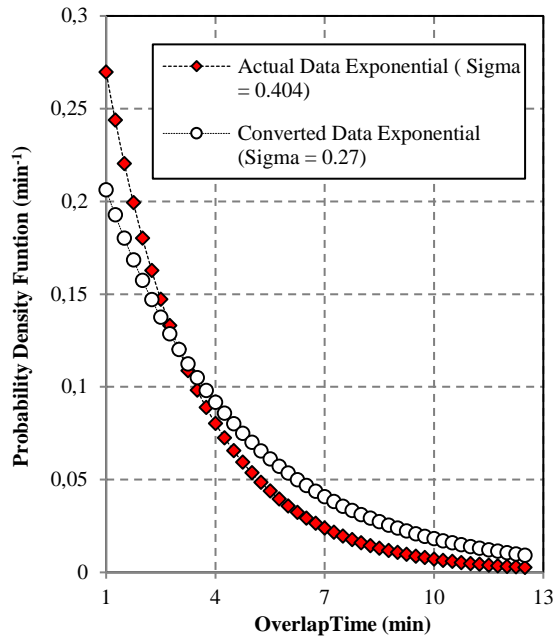
The overlap times of the converted and measured 30-second data are exponentially distributed as shown in Figure 4.12. At 0.1% significant level, the Chi-square error test does not reject the null hypothesis as shown in Table 4.6; hence these two PDFs represent the same process. Additionally, the Kolmogorov-Smirnov error test does not reject the null hypothesis at 0.1% significant level; hence the two CDFs have insignificant difference. Conclusively, the overlap times of the converted and measured 30-second data behave the same. To this effect, the conversion method is also valid for the overlap time parameter



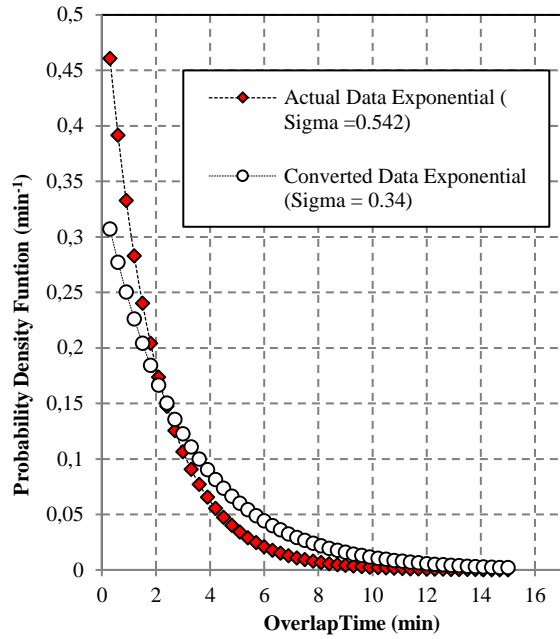
a) Drizzle



b) Widespread



c) Shower

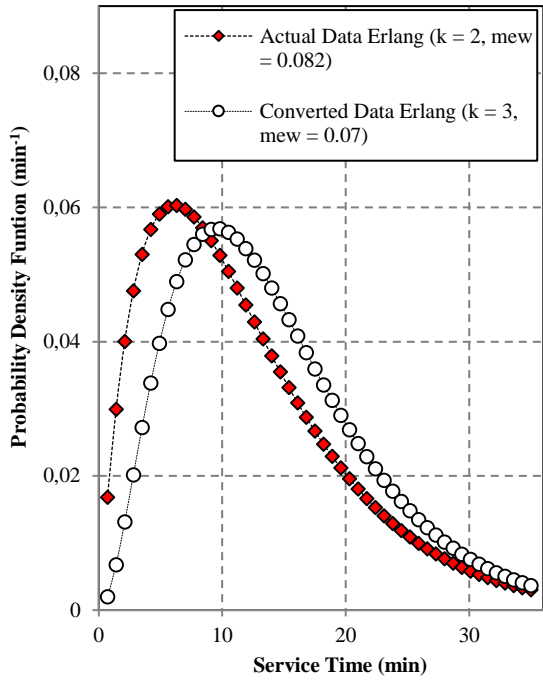


d) Thunderstorm

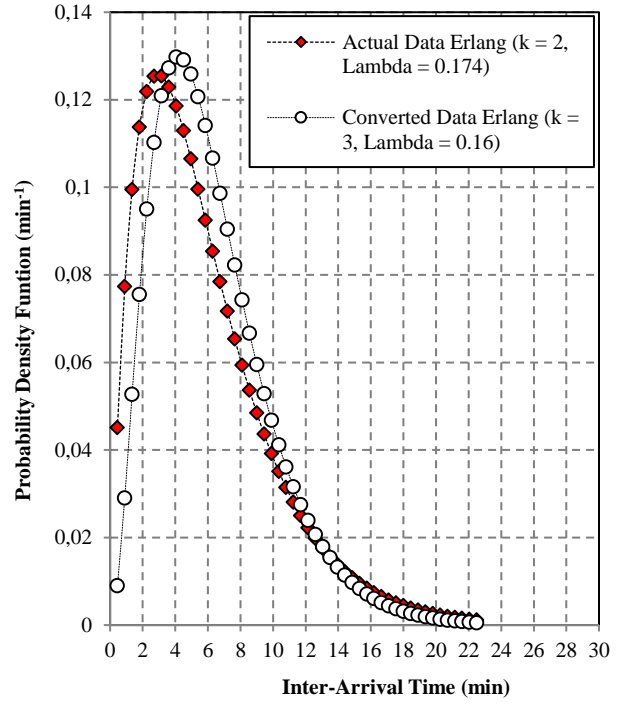
*Figure 4.12: Comparison of the Overlap Times Proposed Models for the 30-second Actual Data and Converted Data.*

#### 4.5.4 Overall Queue Parameters Comparison

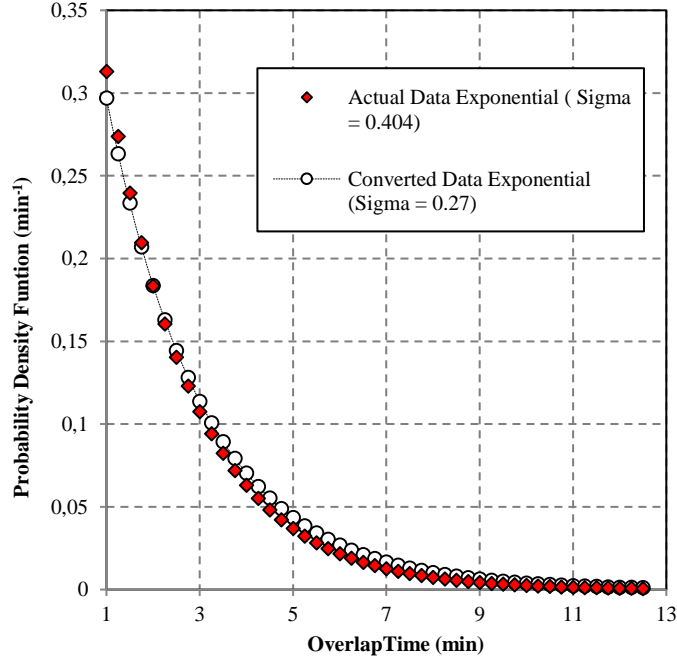
Finally, the error analysis results between the converted and measured 30-second overall queue parameters are presented in Table 4.7. The overall service and inter-arrival times of the converted and measured 30-second data are Erlang-k distributed; whereas the overall overlap times are exponentially distributed as shown in Figure 4.13. The Chi-square test statistics at 0.1% significant level does not reject the null hypothesis for all the three queue parameters. Hence the difference between the respective pairs of PDFs is insignificant. Moreover, the Kolmogorov-Smirnov error test does not reject the null hypothesis at 0.1% significant level for all the three queue parameters; hence the two CDFs for each queue parameter have insignificant differences. In this regard, it is concluded that the converted and measured 30-second overall queue parameters resemble each other. Hence the conversion method is still valid for the overall queue parameters.



a) Overall Service Time



b) Overall Inter-Arrival Time



a) Overall Overlap Time

**Figure 4.13:** Comparison of the Overall Queue Parameters Proposed Models for the 30-second Actual Data and Converted Data

#### 4.6 Long Term Modeling Results Analysis

Due to advances in technology, it is apparent that the quality of measurement instrumentation improves over time and rain sensing equipment is no different. Sampling time is one of the features which designers of such instruments strives to reduce as much as necessary. However, the long-term statistics of rainfall is very important such that even in the advent of new and high-sampling rate instrumentation, historical data remains valuable in the quest for long-term modeling. It is therefore necessary to continue to utilize historical data as part of a bulk measurement campaign spanning several years. With the understanding that the sampling rate may not have been adequate in previous campaigns, this work has taken the initiative to convert such data into a finely sampled one making it possible to integrate with current on-going measurement data. The combined bulk data is then used for rainfall long-term statistical analysis by applying queueing theory once again. In this case sixty six (66) months' worth of data will be used for long-term modeling of rainfall in Durban, South Africa.

**Table 4.8:** LONG-TERM RAINFALL QUEUE PARAMETERS MODELING RESULTS AT 30-SECOND SAMPLING TIME

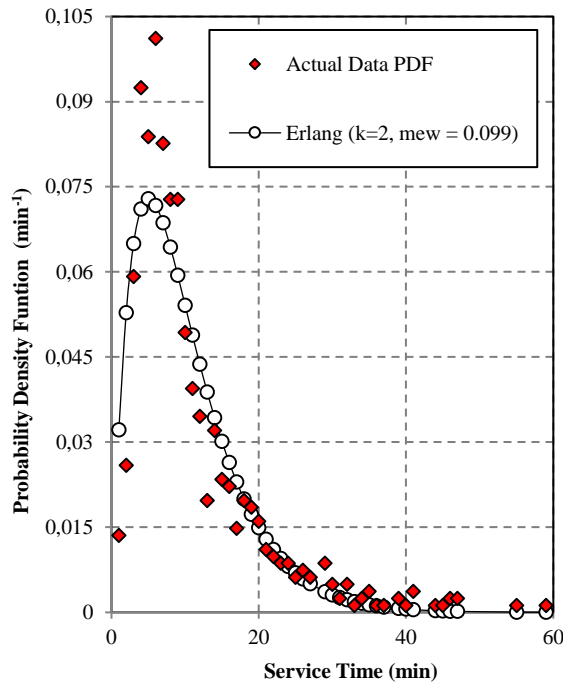
QUEUE PARAMETER	REGIME	AVERAGE TIME ( $\bar{t}_s$ )	RATE ( $\mu_s$ )	NUMBER OF STAGES k
SERVICE TIME	Drizzle	10.098	0.099	2
	Widespread	11.707	0.085	3
	Shower	14.636	0.068	2
	Thunderstorm	14.285	0.070	3
QUEUE PARAMETER	REGIME	AVERAGE TIME ( $\bar{t}_a$ )	RATE ( $\lambda_a$ )	NUMBER OF STAGES k
INTER-ARRIVAL TIME	Drizzle	4.882	0.205	4
	Widespread	4.123	0.243	3
	Shower	5.737	0.174	2
	Thunderstorm	9.210	0.109	2
QUEUE PARAMETER	REGIME	AVERAGE TIME ( $\bar{t}_o$ )	RATE ( $\sigma_o$ )	NUMBER OF STAGES k
OVERLAP TIME	Drizzle	1.506	0.664	1
	Widespread	1.974	0.507	1
	Shower	2.720	0.368	1
	Thunderstorm	2.243	0.446	1

### 4.6.1 Long-Term Service Time

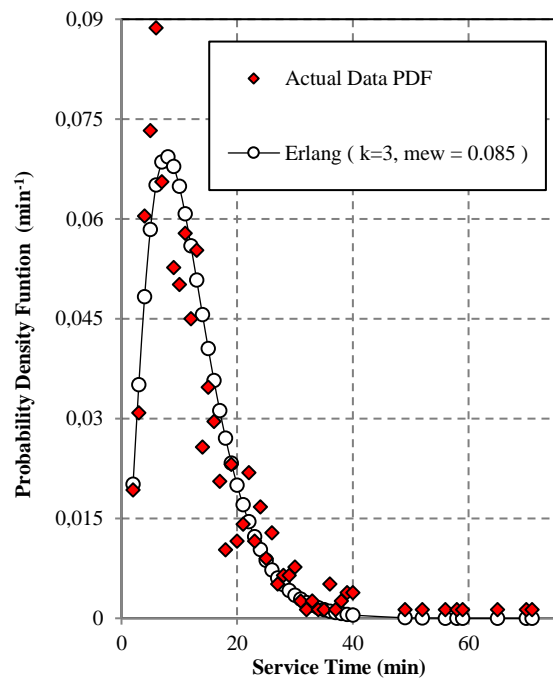
By utilizing the obtained long-term data, the service time is found to be Erlang-k distributed with either 2 or 3 number of stages for all rainfall regimes as shown in Table 4.8 and Figure 4.14. The highest average service time,  $\bar{t}_s = 14.636$ , is found under the shower regime. The drizzle regime has the highest service rate,  $\mu = 0.099$ , as compared to all other regimes. It is notable that the long-term service time resembles the characteristics of the short-term service time (actual 30-second data) for all rainfall regimes. According to the results presented in Table 3.2, the highest average service time is found under the shower regime for both the long-term and short-term data and has a value of approximately 15 minutes. Again, the highest service rate,  $\mu = 0.099$ , for both datasets is found under the drizzle regime. It is observed that the statistical behavior of the long-term and short-term rainfall time series resemble each other.

### 4.6.2 Long-Term Inter-Arrival Time

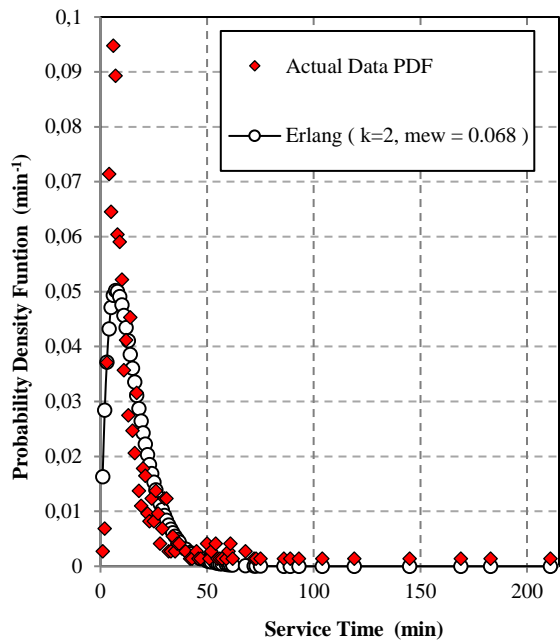
Similarly, the long-term inter-arrival time is Erlang-k distributed with the number of stages ranging from 2 to 4 for all rainfall regimes as shown in Table 4.8 and Figure 4.15. The thunderstorm regime has notably the highest average inter-arrival time,  $\bar{t}_a = 9.210$ , as compared to all other regimes. On the other hand, widespread regime is observed to have the highest arrival rate,  $\mu = 0.243$ , in comparison to all other



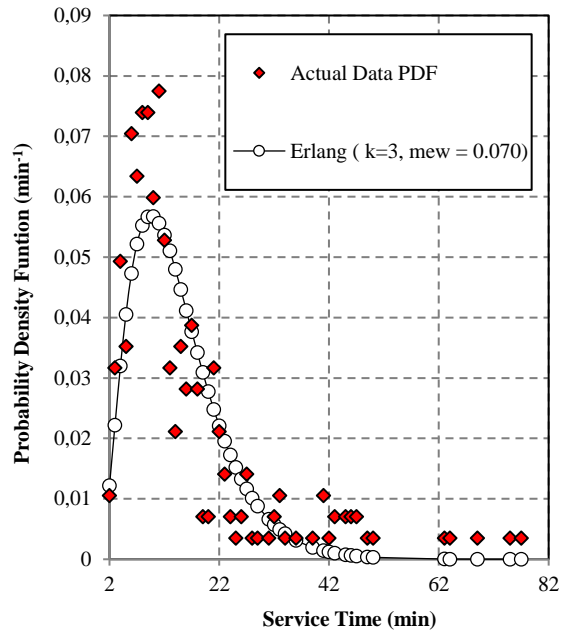
a) Drizzle



b) Widespread

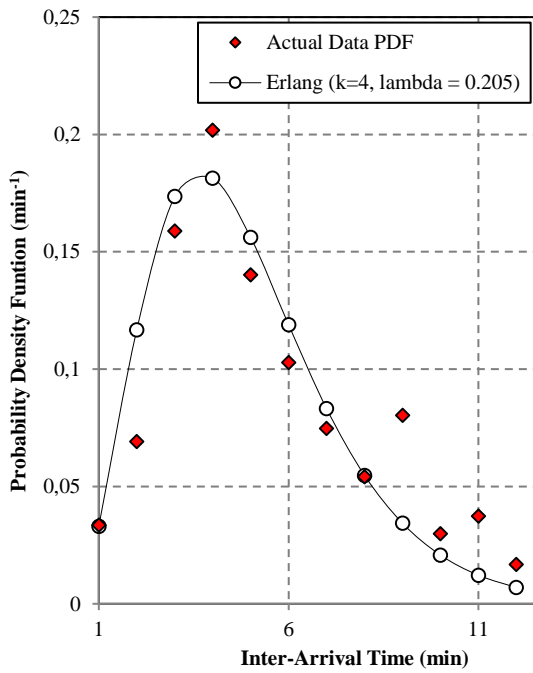


c) Shower

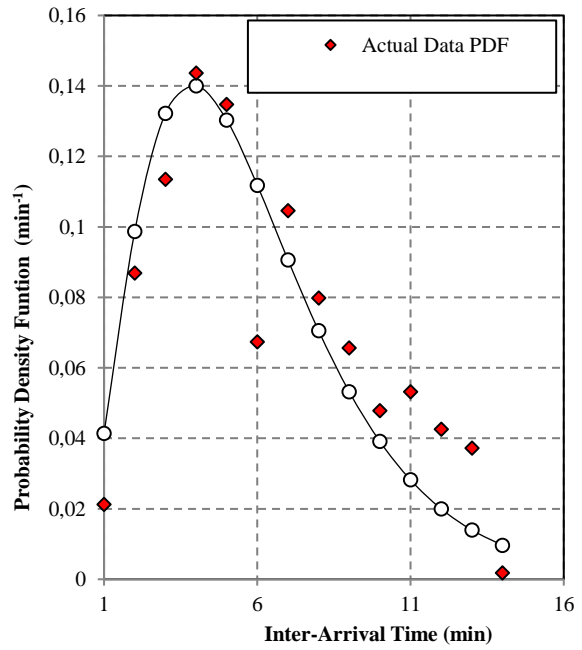


d) Thunderstorm

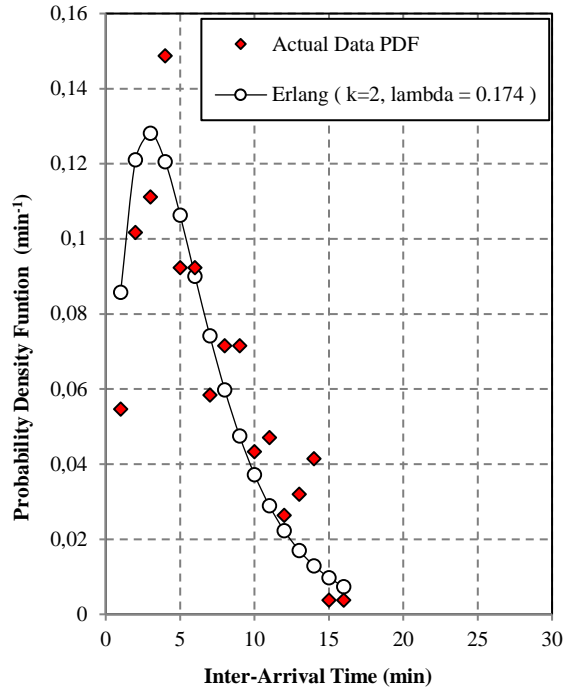
**Figure 4.14:** Long-Term Modeling Plots of the Service Time Parameter at 30-second Sampling Time in Durban.



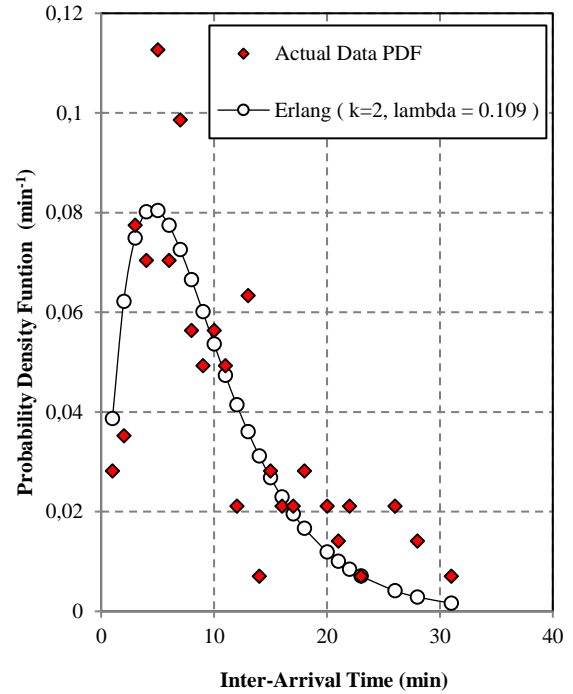
a) Drizzle



b) Widespread



c) Shower



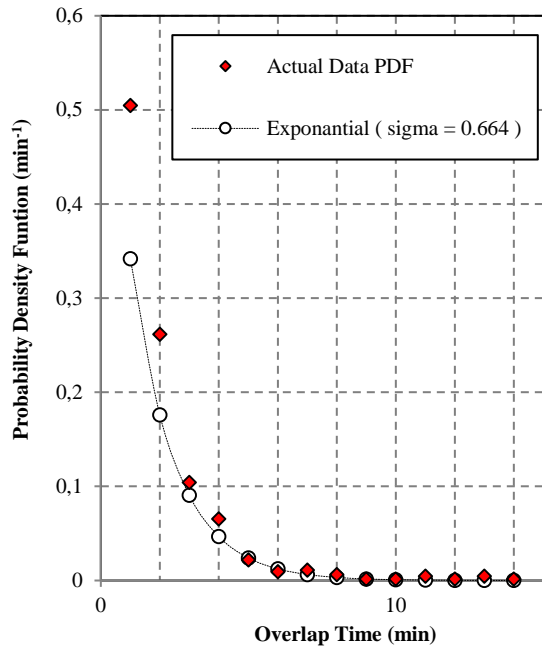
d) Thunderstorm

**Figure 4.15:** Long-Term Modeling Plots of the Inter-Arrival Time Parameter at 30-second Sampling Time in Durban.

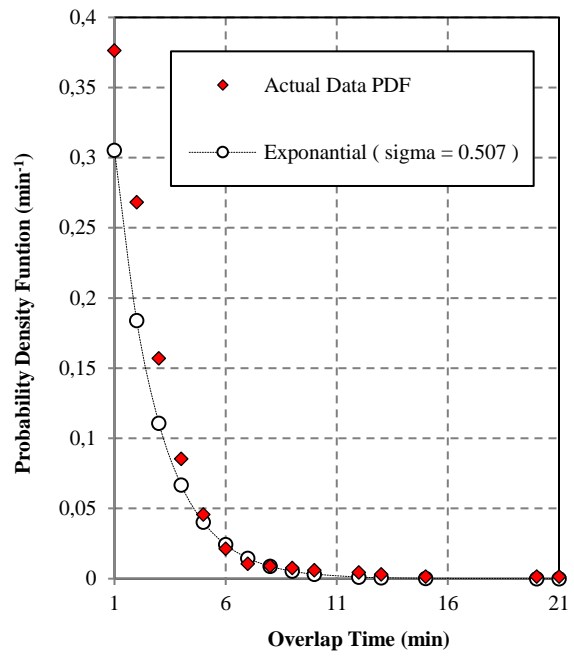
regimes. The regime-based long-term inter-arrival times possess the characteristics of their short-term counterparts. In both cases the highest average inter-arrival times are found under the thunderstorm regime and are approximately 10 minutes. The difference in their statistical characteristics is not enough to suggest that the two datasets may be generated from two different processes.

### 4.6.3 Long-Term Overlap Time

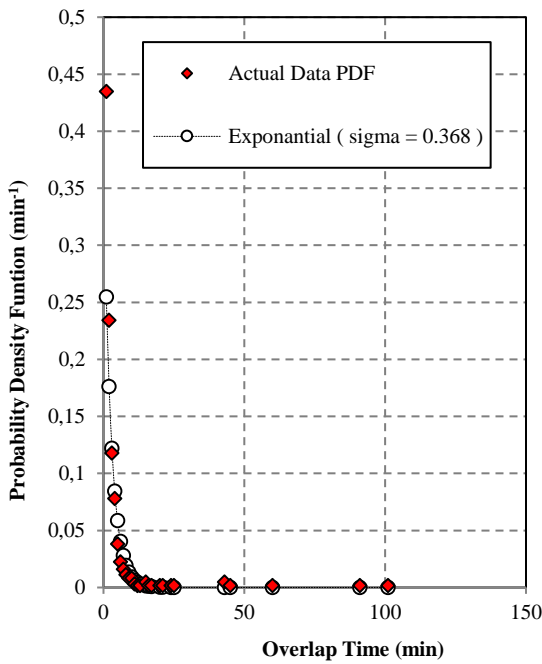
The long-term overlap time is exponentially distributed for all the rainfall regimes as shown in Table 4.8 and Figure 4.16. The shower regime is found to have the highest average overlap time,  $\bar{t}_o = 2.720$ , compared to all other regimes. The drizzle regime on the other hand exhibits the highest overlap rate,  $\sigma = 0.664$ , compared to all other regimes. Similar conclusions can be drawn with respect to the statistical behavior of the long-term overlap time as seen before with other queue parameters. It is evident that the long-term and short-term statistical characteristics of the overlap time are similar. In addition to both the processes being exponentially distributed, their highest average overlap times are recorded under the shower regime and the lowest overlap rates are found on the same regime.



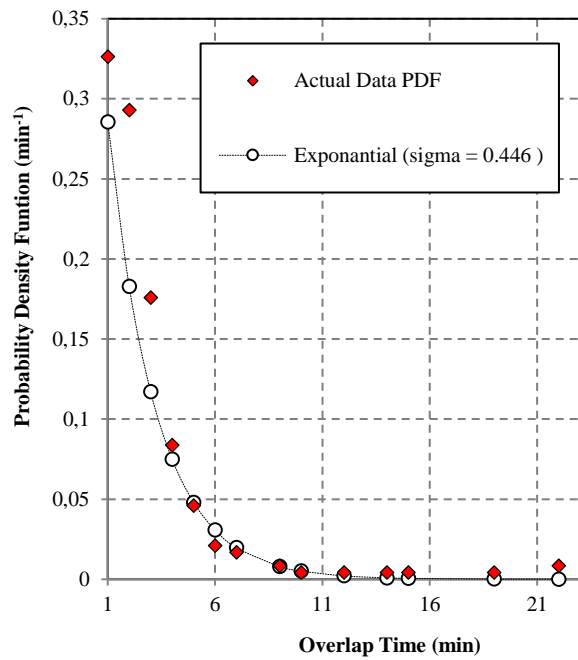
a) Drizzle



b) Widespread



c) Shower



d) Thunderstorm

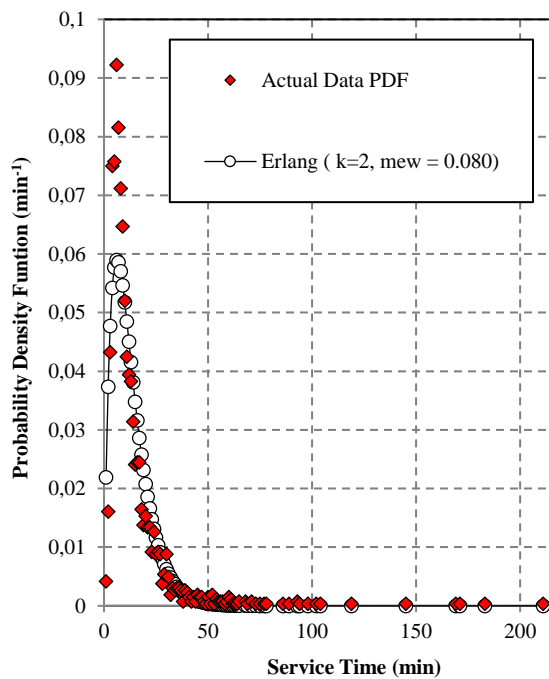
Figure 4.16: Long-Term Modeling Plots of the Overlap Time Parameter at 30-second Sampling Time in Durban.

**TABLE 4.9: LONG-TERM RAINFALL OVERALL QUEUE PARAMETERS MODELING RESULTS AT 30-SECOND SAMPLING TIME**

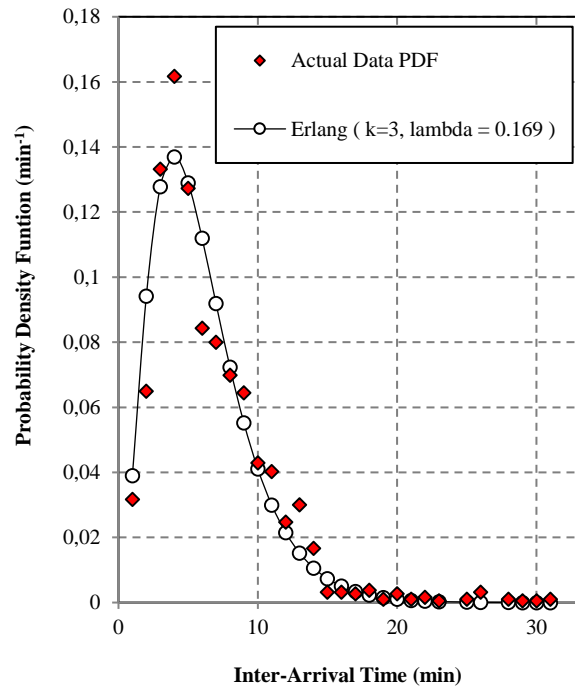
QUEUE PARAMETER	AVERAGE TIME	RATE PARAMETER	NUMBER OF STAGES
Service Time	$\bar{t}_s$ 12.466	$\mu$ 0.080	<b>k</b> 2
Inter-Arrival Time	$\bar{t}_a$ 5.929	$\lambda$ 0.169	<b>k</b> 3
Overlap Time	$\bar{t}_o$ 1.919	$\sigma$ 0.521	<b>k</b> 1

#### 4.6.4 Long-Term Overall Parameters

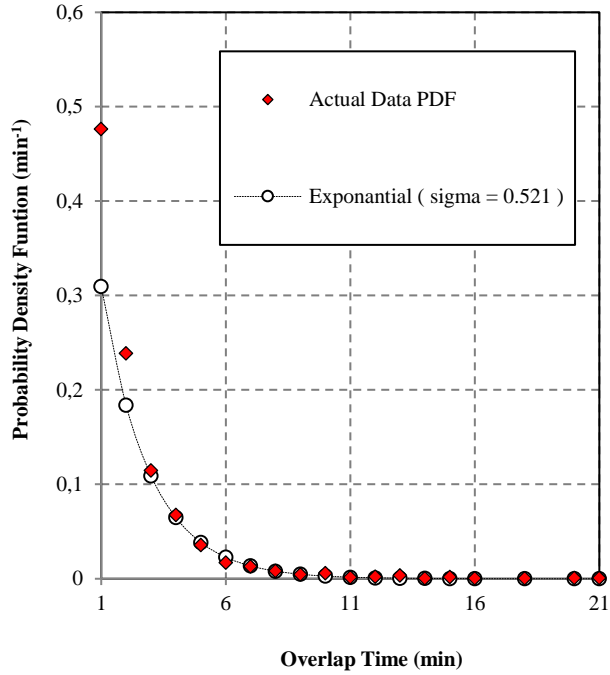
With regards to the long-term overall queue parameters, the service and inter-arrival times are found to be Erlang-k distributed with 2 and 3 number of stages respectively. Conversely the overall overlap time follows exponential distribution as shown in Table 4.9 and Figure 4.17. The average service, inter-arrival and overlap times are  $\bar{t}_s = 12.466$ ,  $\bar{t}_a = 5.929$  and  $\bar{t}_o = 1.919$ , respectively. Hence their queue parameters rates are  $\mu = 0.080$ ,  $\lambda = 0.169$  and  $\sigma = 0.521$ , respectively. Therefore comparing with the short-term results displayed in the Table 3.3, the results prove to be statistically similar.



a) Overall Service Time



b) Overall Inter-Arrival Time



c) Overall Overlap Time

**Figure 4.17:** Long-Term Modeling Plots of the Overall Parameters at 30-second Sampling Time in Durban.

#### 4.6.5 Error Analysis of the Long-Term Proposed Distribution

The RMSE for the long-term service time is between 0.86% and 1.4% for all rainfall regimes as presented in Table 4.10. In this regard, at 5% significant level the null hypothesis is not rejected. Also under the  $\chi^2$  test statistic, the null hypothesis is not rejected. Therefore, the long-term service time is best described by an Erlang-k distribution. The long-term inter-arrival time has an RMSE that ranges between 1.10% and 2.30% for all rainfall regimes. Hence the null hypothesis is not rejected. Again by the  $\chi^2$  test, the null hypothesis is not rejected. Therefore, the long-term inter-arrival time is fully described by the Erlang-k distribution. The long-term overlap time RMSE is between 2.60% and 4.96% for all rainfall regimes. Therefore with both RMS and  $\chi^2$  error tests, the null hypothesis is not rejected. Thus, the long-term overlap time is exponentially distributed.

Lastly, the RMSE for the long-term overall queue parameters lies between 0.7% and 3.3% for all queue parameter as displayed in Table 4.11. When using the RMS and  $\chi^2$  error tests, the null hypothesis is not rejected. This confirms that the proposed distributions for modeling the overall queue parameters are satisfactory.

**TABLE 4.10:** ERROR ANALYSIS OF THE LONG-TERM QUEUE PARAMETERS PROPOSED DISTRIBUTIONS

QUEUE PARAMETER	RAINFALL REGIME	PROPOSED MODEL	REGIME RMSE	REGIME $\chi^2$	DF	SL
SERVICE TIME	DRIZZLE	<i>Erlang-k</i>	0.0091	0.127	810	918.937
	WIDESPREAD	<i>Erlang-k</i>	0.0086	0.123	777	866.911
	SHOWER	<i>Erlang-k</i>	0.0100	0.363	727	814.822
	T/STORM	<i>Erlang-k</i>	0.0140	0.206	283	341.395
INTER-ARRIVAL TIME	DRIZZLE	<i>Erlang-k</i>	0.0230	0.093	534	605.667
	WIDESPREAD	<i>Erlang-k</i>	0.0190	0.133	563	658.094
	SHOWER	<i>Erlang-k</i>	0.0160	0.073	530	605.667
	T/STORM	<i>Erlang-k</i>	0.0110	0.378	230	265.301
OVERLAP TIME	DRIZZLE	<i>Exponential</i>	0.0496	0.103	641	710.421
	WIDESPREAD	<i>Exponential</i>	0.0260	0.057	655	762.661
	SHOWER	<i>Exponential</i>	0.0380	0.164	627	710.421
	T/STORM	<i>Exponential</i>	0.0350	0.092	240	277.138

**TABLE 4.11:** ERROR ANALYSIS OF THE LONG-TERM OVERALL QUEUE PARAMETERS PROPOSED DISTRIBUTIONS

PARAMETERS	PROPOSED MODEL	OVERALL RMSE	OVERALL $\chi^2$	DF	SL
SERVICE TIME	<i>Erlang-k</i>	0.007	0.202	2611	1074.679
INTER-ARRIVAL TIME	<i>Erlang-k</i>	0.010	0.060	2172	1074.679
OVERLAP TIME	<i>Exponential</i>	0.033	0.088	1860	1074.679

#### 4.7 Chapter Summary

The typical relationship between the 30-second and 1-minute rainfall data in Durban is best described by a second order polynomial function. This has been confirmed by plotting the CDFs for the two datasets against each other and successfully fitting their relationship to a second order polynomial with a high correlation coefficient. This has been done for all the queue parameters under both the regime-based

approach and the overall case. The conversion method has been validated by comparing the converted 30-second data queue distribution models with those of the measured 30-second sampled data. The error analysis by means of RMSE between these two models confirmed that more than 95% of the converted data belongs to the same process that generated the actual 30-second data. The resultant queue discipline ( $E_k/E_k/s/\infty/FCFS$ ) for the long-term model is similar to that of the short-term modeled data at 30-second sampling. In this regard, the rainfall process exhibits traits of a self-similar process in the period of 66 months. In this view, it might be possible to adequately characterize rainfall behavior in Durban from rainfall data acquired over a fraction of this measurement period.

## CHAPTER FIVE

### Effect of the Sampling Time on Rainfall Attenuation along Radio Links

#### 5.1 Introduction

The ever increasing demand for higher bandwidth has led to an increased interest in deploying communication services at frequencies beyond 10 GHz. However, operating terrestrial and satellite links at such frequencies brings about propagation related challenges. The biggest challenge at microwave and millimeter wave bands is precipitation in the form of rainfall. At these frequencies the raindrop diameter is comparable to the wavelength of the operating frequency hence the effects of scattering and absorption become dominant. Rainfall contributes majorly to the overall attenuation of the propagating signal in free space. For a network designer setting up a radio link, rain attenuation information is essential for link budget calculations in order to determine the appropriate fade margins. Therefore, given the statistical modeling and analysis that has been done in previous chapters it is necessary to examine rain attenuation at a location. At this point in this study, the effect of the sampling time has been investigated on the modeling of rainfall behavior. Therefore, this chapter aims to examine the effect of the sampling time on rain attenuation over radio links in Durban.

#### 5.2 Rain Rate Cumulative Distributions

Sampling time and rain rate cumulative distributions are some of the significant information for rain attenuation modeling. The availability of such information makes it possible for system engineers to predict the percentage of time which the attenuation due to rain is significant within an average year, the future link performance and the availability of communication services [Moupfouma and Martins, 1995]. The outage of a terrestrial radio link may depend on the instantaneous rain rate, but rain rate varies throughout a rain event as well as yearly. In this regard, the rain rate cumulative distribution (CD) is required for rain attenuation prediction. Figure 5.1 provides a graphical representation of rain rate exceeded for different percentage of time in Durban at 30-second and 1-minute sampling time. The 1-minute data is extracted from the previous study of [Alonge and Afullo, 2015]. Generally  $R_{0.01}$  is considered as most useful for rain attenuation predictions over satellite and terrestrial communication links. This parameter,  $R_{0.01}$ , is the rain rate which is exceeded 0.01% of the time in an average year at a given location. From the rain rate investigation results, it is evident from Figure 5.1 that at 30-second sampling time the probability of exceedance is consistently higher than that at 1-minute sampling for the same rain rate.

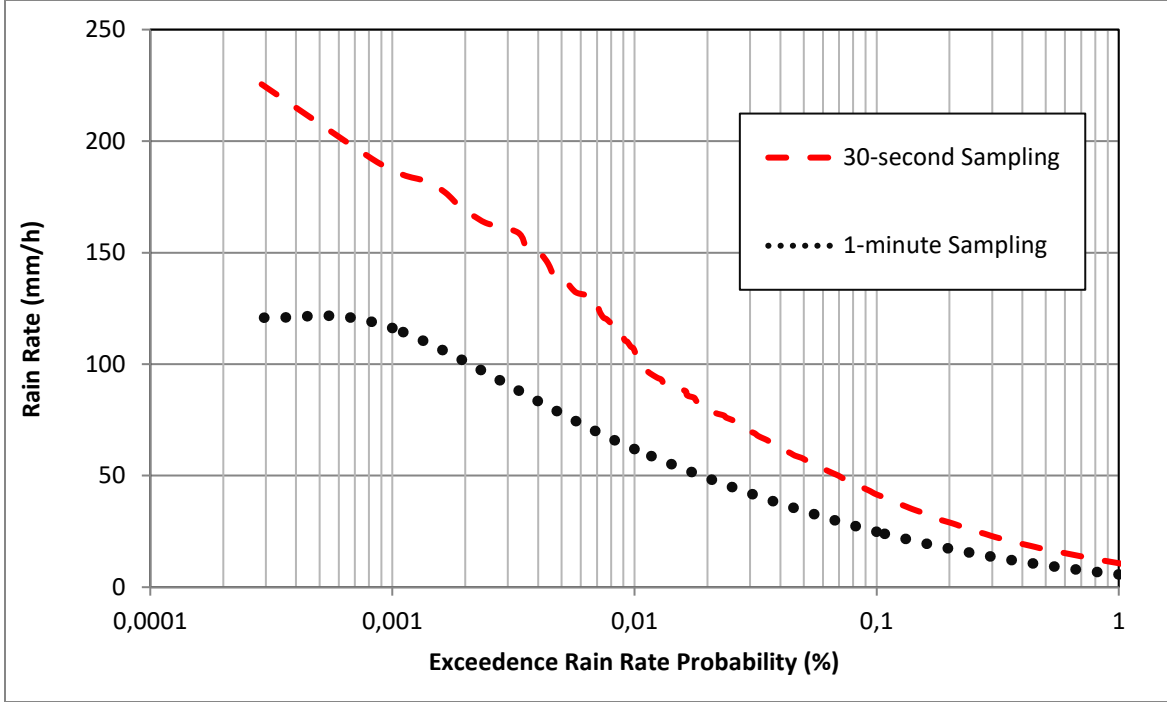


**Figure 5.1:** Rainfall rate cumulative distribution for the 30-second and 1-minute sampling times.

### 5.3 Prediction and Comparison of Specific Attenuation

#### 5.3.1 Determination of Conversion Factors

For long-term attenuation predictions, *ITU-R 530-16* recommends  $R_{0.01}$  to be determined at 1-minute sampling time. Therefore, the rain rate exceedance at 30-second are not applicable for attenuation predictions unless they are converted into 1-minute. *Akuan and Afullo 2011a*, proposed a mathematical method to convert rain rate of any sampling time into 1-minute sampling time. This is executed by converting and substituting values in the power-law function. Therefore, by adopting the same conversion method and *ITU-R P838-3* specific attenuation calculation guide for this current work, the specific attenuation at 30-second and 1-minute sampling is respectively determined as follows:

$$\gamma_{R,30s} = z[\mu R_{30s}^\beta]^\alpha \quad [dB/km] \quad (5.1a)$$

and

$$\gamma_R = z[R_{1min}]^\alpha \quad [dB/km] \quad (5.1b)$$

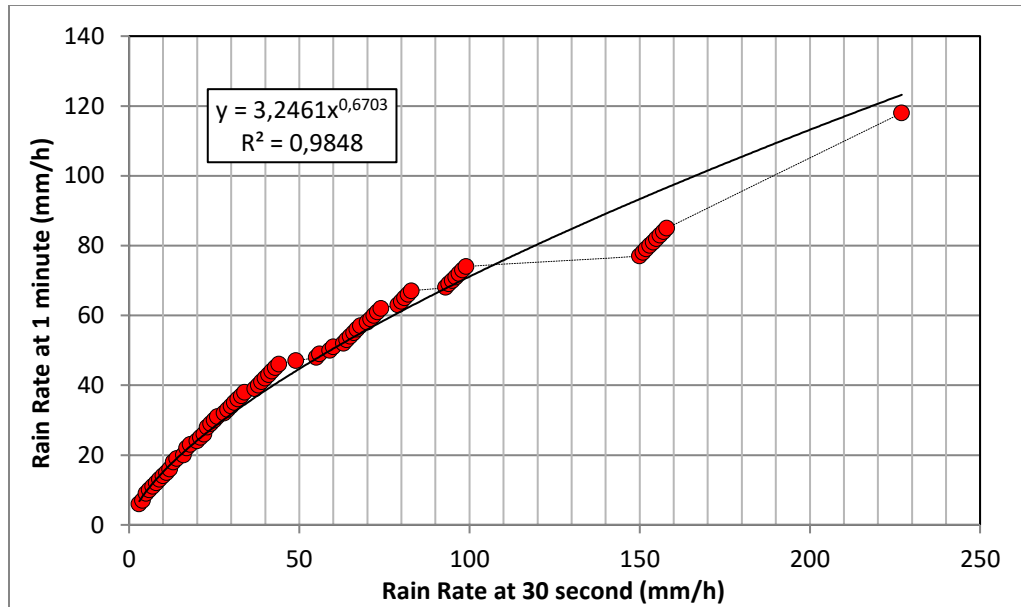


**Figure 5.2:** Conversion of the 30-second rain rate into 1-minute rain rate.

Where:

$R_{30s}$  = rain rate at 30-second sampling in mm/h.

$R_{1min}$  = rain rate at 1-minute sampling in mm/h.

$x$  and  $y$  = power-law coefficient for conversion of 30-second rain rate into 1-minute.

$z$  and  $\alpha$  = frequency and polarization dependence coefficient, found in [ITU-R P838-3].

Figure 5.2 presents the power-law parameters which are required to convert the 30-second rain rates into 1-minute rain rate in Durban. It is found that the ideal power-law coefficients for (5.2a) in Durban are  $x = 3.2461$  and  $y = 0.6703$ .

### 5.3.2 Comparison of the Specific Attenuation at Different Sampling Times

Figure 5.3 presents the comparison of 30-second and 1-minute predicted specific rain attenuation at different frequencies. The rain drop shape is considered to be spherical; hence the frequency polarization difference is insignificant. On figure 5.3 it is observed that the two predicted trends of attenuation almost resemble each other at frequencies less than 10 GHz. However, after 10 GHz the difference between the two attenuation trends gradually increases; where the attenuation estimated at 30-second continuously get higher than attenuation estimated at 1-minute sampling as the frequency increases beyond 10 GHz.

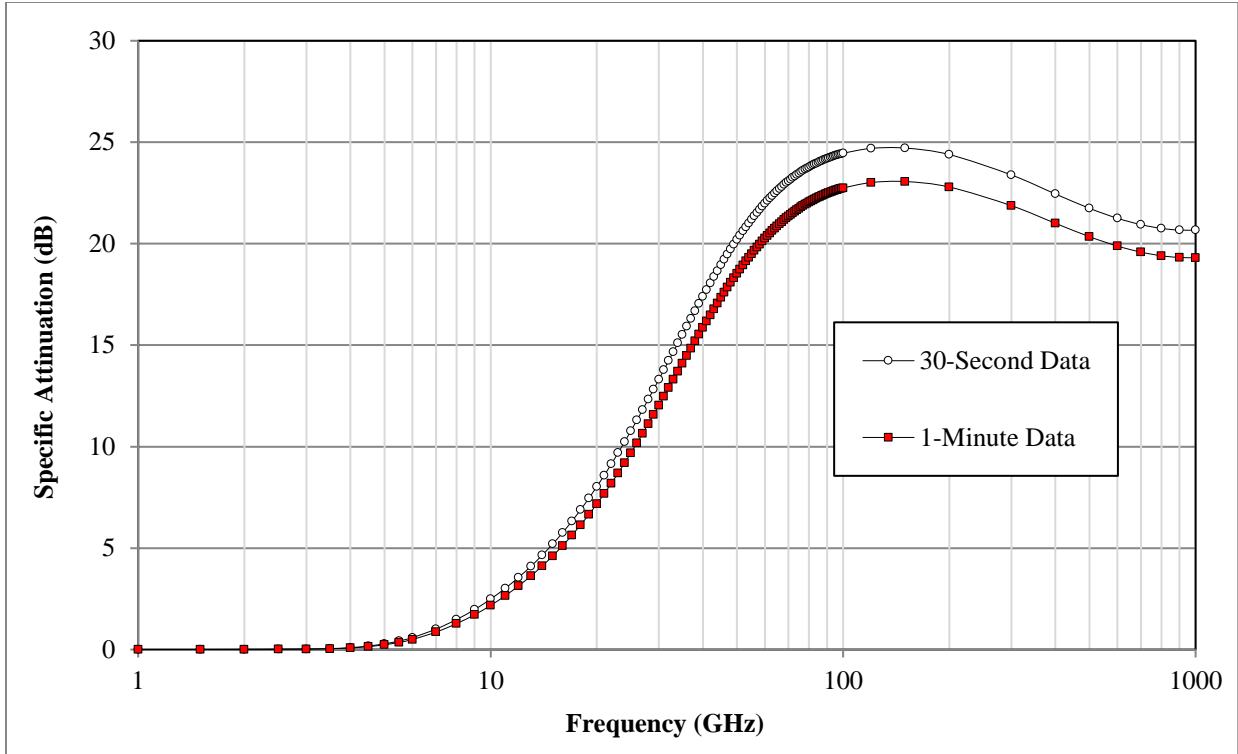
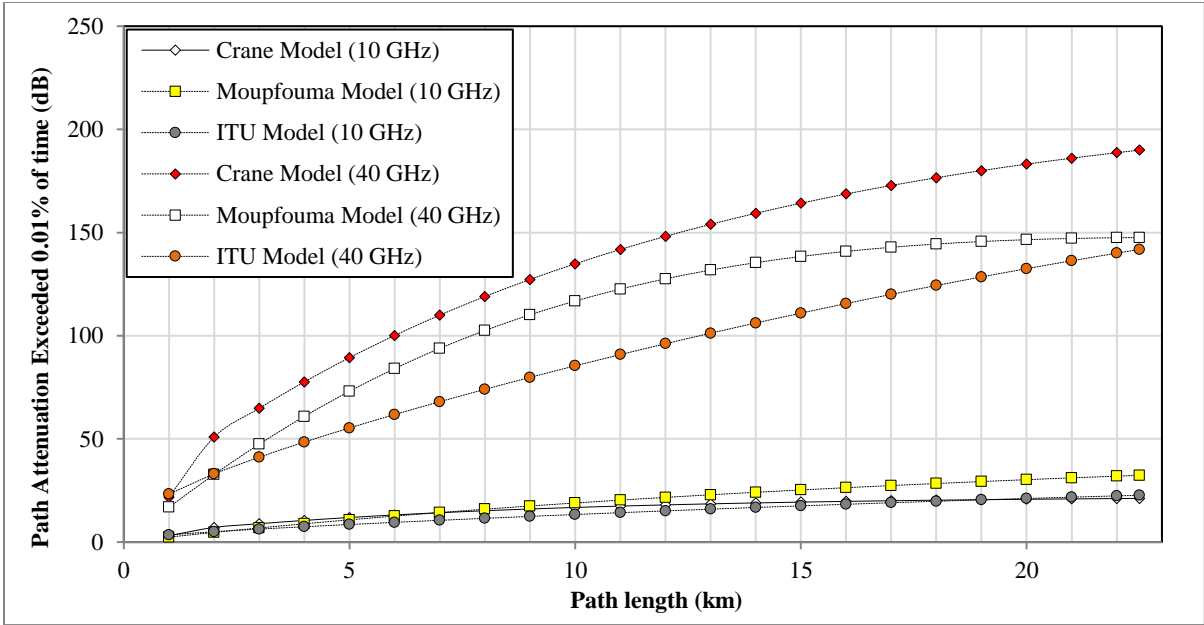


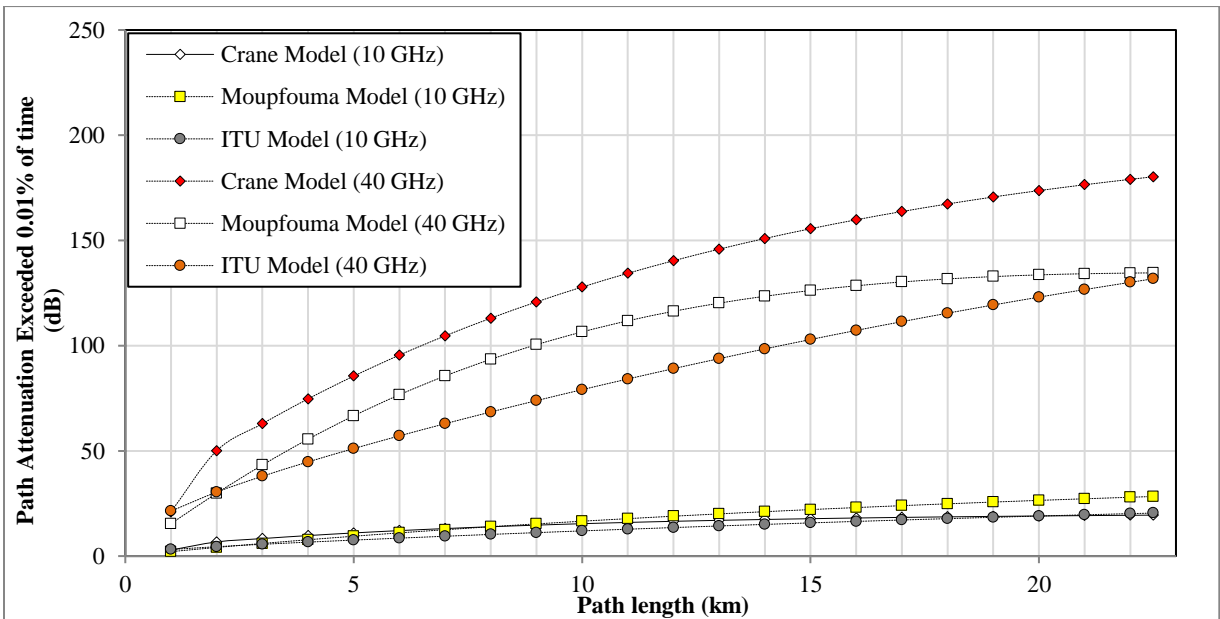
*Figure 5.3: Predicted specific attenuation at 30-second and 1-minute sampling on different frequencies for horizontal frequency polarization.*

#### 5.4 Prediction of Path Attenuation Using Existing Models

This section presents the estimation of rain path attenuation over terrestrial links using existing models based on  $R_{0.01}$ . This gives the attenuation exceeded 0.01% of the time ( $A_{0.01}$  in dB) for different radio path lengths up to 22 km. This is executed at two specific frequencies namely 10 GHz and 40 GHz in Durban. Therefore, Figure 5.4 a) presents attenuation predictions at 30-second sampling time. From the results, it is found that at 10 GHz the Crane Global, Moupfouma and ITU-R models are very close to each other; but beyond a path length of 4 km the Moupfouma model tends to predict higher attenuation compared to the other two models. Conversely at 40 GHz the Crane Global model predicts higher attenuation compared to the ITU-R model, while the Moupfouma varies between Crane Global and ITU-R model after 2 GHz. The general behavior of the attenuation from the models at both 1- minute and 30-second sampling is similar except that the attenuation is consistently higher under 30-second sampling for corresponding models, especially after path length of 5 km as seen in Figure 5.4 b).



a) 30-second Data

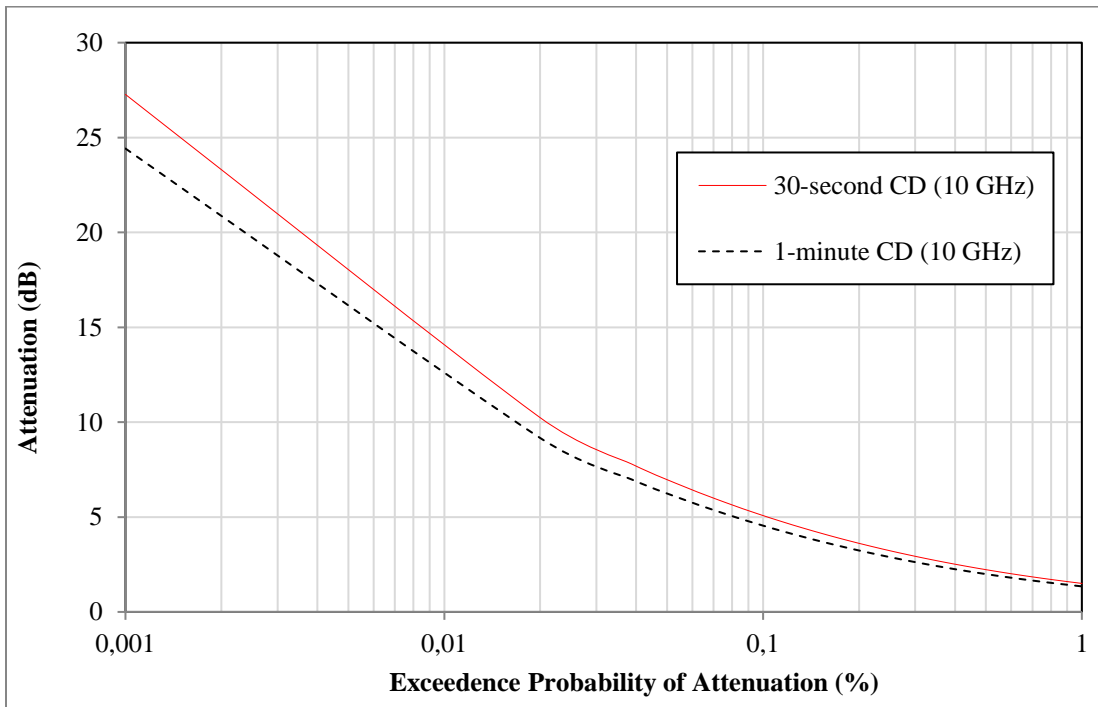


b) 1-minute Data

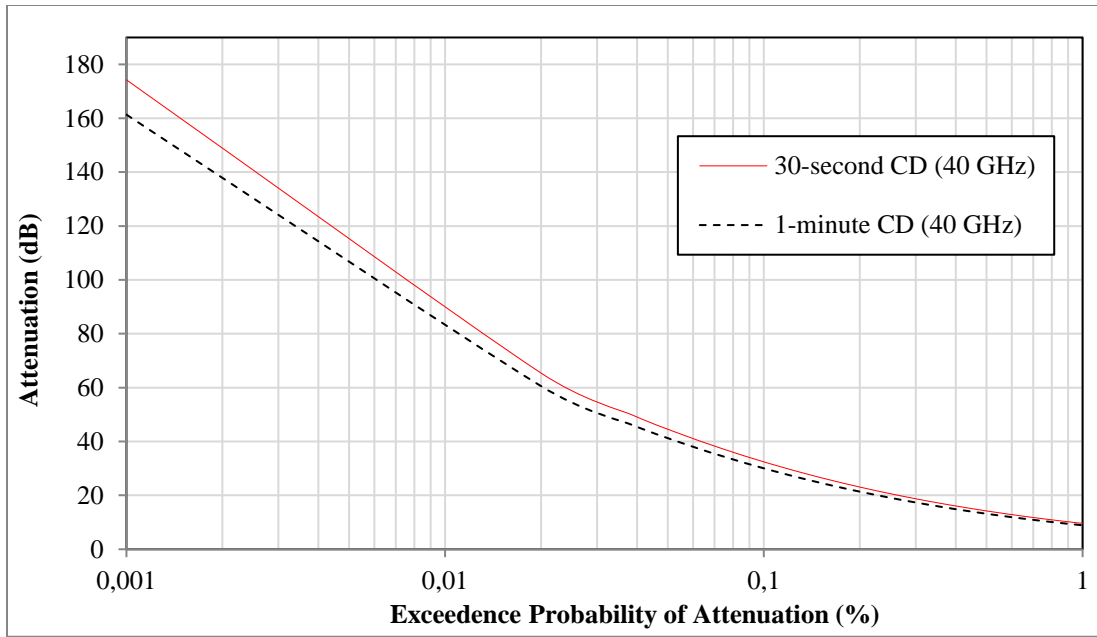
Figure 5.4: Predicted path attenuation using existing models at 30-second and 1-minute sampling on different path length in Durban.

### 5.5 Investigation of Annual Attenuation Exceeded Along the Path Length of 10 km at 10 GHz and 40 GHz.

Rainfall occurrences are randomly distributed throughout the whole year and rain rates vary during rain events. Thus, the required rain fade margin to overcome the rain effects over radio links changes from one rain event to another throughout the year. Therefore, the cumulative distribution (CD) of rainfall attenuation is required to determine the amount of rain attenuation expected to be suffered by a propagating radio signal for different percentages of time over a given year. Table 5.1 and Figure 5.5 present the predicted rain attenuation exceeded for the percentage of time in the range 0.001% to 1% using [ITU-R P.530-16, 2015] along a 10 km path length. These results agree with the general norm that at higher frequencies attenuation is higher than at lower frequencies. It is observed that at both sampling times the attenuation is higher at 40 GHz than at 10 GHz. Also, results show that at both frequencies the predicted attenuation is higher at 30-second sampling than at 1-minute sampling for all the percentage of time.



a) Attenuation at 10 GHz



b) Attenuation at 40 GHz

**Figure 5.5:** Rain attenuation cumulative distribution for the 30-second and 1-minute sampling time data.

**TABLE 5.1:** RAIN ATTENUATION EXCEEDANCE AT DIFFERENT PERCENTAGE OF TIME FOR THE 30-SECOND AND 1-MINUTE DATA.

FREQUENCY	PERCENTAGE (%)	ATTENUATION (dB) AT 30-SECOND	ATTENUATION (dB) AT 1-MINUTE
10 GHz	0.001	27.27	24.42
	0.01	19.17	16.74
	0.1	5.09	4.56
	1	1.502	1.345
40 GHz	0.001	174.27	161.35
	0.01	122.47	113.40
	0.1	31.64	30.11
	1	9.60	8.89

## 5.6 Significance of Lower Sampling Time on Rainfall Data.

Considering the high data rates that are demanded in digital broadcasting technology, many researchers have investigated the direct level of influence of rainfall attenuation towards video quality during satellite video transmission [Ma et al, 2012]. Similarly, Lee and Winkler (2011) analyzed the correlation between video quality of service, video quality of experience, and rainfall rate on Ka-band satellite links. They used

the V-Factor metric for video quality, where the algorithm is mainly designed for MPEG-2 and H.264 video streaming over IP networks. From their analyses, it was found that the increase in rain rate results in severe packet loss on the link, hence the video quality gets badly affected. Thus, rain rate is inversely proportional to the video quality.

In such cases where rain attenuation is one of the main causes of packet loss, one of the methods to mitigate rain attenuation is by increasing the fade margin such that it exceeds the highest attenuation level possible [Manabe et al, 1995]. Therefore, for accurate fade margin calculations it is required that rain attenuation statistics information be accurate. Due to generally known fact that at wider sampling the averaging is big, as a result some important information gets omitted. It is very crucial that lower sampling time data get first preference in order to achieve accurate predictions. This observation is evident in Figure 5.3 through Figure 5.5, the rain attenuation predicted under 30-second sampling consistently indicates that higher attenuation levels are to be expected in contrast to that at 1-minute sampling. At 1-minute sampling it is observable that some spikes are not accurately resolved due to the mentioned reason of averaging; therefore it is ideal to use 30-second sampling for improved prediction of rain attenuation. The rain attenuation prediction method recommended by the ITU-R is one of the popular models used worldwide. Nevertheless, when applied to the tropical regions, it has been shown to be inadequate as reported in [Manabe et al, 1987; Yeo et al, 1990; Zhou et al, 1999 and Obiyemi et al, 2014]. Given that ITU-R recommends 1-minute sampling time, it is highly possible that the sampling time may be the cause of the inaccuracy. Therefore based on the results of this study, it is evident that the 1-minute sampling recommended by the ITU-R results in the attenuation experienced by a link under rainy conditions being underestimated. To address this issue, owing to the current complexity and data rates produced by modern communication systems, it is vital that the ITU-R revise their model by considering lower sampling times in order to develop a realistic model.

## **5.7 Chapter Summary**

This chapter focused on the investigation of rain attenuation at the chosen frequencies, distances and sampling times. Based on the results, specific rain attenuation is found to be increasing as the frequency increases in the frequency range 1 GHz to 200 GHz. Moreover, by using the existing models it is found that as the distance increases so does the attenuation. As expected, the attenuation predicted at 1-minute sampling is found to be lower than that estimated at 30-second sampling. This means that at 1-minute sampling the expected attenuation is underestimated.

# CHAPTER SIX

## Conclusion and Future Work

### 6.1 Conclusions

Rainfall process is one of the most complex and unpredictable processes which are naturally occurring. However, the understanding of this process is very crucial in telecommunications since most of the time the presence of rainfall over radio links causes signal loss. Hence by understanding rain process the loss can be minimized. Owing to this, different techniques have been proposed by many researchers for the purpose of understanding the behavior of the rainfall process. Recently, the Queueing Theory Technique (QTT) has been developed in order to understand the rain process and the time-variation of rain attenuation [Alonge, 2014]. The results produced by QTT demonstrated that at subtropical and equatorial Africa rain rate queues follow a semi-Markovian queue discipline [Alonge et al, 2014b]. In this study, the objective was to investigate the effect of sampling time on rainfall queues and attenuation; hence the following conclusions are made based on the obtained results.

Chapter 3 presented the investigation of rainfall spikes at 30-second sampling and the comparison of rainfall spikes at 1-minute and 30-second sampling in Durban. From the 30-second rainfall spikes investigation, it is found that rainfall queues follow a non-Markovian queue discipline ( $E_k/E_k/s/\infty/FCFS$ ). The service and inter-arrival times are found to be best described by an Erlang-k distribution; conversely the overlap time is exponentially distributed. The rainfall spikes inter-arrival times during thunderstorm events are found to be the longest compared to all other rainfall regimes. Drizzle events are characterized by many rain spikes arrival compared to all other rainfall regimes. However, drizzle events are also characterized by the lowest spikes average inter-arrival time, service time, overlap time and rain rates compared to all other regimes. Give all these facts, drizzle events are least expected to cause network outage. Conversely, shower rain spikes are observed to have the longest average service time, overlap time and belong to the second highest rain rate range ( $10 < R \leq 40 \text{ mm/h}$ ). Therefore, network outages are highly possible during shower events at 30-second sampling. During the comparison of the 30-second and 1-minute sampling time rain data, it is found that the average inter-arrival, service and overlap time at 1-minute is larger than at 30-second sampling. This is due to the fact that at wider interval the averaging is large. Hence this may serve as a disadvantage to someone with 1-minute data expecting accurate results, since at large averaging some information is omitted. Further on, from both results is identified that the average service time of rainfall spikes in Durban is between  $10 < t < 21 \text{ minutes}$  irrespective of the two sampling times. Lastly, all the queue parameters at 30-second sampling have higher rates than those at 1 minute sampling. Hence more

rainfall spikes are identified at 30-second data compared to the 1-minute data. Conclusively, at lower sampling time more rainfall spikes statistical information is revealed.

Chapter 4 presented the long-term modeling of rainfall spikes at 30-second sampling time. It is found that there typical relationship between the 30-second and 1-minute rainfall data which is best described by a polynomial function. This is proven by the higher coefficient of determination,  $R^2$ , obtained under the polynomial function for all the queue parameters under all rainfall regimes. In this regards, the polynomial function is used to convert the 1-minute data into 30-second sampling time data. The conversion method is validated by comparing the converted data queue models with the actual 30-second sampling data queue models. The error test between these two models strongly confirmed that the converted data is similar to the actual 30-second data; hence the conversion method is valid. The resultant queue discipline ( $E_k/E_k/s/\infty/FCFS$ ) on the long-term modeling is similar to the short-term data queue discipline at 30-second sampling in Durban. Therefore, the rainfall process shows some attributes of a self-similar process in the period of 66 months. Hence if 12 months 30-second rain data is available there might be no need for other long-term measurements, since the modeling results will be the same. However, there are many parameters which are assessed for a particular process to be considered a self-similar process. Hence an extensive study needs to be taken in order to conclude if rainfall is a self-similar process. Therefore, we propose that study in the future work.

Chapter 5 presented the investigation of the effect of the sampling time on rain attenuation statistical information. From specific attenuation results, it is found that at frequencies less than 10 GHz the predicted attenuation at both 30-second and 1-minute sampling is almost the same. Conversely, after 10 GHz the difference between the attenuation predicted at both sampling times gradually increase; where at 30-second higher attenuation is predicted than at 1-minute. Attenuation exceeded at 0.01% of the time ( $A_{0.01}$ ) is considered as a parameter of interest for radio system designers. Therefore, in this study this parameter of interest ( $A_{0.01}$ ) is examined using the three existing attention models namely Crane Global, Moupfouma and ITU-R model. It is found that each model predict higher attenuation at 30-second compared at 1-minute. Further on, examining rain attenuation exceeded for the percentage of time in the range 0.001% to 1% by using [ITU-R P.530-16, 2015]; it is also found that the predicted rain attenuation at 30-second is higher compared at 1-minute sampling. From all the presented rain attenuation results, it is seen that at all aspects predicted rain attenuation at 30-second sampling is higher than at 1-minute sampling. This is due to the fact that at 1-minute sampling the averaging is larger compared at 30-second sampling; hence some rainfall spikes are not considered as independent spikes, instead are identified as portions of some larger rainfall spikes. That is disadvantageous for the 1-minute sampling time because failure to recognize some spikes as independent rainfall spikes, results failure to recognize their total contribution toward link rain

attenuation. Hence at 1-minute sampling the predicted rain attenuation is lower compared at 30-second sampling, since some rain attenuation information get omitted at wider sampling. Therefore, given that one of the strong suggested methods to compensate rain attenuation is to increase fade margin such that it exceeds the highest attenuation level [*Manabe et al, 1995*], therefore it adequate to use 30-second sampling data for accurate calculations of fade margin. Conclusively, given that ITU-R recommends 1-minute sampling time; we strongly recommend that ITU-R revise their prediction methods using 30-second sampling time data.

## **6.2 Future Work**

- Investigation of a Self-Similar process Attributes on Rainfall Process over Radio Links using Queueing Theory Technique.
- Elliptical Analysis of Rain Cell Characteristics from Queueing Theory for Wireless Radio Link Designs.

## References

- Acosta R. J. (1997): 'Rain Fade Compensation Alternatives for Ka-Band Communication Studies', *3rd Ka-Band Utilization Conference*, Sorrento, Italy, pp. 225-231.
- Adan I. and Resing J. (2015): Handbook on Queueing Systems, *MB Eindhoven*, Netherlands pp. 23-28.
- Adimula, I.A and Ajayi G.O. (1996): 'Variation in raindrop size distribution and specific attenuation due to rain in Nigeria', *Ann. Telecommun.*, Vol.51, No. 1-2 pp. 87-93.
- Adhikari P. (2008): 'Understanding Millimeter Wave Wireless Communication', *VP of Business Development for Network Solution*, Loea Corporation, San Diego pp. 1-3.
- Afullo T. J. O. (2011): 'Raindrop size Distribution Modeling for Radio Link Design along the Eastern Coast of South Africa,' *Progress in Electromagnetic Research B*, Vol. 34, pp. 345- 366.
- Ajayi G. O. and Olsen R. L, (1985): 'Modelling of a tropical raindrop size distribution for microwave and millimeter wave applications', *Radio Science*, Vol. 20, No. 2, pp. 193-202.
- Ajayi, G. O., and Adimula I. A., (1996): 'Variations in raindrop size distribution and specific attenuation due to rain in Nigeria', *Ann. Telecommun.*, Vol.51, No. 1-2 pp. 87-93.
- Akuon P.O. and Afullo T.J.O., (2011a): 'Rain cell sizing for the design of high capacity radio link systems in South Africa', *Progress in Electromagnetics Research B*, Vol. 35, pp. 263-285.
- Akuon P.O. and Afullo T.J.O., (2011b): 'Path Reduction Factor Modelling for Terrestrial Links based on Rain Cell Growth,' *Proc. IEEE AFRICON 2011 conf.*, Livingstone, Zambia, ISBN 978-1-61284-991-1, pp. 1-5.
- Alasseur A. C, Núñez A. B, Fontán F.P., Hussona L., Fiebigc U.C. and Mariño P., (2006): 'Two approaches for effective modelling of rain-rate time-series for radio communication system simulations', *Space Communications IOS Press 20*, Vol. 69, pp. 69-83.
- Alonge A. A., (2011): 'Msc. Thesis on Correlation of rain dropsize distribution with rain rate derived from disdrometers and rain gauge networks in Southern Africa', *University of KwaZulu Natal*, South Africa, pp. 51-63.
- Alonge A. A. and Afullo T. J., (2012a): 'Regime analysis of rainfall drop-size distribution models for microwave terrestrial network', *IET Microwaves Antennas Propagation*, Vol 6, No. 4, pp. 393-403.
- Alonge A. A. and Afullo T. J. O., (2012b): 'Seasonal analysis and prediction of rainfall effects in Eastern Southern Africa at microwave frequencies', *Prog. Electromagn. Res. B*, Vol. 40, No. 3, pp. 279-303.
- Alonge, A.A and Afullo T.J., (2014a): 'Fractal analysis of rainfall event duration for microwave and millimetre networks: rain queueing theory approach', *IET Microwaves Antennas Propagation*, Vol. 9, No. 4, pp. 291-294.

- Alonge A.A and Afullo T.J., (2014b): ‘Characteristics of rainfall queues for rain attenuation studies over radio link at subtropical and equatorial Africa’, *Radio Science*, Vol 49, doi:10.1002/2014RS005424, pp. 583-591.
- Alonge A.A., (2014): ‘PhD Thesis on Queueing Theory Approach to Rain Fade Analysis at Microwave and Millimeter Bands in Tropical Africa’, *University of KwaZulu-Natal*, pp. 53-63.
- Alonge A.A. and Afullo T.J., (2015): ‘Rainfall time series synthesis from queue scheduling of rain event fractals over radio links’, *Radio Science*, Vol. 50, doi:10.1002/2015RS005791, pp. 1209-1210.
- Atlas D. and Ulbrich C.W., (1974): ‘The physical basis for attenuation-rainfall relationships and the measurement of rainfall parameters by combined attenuation and radar methods,’ *J. Rech.Atmos.*, Vol. 8, No. 1-2 , pp. 275–298.
- Bolch G., Greiner S., de Meer H. and Trivedi K.S, (1998): ‘Handbook on Modelling and Performance with Computer Science Application’, *John Wiley and Sons*, Chapter 6, pp. 209-233.
- Braten L. E. and Tjelta T., (2000): ‘An improved three-state semi-Markov propagation model optimised for land mobile satellite communication’, *Proc. AP 2000 Millennium Conference on Antennas & Propagation*, Davos, Switzerland pp. 165-172.
- Carey D.I. and Haan, C.T., (1978): ‘Markov process for simulating daily point rainfall’, *Journal of the Irrigation and Drainage Division*, Vol 104, IR1, pp. 111 – 125.
- Crane R.K., (1980): ‘Prediction of Attenuation by Rain’, *IEEE Trans. Commun.*, Vol.28, No.6, pp. 1717-1733.
- Crane R.K., (1985): ‘Evaluation of Global and CCIR models for estimation of rain rate statistics’, *Radio Science*, New York, Vol.20, No.4, pp. 865-879.
- Crane R.K., (1996): ‘Electromagnetic Wave Propagation Through Rain’, *John Wiley and Sons Inc.*, New York, Vol. 24, No.3, pp 1-4 and pp. 39-40.
- Crane R. K., (2003): ‘Propagation Handbook for Wireless Communication System Design’, *CRC Press*, New York pp. 35-70.
- Das S., Maitra A. and Shukla A. K., (2010): ‘Rain attenuation modelling in the 10-100 GHz frequency using drop size distributions for different climatic zones in Tropical India’, *Progress In Electromagnetics Research B*, Vol. 25, doi:10.2528/PIERB10072707, pp. 211-224.
- Dissanayake A., Allnut J. and Haidara F., (1997): ‘A prediction Model that combines Rain Attenuation and other propagation impairments along earth-satellite paths’, *IEEE Transactions and Propagation*, Vol. 45, No.10, pp. 1548-1552.
- Fashuyi M .O., Owolawi P. A. and Afullo T. O. (2006): ‘Rainfall rate modelling for LoS radio systems in South Africa’, *Trans. of South African Inst. of Elect. Engineers (SAIEE)*, Vol. 97, No. 1, pp. 74-81.

- Diba F., Afullo T. and Alonge A., (2016): “Time Series Rainfall Spike Modelling from Markov Chains and Queueing Theory Approach for Rainfall Attenuation over Terrestrial and Earth-space Radio Wave Propagation in Jimma, Ethiopia” *Progress In Electromagnetic Research Symposium (PIERS)*, Shanghai, China, pp. 4991- 4995.
- Freeman R. L., (2007): ‘Handbook on Radio System Design for Telecommunications’, *John Wiley and Sons*, New York, pp. 60-77.
- Gabriel K. R. and Neumann J., (1962): ‘A Markov chain model for daily rainfall occurrences at Tel Aviv’, *Quar. J. Roy. Meteor. Soc.*, Vol. 88, No. 375, pp. 90–95.
- Green H. E., (2004): Propagation Impairment on Ka-Band SATCOM links in tropical and equatorial regions, *IEEE Antennas Propag. Mag.*, Vol. 46, No. 2, pp. 31–44.
- Heder B. and Bitos J., (2008): ‘General N-state Markov model for rain attenuation times series generation’, *Wireless Pers. Comm.*, Vol. 4, No. 3, pp. 99–113.
- Hillier S.F. and Lieberman J.G., (2010): ‘Handbook on Introduction to operation research’, (7<sup>th</sup> Edition), *McGraw-Hill*, New York pp. 760-812.
- Ishimaru A., (1978): ‘Wave Propagation and Scattering in Random Media’, *Academic Press*, New York, Vol. 1 and 2, No.4, pp. 434-437.
- Islam M.R., Chebil J. and Rahman T.A., (1997): ‘Review of Rain Attenuation Studies for Communication Systems operating in Tropical region’, *Proc. IEEE Malaysia International Conference on Communications*, Malaysia, pp. 1-4.
- Ivanovs G. and Serdega D., (2006): ‘Rain Intensity Influence on Microwave Line Payback Terms’, *Electronic and Electrical Engineering*, Vol. 6, No. 70, pp. 243-248.
- Ippolito L. J. Jr., (2008): ‘Handbook on Satellite Communications Systems Engineering: Atmospheric Effects, Satellite Link Design and System Performance’, *John Wiley and Sons Ltd*, UK, pp. 284-289.
- ITU-R P.837-1, (1994): ‘Characteristics of precipitation for propagation modelling’, *ITU-R Recommendation*, Geneva.
- ITU-R P.530-10, (2001): ‘Propagation prediction techniques and data required for design of terrestrial line-of-sight systems, *ITU-R Recommendation*, Geneva.
- ITU-R P.1703, (2005): ‘Availability objectives for real digital fixed wireless links in 27,500 km hypothetical reference paths and connections’, *ITU-R Recommendation*, Geneva.
- ITU-R P.838-3, (2005): ‘Specific attenuation model for use in prediction methods’, *ITU-R Recommendation*, Geneva.
- ITU-R P.530-16, (2015): ‘Propagation data and prediction methods required for the design of terrestrial line-of-sight systems’, *ITU-R Recommendation*, Geneva.

- Jonathan H. and Dong L., (2004): ‘Ice and water permittivity for millimeter and sub-millimeter remote sensing applications’, *Atmospheric Science Letters*, Vol. 5, doi: 10.1002/asl.77, pp. 146-151.
- Kozu T. and Nakamura K., (1991): ‘Rainfall parameter estimation from dual-radar measurements combining reflectivity profile and path-integrated attenuation’, *J. of Atmos. and Oceanic Tech.*, Vol. 8, No.2, pp 259–270.
- Kumar L.S. and Lee Y.H., (2010): ‘Shape Slope parameter distribution modelling for electromagnetic scattering by rain drops’, *Progress In Electromagnetics Research B*, Vol. 25, No. 10, pp. 191-209.
- Laskshmi S. K., Lee Y. H. and Ong J. T., (2010): ‘Truncated gamma drop size distribution models for rain attenuation in Singapore’, *IEEE Trans Antennas Propag (USA)*, Vol. 58, No. 4, pp. 1325-1335.
- Lee Y. H and Winkler S., (2011): ‘Effects of Rain Attenuation on Satellite Video Transmission’, *Vehicular Technology Conference (VTC Spring)*, IEEE 73rd, Budapest, Hungary, pp. 246-248.
- Lutz E., Cygan D., Dippold M., Dolainsky F., and Papke W., (1991): ‘The land mobile satellite communication channel-recording, statistics, and channel model’, *IEEE Transactions on Vehicular Technology*, Vol. 40, No. 2, ISSN: 0018-9545, pp. 375–386.
- Ma T., Lee Y. H., Ma M., and Winkler S., (2012) : ‘The Rain Attenuation on Real-Time Video Streaming via Satellite Links’, *International Journal of Computer Theory and Engineering*, Vol. 4, No.4, pp.524-529.
- Malinga S. J., Owolawi P. A. and Afullo T. J. O., (2013): ‘Computation of rain attenuation through scattering at microwave and millimeter bands in South Africa’, *Progress in Electromagnetics Research Symposium Proceedings*, Taipei, pp. 959-971.
- Manabe T. and Yashida T., (1995): ‘Rain attenuation characteristics on radio links’, *IEEE Proceedings*, San Francisco, USA, pp. 77–80.
- Manabe T., Ihara T., Awaka J., and Furuhashi Y., (1987): “The relationship of raindrop-size distribution to attenuation experiments at 50, 80, 140, and 240 GHz,” *IEEE Trans. Antennas Propag.* , Vol. 35, No. 11, pp. 1326–1330.
- Marayuma T., Shirato Y., Akimoto M., and Nakatsugawa M., (2008): ‘Service area expansion of Quasi-Millimeter FWA systems through site diversity based on detailed rainfall intensity data’, *IEEE Trans. Antennas Propag.*, Vol. 56, No. 10, doi:10.1109/TAP.2008.929432, pp. 3285–3292.
- Massambani O. and Rodriguez C.A.M., (1990): ‘Specific attenuation as inferred from drop size distribution measurements in the tropics’, *Proc. URSI Comm. F. Sym. on Regional Factors in predicting Radiowave Attenuation*, Rio de Janeiro, Brazil, Vol. 6, pp. 25-28.
- Medeiros Filho F. C, Cole R. S. and Sarma A. D., (1986): ‘Millimeter-wave induced attenuation: Theory and Experiment’, *IEE Proc.*, part H, Microwave Antennas Propag., Vol. 133, No. 4, pp. 308-314.

- Moupfouma F., (1987): 'More about rainfall rates and their prediction for radio systems', *IEEE Proceedings*, Vol. 134, No. 6 pp. 527-537.
- Moupfouma F. and Martins S., (1995): 'Modeling of the rainfall rate cumulative distribution for design of satellite and terrestrial communication systems', *International Journal of Satellite Communication*, Vol. 13, No. 2, pp. 105-115.
- Moupfouma F. (1982): 'Empirical model for rainfall rate distribution,' *Electron. Lett*, Vol. 18, No.11, pp. 460–461.
- Moupfouma F. (1984): "Improvement of rain attenuation prediction method for terrestrial microwave links", *IEEE Trans. Antennas Propag.*, Vol. 32, No. 12, pp. 1368–1372.
- Murrell J. N. and Jenkins A. D. (1994): 'Handbook on Properties of Liquids and solutions', *2nd Ed. John Wiley & Sons*, Chichester, England, pp.442-445.
- Nakazawa S., Nagasaka M., Tanaka S. and Shogen K., (2010): 'A method to control phased array for rain fading mitigation of 21-GHz band broadcasting satellite', in *Proceedings of the Fourth European Conference on Antennas and Propagation (EuCAP) IEEE*, Barcelona, Spain, pp. 1–5.
- Nemarich J., Ronald J. and James L., (1988): 'Backscatter and attenuation by falling snow and rain at 96, 140, and 225 GHz', *IEEE Trans. Geoscience and Remote Sensing*, Vol. 26, No. 3, pp. 319-329.
- Obiyemi O. O., Ojo J. S. and Ibiyemi T. S., (2014): "Performance analysis of rain rate models for microwave propagation designs over tropical climate," *Progress In Electromagnetics Research M*, Vol. 39, doi: 10.2528/PIERM14083003, pp. 115–122.
- Odedina M.O. and Afullo T.J., (2008): 'Characteristics of seasonal attenuation and fading for line-of-sight links in South Africa,' *Proc. of SATNAC*, South Africa, Durban, pp. 203–208.
- Odedina M.O. and Afullo T.J., (2010): 'Determination of rain attenuation from electromagnetic scattering by spherical raindrops: Theory and experiment,' *Radio Sci.*, Vol. 45, No. 1, pp. 250-254.
- Owolawi P.A, (2011): 'Rainfall Rate Probability Density Evaluation and Mapping for the Estimation of Rain Attenuation in South Africa and Surrounding Island,' *Progress in Electromagnetics Research B*, Vol. 112, doi: 10.2528/PIER1008250, pp. 155-181.
- Owolawi P. A., (2011): 'Derivation of one-minute rain rate from five-minute equivalent for the calculation of rain attenuation in South Africa', *PIERS Online*, Vol.7, No.6, pp 524-535.
- Pawlina A., (2002): 'No rain intervals within rain events: some statistics based on Milano radar and rain-gauge data', *COST Action 280 1st International Workshop*, pp. 382-385.
- Pozar D.M., (1998): 'Handbook on Microwave Engineering, Second Edition', *John Wiley and Sons Inc.*, New York. pp. 6.
- Rappaport S., Heath W. Jr, Daniels C., Murdock N., (2014): Handbook on 'Millimeter wave wireless communications', *U.S Prentice Hall*, USA, pp. 3-14.

- Rice P.L. and Holmberg N.R., (1973): 'Cumulative Time Statistics of Surface-Point Rainfall Rates', *IEEE Transactions on Communications*, Vol. 21, doi: 10.1109/TCOM.1973.1091546, pp. 1131-1136.
- Rodgers D. V. and Olsen R. L., (1976): 'Calculation of radiowave attenuation due to rain at frequencies up to 1000 GHz', *Commun. Res. Cent. Rep. 1299*, Ottawa Ont., Canada, pp. 425-428.
- Rodriguez R.I.F., Prez G.A.C., Werner M., Castaño A.G. and Cano A.M., (2012): 'Rainfall Estimation by a Signal Attenuation Analysis in Mobile Systems,' *XV Symposium SELPER*, November, pp. 222-225.
- Seybold J.S., (2005): 'Handbook on Introduction to RF Propagation', *John Wiley and Sons*, New York, pp. 218-245.
- Timothy K.I., Ong J. T. and Choo E. B. I., (2002): 'Raindrop size distribution using methods of moments for terrestrial and satellite communication applications in Singapore', *IEEE Transactions on Antennas and Propagation*, Vol. 50, No. 10, pp. 140-1424.
- Tseng, C.H., Chen K.S. and Chu C.H., (2005): 'Prediction of KA-band terrestrial rain attenuation using 2-year raindrop size distribution measurements in Northern Taiwan', *J. of Electromagn. Waves and Appl.*, Vol. 19, No. 13, pp. 1833-1841.
- Ulbrich C.W. (1983): 'Natural variation in the analytical form of the raindrop size distribution,' *J. of Climate and Applied Meteor.*, Vol. 22, No. 10, pp. 1764-1775.
- Umebayashi K., Morelos-Zaragoza R. H. and Kohno R., (2005): 'Modulation identification and carrier recovery system for Adaptive modulation in satellite communication', *Proceedings of IEEE 61st Vehicular Technology Conference*, VTC-Spring, Sweden, pp. 2697-2701.
- Vucetic B. and Du J., (1992): 'Channel modeling and simulation in satellite mobile communication systems', *IEEE Journal on Selected Areas in Communications*, Vol. 10, No. 8, pp. 1209-1218.
- Yakubu M. L., Yusop Z. and Yusof F., (2014): 'The modelled raindrop size distribution of Skudai, Peninsular Malaysia, using exponential and lognormal distributions', *The Scientific World Journal*, Vol. 2014, Article ID 361703, pp. 1-7.
- Yeo T. S., Kooi P. S., Leong M. S. and Ng S. S., (1990): 'Microwave attenuation due to rainfall at 21.225 GHz in the Singapore environment', *Electron. Lett.*, Vol. 26, No. 14, pp. 1021-1022.
- Zhang G. J., Vivekanandan J. and Brandes E., (2000): 'A method of estimating rain rate and drop size distribution from polarimetric radar measurements', *IEEE Transactions on Geoscience and Remote Sensing Conference*, pp. 350-352.
- Zhou Z. X., Li L. W., Yeo T. S. and Leong M. S., (1999): 'Analysis of experimental results on microwave propagation in Singapore's tropical rainfall environment', *Microwave Opt. Technol. Lett.*, Vol. 21, No. 6, pp. 470-473.

## Internet Sources

- [1] <http://www.medcalc.org/manual/chi-square-table.php>
- [2] <http://www.livescience.com/50399-radio-waves.html>
- [3] <http://www.real-statistics.com/non-parametric-tests/goodness-of-fit-tests/two-sample-kolmogorov-smirnov-test/>
- [4] [https://en.wikipedia.org/wiki/Kolmogorov%E2%80%93Smirnov\\_test](https://en.wikipedia.org/wiki/Kolmogorov%E2%80%93Smirnov_test)
- [5] <https://onlinecourses.science.psu.edu/stat464/node/54>

## Appendix A

**TABLE A-1:** FREQUENCY-DEPENDENT COEFFICIENTS FOR ESTIMATION OF SPECIFIC  
RAIN ATTENUATION [ITU-R P.838-3, 2005]

Frequency (GHz)	$k_H$	$\alpha_H$	$k_V$	$\alpha_V$
1	0.0000259	0.9691	0.0000308	0.8592
1.5	0.0000443	1.0185	0.0000574	0.8957
2	0.0000847	1.0664	0.0000998	0.9490
2.5	0.0001321	1.1209	0.0001464	1.0085
3	0.0001390	1.2322	0.0001942	1.0688
3.5	0.0001155	1.4189	0.0002346	1.1387
4	0.0001071	1.6009	0.0002461	1.2476
4.5	0.0001340	1.6948	0.0002347	1.3987
5	0.0002162	1.6969	0.0002428	1.5317
5.5	0.0003909	1.6499	0.0003115	1.5882
6	0.0007056	1.5900	0.0004878	1.5728
7	0.001915	1.4810	0.001425	1.4745
8	0.004115	1.3905	0.003450	1.3797
9	0.007535	1.3155	0.006691	1.2895
10	0.01217	1.2571	0.01129	1.2156
11	0.01772	1.2140	0.01731	1.1617
12	0.02386	1.1825	0.02455	1.1216
13	0.03041	1.1586	0.03266	1.0901
14	0.03738	1.1396	0.04126	1.0646
15	0.04481	1.1233	0.05008	1.0440
16	0.05282	1.1086	0.05899	1.0273
17	0.06146	1.0949	0.06797	1.0137
18	0.07078	1.0818	0.07708	1.0025
19	0.08084	1.0691	0.08642	0.9930
20	0.09164	1.0568	0.09611	0.9847
21	0.1032	1.0447	0.1063	0.9771
22	0.1155	1.0329	0.1170	0.9700
23	0.1286	1.0214	0.1284	0.9630
24	0.1425	1.0101	0.1404	0.9561
25	0.1571	0.9991	0.1533	0.9491
26	0.1724	0.9884	0.1669	0.9421
27	0.1884	0.9780	0.1813	0.9349

<b>Frequency (GHz)</b>	$k_H$	$\alpha_H$	$k_V$	$\alpha_V$
28	0.2051	0.9679	0.1964	0.9277
29	0.2224	0.9580	0.2124	0.9203
30	0.2403	0.9485	0.2291	0.9129
31	0.2588	0.9392	0.2465	0.9055
32	0.2778	0.9302	0.2646	0.8981
33	0.2972	0.9214	0.2833	0.8907
34	0.3171	0.9129	0.3026	0.8834
35	0.3374	0.9047	0.3224	0.8761
36	0.3580	0.8967	0.3427	0.8690
37	0.3789	0.8890	0.3633	0.8621
38	0.4001	0.8816	0.3844	0.8552
39	0.4215	0.8743	0.4058	0.8486
40	0.4431	0.8673	0.4274	0.8421
41	0.4647	0.8605	0.4492	0.8357
42	0.4865	0.8539	0.4712	0.8296
43	0.5084	0.8476	0.4932	0.8236
44	0.5302	0.8414	0.5153	0.8179
45	0.5521	0.8355	0.5375	0.8123
46	0.5738	0.8297	0.5596	0.8069
47	0.5956	0.8241	0.5817	0.8017
48	0.6172	0.8187	0.6037	0.7967
49	0.6386	0.8134	0.6255	0.7918
50	0.6600	0.8084	0.6472	0.7871
51	0.6811	0.8034	0.6687	0.7826
52	0.7020	0.7987	0.6901	0.7783
53	0.7228	0.7941	0.7112	0.7741
54	0.7433	0.7896	0.7321	0.7700
55	0.7635	0.7853	0.7527	0.7661
56	0.7835	0.7811	0.7730	0.7623
57	0.8032	0.7771	0.7931	0.7587
58	0.8226	0.7731	0.8129	0.7552
59	0.8418	0.7693	0.8324	0.7518
60	0.8606	0.7656	0.8515	0.7486
61	0.8791	0.7621	0.8704	0.7454
62	0.8974	0.7586	0.8889	0.7424

<b>Frequency (GHz)</b>	$k_H$	$\alpha_H$	$k_V$	$\alpha_V$
63	0.9153	0.7552	0.9071	0.7395
64	0.9328	0.7520	0.9250	0.7366
65	0.9501	0.7488	0.9425	0.7339
66	0.9670	0.7458	0.9598	0.7313
67	0.9836	0.7428	0.9767	0.7287
68	0.9999	0.7400	0.9932	0.7262
69	1.0159	0.7372	1.0094	0.7238
70	1.0315	0.7345	1.0253	0.7215
71	1.0468	0.7318	1.0409	0.7193
72	1.0618	0.7293	1.0561	0.7171
73	1.0764	0.7268	1.0711	0.7150
74	1.0908	0.7244	1.0857	0.7130
75	1.1048	0.7221	1.1000	0.7110
76	1.1185	0.7199	1.1139	0.7091
77	1.1320	0.7177	1.1276	0.7073
78	1.1451	0.7156	1.1410	0.7055
79	1.1579	0.7135	1.1541	0.7038
80	1.1704	0.7115	1.1668	0.7021
81	1.1827	0.7096	1.1793	0.7004
82	1.1946	0.7077	1.1915	0.6988
83	1.2063	0.7058	1.2034	0.6973
84	1.2177	0.7040	1.2151	0.6958
85	1.2289	0.7023	1.2265	0.6943
86	1.2398	0.7006	1.2376	0.6929
87	1.2504	0.6990	1.2484	0.6915
88	1.2607	0.6974	1.2590	0.6902
89	1.2708	0.6959	1.2694	0.6889
90	1.2807	0.6944	1.2795	0.6876
91	1.2903	0.6929	1.2893	0.6864
92	1.2997	0.6915	1.2989	0.6852
93	1.3089	0.6901	1.3083	0.6840
94	1.3179	0.6888	1.3175	0.6828
95	1.3266	0.6875	1.3265	0.6817
96	1.3351	0.6862	1.3352	0.6806
97	1.3434	0.6850	1.3437	0.6796

<b>Frequency (GHz)</b>	$k_H$	$\alpha_H$	$k_V$	$\alpha_V$
98	1.3515	0.6838	1.3520	0.6785
99	1.3594	0.6826	1.3601	0.6775
100	1.3671	0.6815	1.3680	0.6765
120	1.4866	0.6640	1.4911	0.6609
150	1.5823	0.6494	1.5896	0.6466
200	1.6378	0.6382	1.6443	0.6343
300	1.6286	0.6296	1.6286	0.6262
400	1.5860	0.6262	1.5820	0.6256
500	1.5418	0.6253	1.5366	0.6272
600	1.5013	0.6262	1.4967	0.6293
700	1.4654	0.6284	1.4622	0.6315
800	1.4335	0.6315	1.4321	0.6334
900	1.4050	0.6353	1.4056	0.6351
1 000	1.3795	0.6396	1.3822	0.6365